



# ANTIOXI - Development of oxide model for activity build-up in LWRs - PWR and WWER plant data analysis

Author	Klas Lundgren (ALARA Engineering)
Confidentiality	Public

Report's title ANTIOXI - Development of oxide model for activity build-up in LWRs - PWR and WWER plant data analysis	
Customer, contact person, address EC / Marc Deffrennes, Commission européenne, Rue du Champ de Mars 21, B-1050 Brussels, Belgium	Order reference
Project name ANTIOXI	Project number/Short name 6402 ANTIOXI
Author Klas Lundgren, ALARA Engineering AB, Skultuna, Sweden	Pages 66 p.
Keywords PWR, WWER, activity build-up, water chemistry, LWR	Report identification code VTT-R-03907-08
<p>Summary</p> <p>The objective of the ANTIOXI projects is to develop a deterministic model for the build-up and properties of the oxide layers formed on LWR out-of-core primary system surfaces. The main focus in the development is to be able to model and predict the radioactivity build-up occurring on these surfaces.</p> <p>This report presents an evaluation of PWR and WWER data. The PWRs specifically reviewed are the 3 Swedish Ringhals plants, and the WWERs the two Finnish Loviisa plants. These plants are of two different types, with different steam generator tubing materials and somewhat different primary water chemistry conditions.</p> <p>Data are normally covered from the initial start up to the 2006 outage, and represent more than 100 operation years. A data review for each plant is presented. An analysis of the data is provided, discussing the influence of different water chemistry and other factors. The report ends with a summary and conclusions.</p> <p>The field experience compiled in this report does support the approach that surface chemistry, as studied by surface complexation methods, is an appropriate technique in assessing the real activity build-up mechanism as well as the impact of the water chemistry on the oxide formation mechanism in PWR and WWER environments. Conclusions are also provided to improve sampling of activated corrosion products in the primary coolant.</p>	
Confidentiality	Public
Espoo, 6 <sup>th</sup> June 2008 Signatures   Liisa Heikinheimo                      Petri Kinnunen Technology Manager                      Senior Research Scientist, Coordinator	
VTT's contact address VTT Technical Research Centre of Finland, P.O. Box 1000 (Kemistintie 3, Espoo), FI-02044 VTT, FINLAND. Tel. +358 20 722 111, Fax +358 20 722 7002	
Distribution (customer and VTT) European Commission 1 original ALARA Engineering 1 original VTT 1 original	
<i>The use of the name of the Technical Research Centre of Finland (VTT) in advertising or publication in part of this report is only permissible with written authorisation from the Technical Research Centre of Finland.</i>	

## Preface

The work discussed in the present report has been carried out as a part of the Work Package 3 of the project FP6036367 A deterministic model for corrosion and activity incorporation in nuclear power plants (ANTIOXI) in 2006 - 2008. The ANTIOXI project is a part of the EURATOM FP6 Programme “Advanced tools for nuclear safety assessment and component design”.

The ANTIOXI project in EURATOM FP6 concentrates on development of modelling tools for activity incorporation and corrosion phenomena into oxide films on construction materials in light water reactor environments.

The main funding source of the work has been the Sixth Framework Programme of the European Commission. The cooperation of the Members of the Advisory Board of the ANTIOXI project is gratefully acknowledged.

Espoo, Finland, 6th June 2008

Author

# Contents

1	Introduction	4
2	Plant data	6
2.1	PWR plants	9
2.1.1	Ringhals unit 2 (R2)	9
2.1.2	Ringhals unit 3 (R3)	18
2.1.3	Ringhals unit 4 (R4)	25
2.2	WWER plants	33
2.2.1	Loviisa unit 1 (LO1)	33
2.2.2	Loviisa unit 2 (LO2)	39
3	Analysis	47
3.1	Plant comparison	47
3.1.1	Co-58 and Co-60	47
3.1.2	Mn-54	49
3.1.3	Sb-122 and Sb-124	50
3.2	Influence of sampling system design	52
3.3	Corrosion release from Inconel	58
3.4	Influence of zinc	61
4	Summary and conclusions	64
	References	66

# 1 Introduction

The objective of the LWROXI/ANTIOXI<sup>1</sup> project is to develop a deterministic model for the build-up and properties of the oxide layers formed on LWR out-of-core primary system surfaces. The main focus in the development is to be able to model and predict the radioactivity build-up occurring on these surfaces. Work package 1 (WP-1) of the ANTIOXI project includes refinement and improvement of the earlier developed model for interaction between the oxide on a structural material and the coolant originating species. WP-2 contains quantifications of the surface complexation / deposition constants through high-temperature laboratory measurements. WP-3 includes critical evaluation of BWR, PWR and WWER reactor water and activity build-up data for validation and benchmarking of the developed model.

This report presents the WP-3 evaluation of PWR and WWER data. The PWRs specifically reviewed are the 3 Swedish Ringhals plants, and the WWERs are the two Finnish Loviisa plants. The reviewed plants and their main data are:

## 1. PWRs:

- a. Ringhals 2 (R2): 1975 - , 2660 MWt
  - i. Westinghouse design
  - ii. Steam Generator (SG) replacement 1989 (Inconel 600 à Inconel 690)
- b. Ringhals 3 (R3): 1981 - , 2775 MWt
  - i. Westinghouse design
  - ii. SG replacement 1995 (Inconel 600 à Inconel 690), a power uprate project is in progress
- c. Ringhals 4 (R4): 1983 - , 2775 MWt
  - i. Westinghouse design
  - ii. SG replacement planed to 2011 (Inconel 600 à will be changed to Inconel 690), a power uprate is planned

## 2. WWERs:

- a. Loviisa 1 (LO1): 1977 - , 1375 à 1500 MWt
  - i. Russian design
  - ii. Power uprated in 1998, SG tubes: stainless steel
- b. Loviisa 2 (LO2): 1981 - , 1375 à 1500 MWt
  - i. Russian design

---

<sup>1</sup> LWROXI was originally a joint Swedish/Finnish project sponsored by utilities and radiation protection authorities. The project has later been converted to the ANTIOXI project with support from the EU.

- ii. Power uprated in 1998, SG tubes: stainless steel, major primary circuit decontamination in 1994

A data review for each plant is presented in chapter 2. An analysis of the data is provided in chapter 3 discussing the influence of different water chemistry and other factors. The report ends with a summary and conclusions.

## 2 Plant data

Reactor water activity and chemistry data from the plants are based on the ordinary surveillance performed at the plants, and comprise typically weekly measuring campaigns. Reactor water activity and chemistry data covered in the present study are:

- Mn-54, Co-58, Co-60, Zn-65, Cr-51, Fe-59, Sb-122, Sb-124, Ag-110m
- Boron, Li, K, NH<sub>3</sub>
  - High temperature pH (pH<sub>300</sub>) calculated
- Fe, Zn, Ni, Cr, Co, Cu

Main data for treated activated corrosion products are presented in **Table 1**.

*Table 1: Half lives, decay constants, way of production and gamma yields for treated activated corrosion product.*

Nuclide	T <sub>½</sub>	λ [s <sup>-1</sup> ]	Production	γ [MeV/diss]
<b>Cr51</b>	27.7 d	2.90E-07	Cr50 (n,γ) Cr51	0.0326
<b>Mn54</b>	312.5 d	2.57E-08	Fe54 (n,p) Mn54	0.836
<b>Fe59</b>	45.1 d	1.78E-07	Fe58 (n,γ) Fe59	1.188
<b>Co58</b>	70.78 d	1.13E-07	Ni58 (n,p) Co58	0.977
<b>Co60</b>	5.27 y	4.17E-09	Co59 (n,γ) Co60	2.504
<b>Zn65</b>	244.3 d	3.28E-08	Zn64 (n,γ) Zn65	0.584
<b>Ag110m</b>	249.78 d	3.21E-08	Ag109 (n,γ) Ag110m	2.7623
<b>Sb122</b>	2.7 d	2.97E-06	Sb121 (n,γ) Sb122	0.441
<b>Sb124</b>	60.2 d	1.33E-07	Sb123 (n,γ) Sb124	1.857

The activity build-up on primary piping and SG tubing has already from the beginning of operation been followed-up by annual measurements during refuelling outages. Dose rates have been measured on a large number of locations as well as gamma scanning on selected locations to determine the contribution from different radio-nuclides. Standard locations are the large recirculation piping on both sides of the SGs (hot and cold legs), the manway covers to the SG water chambers and on the SG tubings<sup>2</sup>. Most locations are for stainless steel surfaces in contact with primary coolant except the Inconel SG tubing in the Ringhals PWRs.

<sup>2</sup> The activity on SG tubing is measured through the SG vessel wall, i.e. the shielding in the thick wall has to be accounted for.

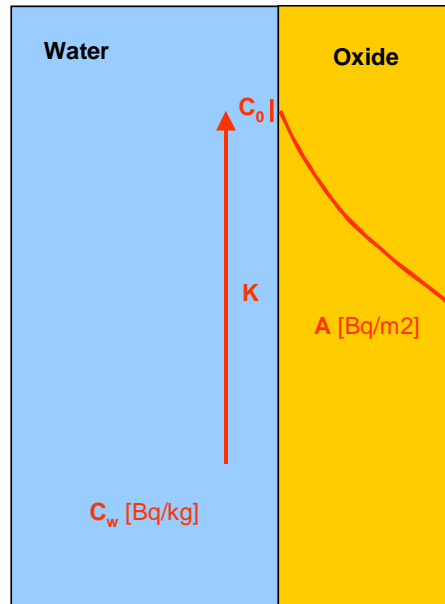


**Figure 1:** Evaluation model for LWR reactor water and system surface activity data

Plant radioactivity data has been evaluated in a generalised way based on a method developed earlier /1/. A similar method has also been used for corresponding evaluation of BWR data /2/. Primary system surface activity levels (A) were recalculated to activity concentrations in the outer oxide layer ( $C_0$ ) assuming an activity profile based on diffusion in the oxide layer, see **Figure 1**. An enrichment factor (K) has thereafter been determined by comparing the concentration in the outer oxide layer with the measured concentration of the same radionuclide in the reactor water, see **Eq. 1**.

$$\text{Eq. 1} \quad C_0 = K_1 \cdot C_w$$

where:

$C_0$  – Concentration in the outer part of oxide layer [Bq/kg]

$C_w$  – Concentration in reactor water during normal operation [Bq/kg]

$K_1$  – Enrichment factor with Model 1 [-]

The evaluation of the time dependent enrichment factor  $K(t)$  has been performed with a generalised expression from /1/ assuming that equilibrium<sup>3</sup> has been reached at every time between the reactor water conditions and the activity content in the oxide.

$$\text{Eq. 2} \quad K_1(t) = \frac{A(t) \cdot \sqrt{\lambda}}{C_w(t) \cdot \rho \cdot \sqrt{D}}$$

where:

$A(t)$  – Activity in oxide film [Bq/m<sup>2</sup>] at time “t”

$\lambda$  – Decay constant [s<sup>-1</sup>]

$\rho$  – Assumed density for oxide layer [=3500 kg m<sup>-3</sup>]

$D$  – Assumed average diffusion rate in oxide layer [=10<sup>-18</sup> m<sup>2</sup> s<sup>-1</sup>]

The above equation, prescribing that the activity build-up is occurring during normal operation of the plant, is designated “**Model 1**”. The equilibrium conditions are normally true for nuclides with rather short half-life compared to reactor operation of several

<sup>3</sup> Equilibrium conditions may be an approximation for long-lived nuclides such as Co-60 ( $T_{1/2} = 5.27$  y). However, after several years of operation at rather constant reactor water conditions also such nuclides are expected to be close to equilibrium in the oxide.



years, e.g. Co-58, but are a simplification in some cases for long-lived nuclides as e.g. Co-60, especially after a short time of activity build-up. Deviations in such cases are not corrected for but commented in the evaluation. The assumed values for oxide density and diffusion rate are based on earlier assessments /1/. Note that other values of the density and the diffusion rate will of course affect the value of the enrichment factor but only as a scaling factor.

An open question when discussing activity build-up in PWRs and VVERs is whether the build-up is mainly determined by the normal operation conditions with rather low reactor water activity or the rather large reactor water activity transient during the shutdown process. The high transient reactor water activity indicates a release of activity especially from the core region, but it can not be excluded that a considerable activity uptake is occurring for some nuclides on system surfaces during the transient. A separate model, **Model 2**, has therefore been used in parallel to the previous Model 1, where the activity build-up is assumed to be completely determined by the shutdown reactor water transient:

$$\text{Eq. 3} \quad K_2(t) = \frac{A(t)}{C_{\max}(t) \cdot \rho \cdot \delta}$$

where:

$C_{\max}(t)$  – Maximum shutdown reactor water activity transient [Bq/kg]

$\delta$  – Affected surface layer [assumed to be 0.1  $\mu\text{m}$ ]

Note that the activity build-up according to Model 1 is proportional to the square root of the decay constant, but not affected by the decay constant in the case of Model 2. A comparison of different radioisotopes with different decay constants, e.g. Co-58 and Co-60, may provide information whether the activity build-up is according to Model 1 or 2.

## 2.1 PWR plants

### 2.1.1 Ringhals unit 2 (R2)

R2 is the oldest Scandinavian PWR, which started operation already in 1975. The reactor water boron, Li and resulting high temperature pH are presented in **Table 2** and **Figure 2**. The measured concentrations of reactor water corrosion products and the evaluation of fuel cycle average values and maximum reactor transient concentrations are presented in **Table 3** and **Figure 3**<sup>4</sup>. The corresponding data for the activated corrosion products are presented **Table 4** and **Figure 4**.

The characteristics of the R2 plant from the water chemistry point of view can be summarised in the following way:

- The SG replacement in 1989 affected the corrosion product balance with initially quite high shutdown transient reactor water Ni. Pre-1989 chemistry data, i.e. during the period with the previous Inconel 600 SGs, are not covered in the present evaluation.
- The pH strategy was changed in the fuel cycle 1999-2000 from  $\text{pH}_{300} = 7.2$  to  $\text{pH}_{300} = 7.4$  during most of the cycle (but not at BOC due to the Li restrictions). This was accomplished by increasing the maximum reactor water Li from 2.2 ppm to 3.5 ppm. A further change was introduced in the fuel cycle 2006-2007 allowing reactor water Li >3.5 ppm to start up the fuel cycle with  $\text{pH}_{300} \approx 7.2$ , see **Figure 2**.
- The introduction of  $\text{pH}_{300} = 7.4$  operation has clearly affected the reactor water chemistry, especially in gradually reduced transients of Ni (**Figure 3**) as well as Co-58 (**Figure 4**).

---

<sup>4</sup> Two types of measurements are performed for the corrosion and activated corrosion products in the Ringhals PWRs:  
“**Grab**” – A water sample is taken and analysed in the laboratory. This method has normally rather high detection limits, and normal operation concentrations are in many cases below the detection limit. The method is, however, effective during the reactor shutdown transient when the concentrations are significantly increased.  
“**Integrated**” – Corrosion and activated corrosion products are accumulated on filter membranes (0.47  $\mu\text{m}$  for particles, cat ion membranes for soluble corrosion products). Totally up to 1000 litre of reactor water is filtered, which considerably lowers detection limits compared to grab samples. The filter membranes are brought to the laboratory, dissolved and analysed.

*Table 2: Ringhals 2–Boron, Li and high temperature – Annual data in beginning (BLX<sup>5</sup>) and end of cycle (EOC)*

Year	Boron [ppm]		Li [ppm]		pH <sub>300</sub>	
	BLX	EOC	BLX	EOC	BLX	EOC
1989	550	4	3.5	0.7	7.37	7.40
1990	760	15	2.5	0.6	7.20	7.30
1991	750	6	2.3	0.5	7.16	7.26
1992	960	8	2.9	0.5	7.04	7.24
1993	760	8	2.5	0.5	7.14	7.23
1994	400	20	2.4	0.6	7.20	7.20
1995	720	5	2.5	0.5	7.21	7.21
1996	720	6	2.6	0.5	7.20	7.22
1997	780	6	2.6	0.4	7.21	7.21
1998	720	6	2.4	0.5	7.18	7.20
1999	1000	60	2.7	0.7	7.08	7.21
2000	890	5	3.4	0.7	7.22	7.40
2001	900	5	3.4	0.7	7.24	7.41
2002	760	6	3.4	0.7	7.29	7.40
2003	980	5	3.7	0.7	7.21	7.41
2004	1140	16	3.5	0.7	7.16	7.40
2005	1000	250	3.4	0.8	7.20	7.42
2006	1350	5	3.8	0.8	7.10	7.41

---

<sup>5</sup> BLX – Beginning of cycle but after Xe equilibrium has been reached.

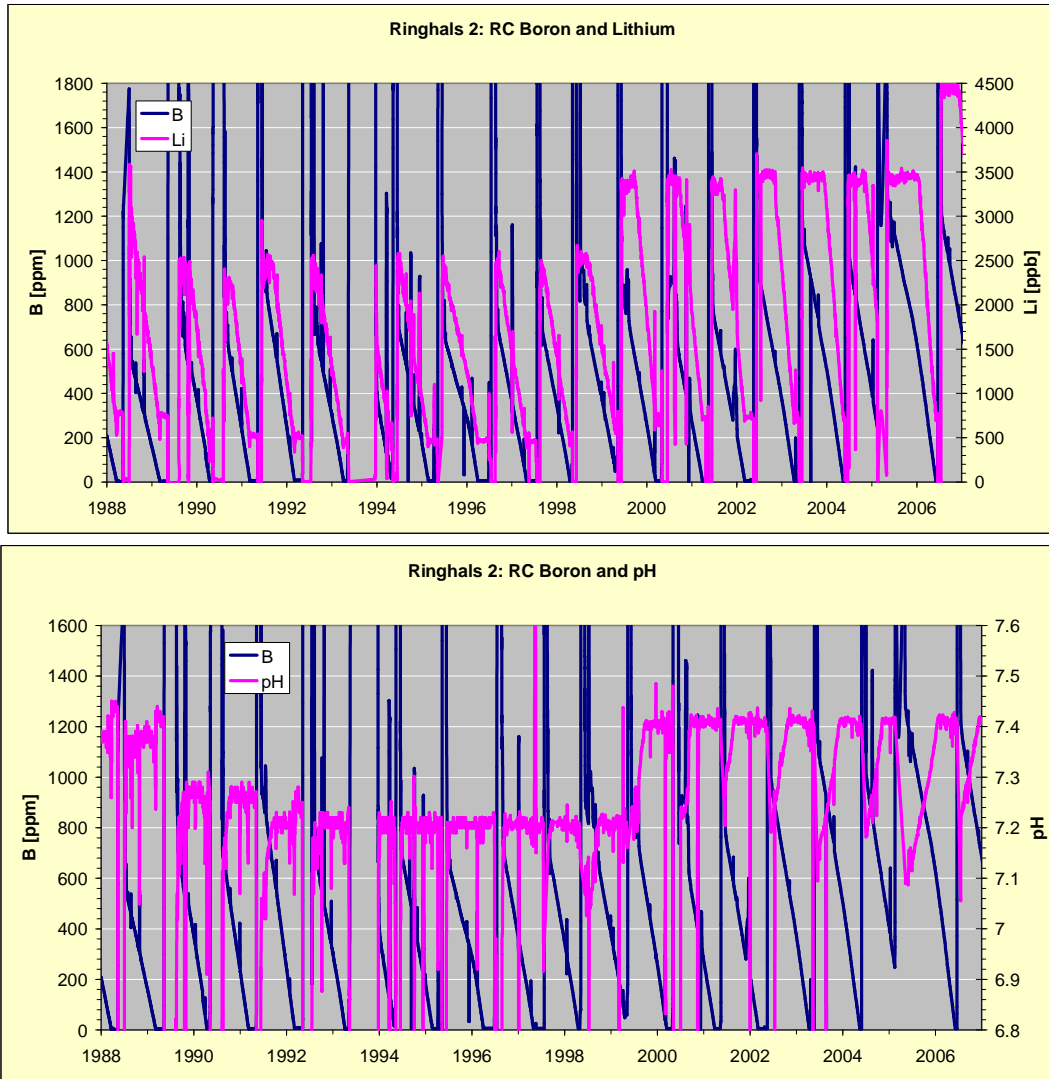


Figure 2: Ringhals 2 – Variation of reactor water boron, Li and pH<sub>300</sub>

Table 3: Ringhals 2– Corrosion product reactor water chemistry data – Annual average reactor operation and maximum shutdown transient data

Year	Fe [ppb]		Ni [ppb]		Co [ppb]		Zn [ppb]		Cr [ppb]		Mn [ppb]		Sb [ppb]	
	Average	Max	Average	Max	Average	Max	Average	Max	Average	Max	Average	Max	Average	Max
1989	1.0E+00	5.4E+02	1.0E-01	3.1E+03	2.5E-03	2.5E+00			1.0E-02	5.2E+01	3.0E-02	7.3E+01		
1990	1.0E+00	3.9E+02	1.0E-01	1.5E+03	2.5E-03	2.0E+00			1.0E-02	9.4E+00	3.0E-02	9.9E+02		
1991	1.0E+00	3.1E+02	1.0E-01	4.3E+03	2.5E-03	2.0E+00			1.0E-02	7.2E+01	3.0E-02	1.0E+03		
1992	1.0E+00	4.1E+02	1.0E-01	4.5E+03	2.5E-03				1.0E-02	3.1E+01	3.0E-02			
1993	1.0E+00		1.0E-01		2.5E-03				1.0E-02		3.0E-02	2.0E+01		
1994	1.0E+00	4.2E+02	1.0E-01	1.8E+03	2.5E-03				1.0E-02		3.0E-02			
1995	1.0E+00		1.0E-01		2.5E-03				1.0E-02		3.0E-02			
1996	1.0E+00	4.4E+02	1.0E-01	3.5E+03	2.5E-03	6.5E-01		3.8E+00	1.0E-02	4.1E+00	3.0E-02	4.4E+00		
1997	1.0E+00	3.2E+02	4.0E-02	3.0E+03	2.5E-03	9.0E-01	5.0E-03	1.5E+00	1.0E-02	3.1E+00	3.0E-02	7.1E+00		
1998	1.0E+00	3.9E+02	8.0E-02	2.8E+03	2.5E-03	1.4E+00	1.0E-02	1.2E+01	1.0E-02	7.2E+00	3.0E-02	5.7E+00		
1999	2.0E+00	3.7E+02	6.0E-02	2.8E+03	2.5E-03	1.0E+00	1.0E-02	8.8E+00	1.0E-02	1.1E+01	4.0E-02	2.3E+01		6.1E+01
2000	2.0E+00	5.4E+02	6.0E-02	2.8E+03	2.5E-03	4.1E+00	1.0E-02	5.9E+00	1.0E-02	8.1E+00	3.0E-02	1.1E+01	3.0E-02	4.0E+01
2001	2.0E+00	3.3E+02	6.0E-02	1.0E+03	2.5E-03	9.9E-01	1.0E-02	2.9E+00	1.0E-02	6.6E+00	3.0E-02	5.0E+00	2.0E-02	2.5E+00
2002	2.0E+00	4.1E+02	6.0E-02	2.2E+03	2.5E-03	5.0E-01	1.0E-02	8.0E-01	1.0E-02	5.5E+00	2.5E-02	4.6E+00	1.5E-02	7.5E-01
2003	2.0E+00	3.3E+02	1.5E-01	1.1E+03	2.5E-03	7.9E-01	1.0E-02	2.9E+00	1.0E-02	3.3E+00	2.5E-02	1.3E+01	1.3E-02	1.4E+00
2004	2.0E+00	2.0E+02	1.5E-01	6.7E+02	2.5E-03	1.1E+00	1.0E-02	3.4E+00	1.0E-02	3.0E+00	2.5E-02	1.0E+01	1.1E-02	1.9E+00
2005	2.0E+00	5.4E+01	1.5E-01	4.0E+02	2.5E-03	1.1E+00	1.0E-02	6.4E+00	1.0E-02	3.7E+00	2.0E-02	5.3E+00	1.1E-02	6.6E+00
2006	2.0E+00	3.3E+02	6.0E-02	4.1E+02	2.0E-03	1.0E+00	1.0E-02	3.4E+00	1.0E-02	4.1E+00	2.0E-02	6.2E+00	1.1E-02	3.3E+00

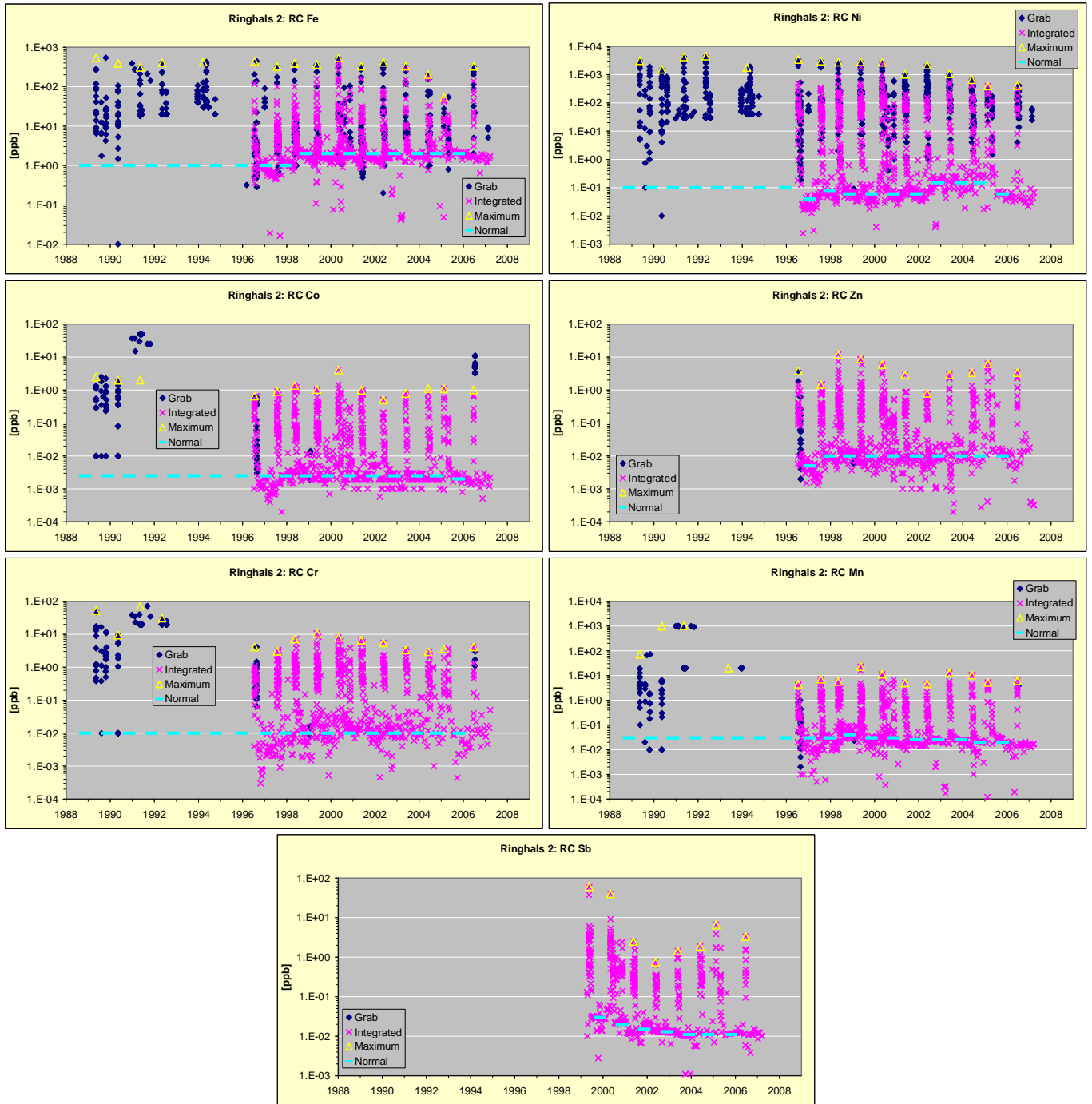
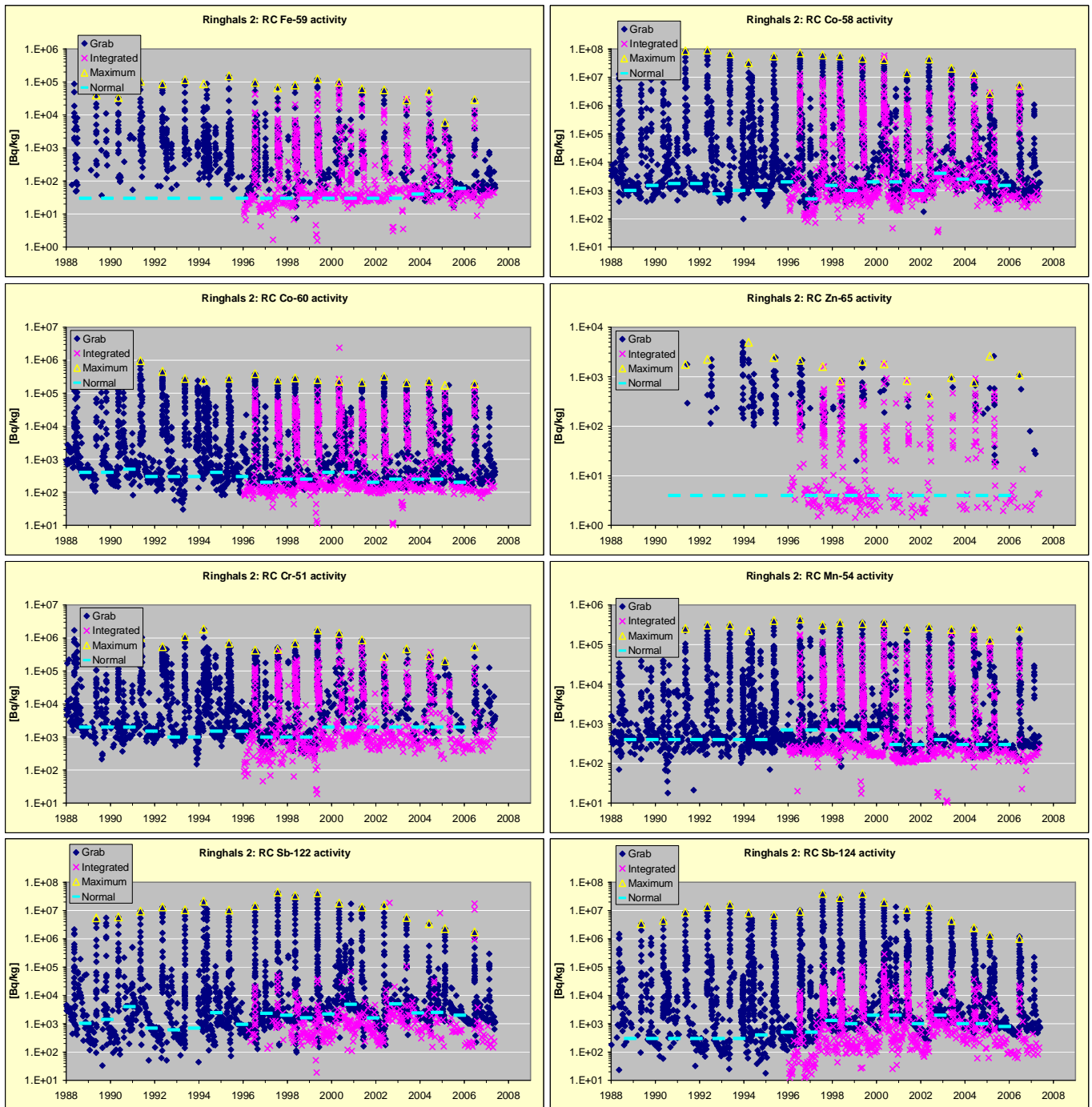


Figure 3: Ringhals 2 – Variation of corrosion products in reactor water

*Table 4: Ringhals 2 – Activated corrosion products in reactor water – Annual average reactor operation and maximum shutdown transient data*

Year	Fe59 [Bq/kg]		Co58 [Bq/kg]		Co60 [Bq/kg]		Zn65 [Bq/kg]		Cr51 [Bq/kg]		Mn54 [Bq/kg]		Sb122 [Bq/kg]		Sb124 [Bq/kg]	
	Average	Max	Average	Max	Average	Max	Average	Max	Average	Max	Average	Max	Average	Max	Average	Max
1989	30	4.0E+04	1000	1.7E+07	400	1.2E+06			2000	5.5E+05	400	4.1E+05	1030	5.5E+06	300	3.5E+06
1990	30	3.4E+04	1500	5.3E+07	400	1.4E+06			2000	4.3E+05	400	1.4E+05	1410	5.9E+06	300	4.5E+06
1991	30	1.1E+05	1750	8.5E+07	500	9.7E+05	4	1.8E+03	2000	1.0E+06	400	2.6E+05	4000	9.6E+06	300	8.7E+06
1992	30	8.7E+04	1750	9.1E+07	300	4.6E+05	4	2.2E+03	1500	5.5E+05	400	3.1E+05	700	1.3E+07	300	1.4E+07
1993	30	1.2E+05	750	6.7E+07	300	2.8E+05	4		1000	1.1E+06	400	3.1E+05	610	1.1E+07	300	1.6E+07
1994	30	8.8E+04	1000	3.2E+07	300	2.5E+05	4	5.0E+03	1000	1.9E+06	400	2.2E+05	700	2.1E+07	300	8.2E+06
1995	30	1.5E+05	1000	5.6E+07	400	2.8E+05	4	2.4E+03	1500	6.9E+05	400	4.1E+05	2450	1.0E+07	400	6.9E+06
1996	30	9.7E+04	2000	7.2E+07	300	3.9E+05	4	2.2E+03	1500	4.3E+05	700	4.4E+05	950	1.5E+07	500	9.3E+06
1997	30	6.6E+04	500	6.1E+07	200	2.5E+05	4	1.6E+03	1000	4.5E+05	700	3.1E+05	2330	4.5E+07	500	4.0E+07
1998	30	8.0E+04	1500	5.7E+07	250	2.9E+05	4	8.2E+02	1000	7.0E+05	700	3.6E+05	2000	3.4E+07	1300	2.9E+07
1999	30	1.2E+05	1000	4.7E+07	250	2.6E+05	4	2.0E+03	1000	1.7E+06	700	3.4E+05	1620	4.2E+07	1000	4.0E+07
2000	30	9.8E+04	2000	4.2E+07	400	2.3E+05	4	1.8E+03	2000	1.4E+06	700	3.6E+05	2200	1.8E+07	2000	2.0E+07
2001	30	6.2E+04	2000	1.4E+07	400	2.1E+05	4	8.3E+02	2000	8.8E+05	300	2.6E+05	4850	1.3E+07	2000	1.1E+07
2002	30	5.8E+04	1000	4.4E+07	200	3.3E+05	4	4.3E+02	2000	2.8E+05	300	2.8E+05	1600	1.6E+07	1000	1.4E+07
2003	30	2.9E+04	4000	2.1E+07	250	2.1E+05	4	9.6E+02	2000	4.7E+05	400	2.4E+05	5000	5.7E+06	2000	4.4E+06
2004	40	5.3E+04	2500	1.3E+07	250	2.3E+05	4	7.7E+02	2000	3.0E+05	300	2.6E+05	2400	3.4E+06	1000	2.5E+06
2005	50	5.9E+03	2000	2.6E+06	250	1.8E+05	4	2.6E+03	2000	2.0E+05	300	1.3E+05	2500	2.3E+06	1000	1.3E+06
2006	60	2.9E+04	1500	5.1E+06	200	1.9E+05	4	1.1E+03	2000	5.5E+05	300	2.6E+05	2000	1.8E+06	800	1.0E+06



*Figure 4: Ringhals 2 – Variation of activated corrosion products in reactor water*

The results from gamma scanning campaigns during shutdown periods are summarized in **Table 5**. The data are divided into activity on hot-side stainless steel, cold-side stainless steel, hot-side Inconel and cold-side Inconel. The stainless steel data are average based on several measurement locations, while the Inconel data are restricted on single measurement locations on the hot and cold side. It has to be also noted that the measurement of activity on the Inconel SG tubing is performed from the outside of the thick SG vessel. The considerable attenuation of photons in the pressure vessel wall reduces the detection limit of some nuclides, especially those with low-energy photons, e.g. Cr-51.

*Table 5: Ringhals 2– Gamma scanning data on hot and cold side stainless steel piping and Inconel SG tubing*

Stainless steel, hot leg [Bg/m <sup>2</sup> ]								
Year	Fe59	Co58	Co60	Zn65	Cr51	Mn54	Sb122	Sb124
1989		1.4E+09	5.1E+09					6.2E+07
1990		4.3E+09	6.0E+09			3.1E+08		
1991		4.8E+09	5.0E+09			2.4E+08		1.9E+08
1992		5.2E+09	5.2E+09					3.2E+08
1993	1.0E+08	6.0E+09	5.4E+09			7.7E+08		6.8E+08
1994	5.2E+07	2.7E+09	3.2E+09		2.1E+08	2.4E+08		9.3E+07
1995		3.7E+09	3.5E+09		3.0E+08	1.8E+08		1.8E+08
1996	3.1E+07	2.9E+09	2.2E+09			2.2E+08		4.6E+07
1997		3.7E+09	3.9E+09			2.0E+08		1.6E+09
1998	5.4E+07	5.5E+09	4.6E+09		3.0E+08	3.8E+08	4.4E+08	2.3E+08
1999		5.5E+09	5.0E+09			3.0E+08		3.6E+09
2000	4.7E+07	2.6E+09	2.4E+09		2.5E+08	2.5E+08		1.4E+08
2001	5.4E+07	2.6E+09	3.7E+09			2.2E+08		1.7E+09
2002	7.7E+07	2.9E+09	3.1E+09		1.4E+08	2.3E+08	1.1E+08	1.4E+08
2003	6.9E+07	5.4E+09	4.7E+09			2.9E+08	9.0E+08	1.1E+09
2004	6.1E+07	3.3E+09	2.5E+09		3.6E+08	3.1E+08	1.5E+08	1.8E+08
2005	3.9E+07	1.8E+09	2.4E+09			1.9E+08	7.9E+08	2.8E+08
2006	5.8E+07	1.6E+09	2.5E+09		4.7E+08	3.0E+08		1.0E+08
Stainless steel, cold leg [Bg/m <sup>2</sup> ]								
Year	Fe59	Co58	Co60	Zn65	Cr51	Mn54	Sb122	Sb124
1989		8.7E+08	4.4E+09					4.2E+07
1990		5.3E+09	6.7E+09			2.5E+08		1.3E+08
1991		4.1E+09	4.6E+09					1.2E+08
1992		9.5E+09	7.7E+09					4.2E+08
1993	1.3E+08	7.1E+09	5.9E+09			7.1E+08		8.7E+07
1994	9.1E+07	3.2E+09	5.9E+09		7.7E+08	4.3E+08		2.3E+08
1995	1.2E+08	5.8E+09	6.4E+09			6.7E+08		2.9E+08
1996	1.0E+08	5.0E+09	6.0E+09	7.3E+07		7.3E+08		1.3E+08
1997		8.2E+09	8.5E+09			3.8E+08		2.6E+09
1998	1.8E+08	7.5E+09	7.5E+09		7.1E+08	1.0E+09	1.2E+09	7.2E+08
1999		6.6E+09	5.7E+09			2.0E+08		3.2E+09
2000	1.1E+08	4.4E+09	4.0E+09		5.2E+08	3.7E+08		5.6E+08
2001	5.8E+07	2.8E+09	3.8E+09			1.6E+08		1.7E+09
2002	1.2E+08	4.2E+09	6.7E+09	2.2E+07	4.9E+08	9.8E+08	5.9E+08	7.6E+08
2003	4.7E+07	4.7E+09	3.7E+09			1.6E+08		7.6E+08
2004	1.3E+08	4.8E+09	6.0E+09		6.3E+08	8.3E+08	3.4E+08	2.6E+08
2005	5.1E+07	2.9E+09	3.9E+09			1.8E+08	5.8E+08	3.9E+08
2006	1.3E+08	2.1E+09	5.9E+09		4.4E+08	6.8E+08		2.4E+08
Inconel, hot tubes [Bg/m <sup>2</sup> ]								
Year	Fe59	Co58	Co60	Zn65	Cr51	Mn54	Sb122	Sb124
1989		1.4E+07	1.3E+07					1.1E+06
1990		2.6E+08	1.1E+08			1.4E+07		2.6E+07
1991		3.9E+08	3.0E+08					1.1E+07
1992		3.2E+08	3.9E+08					1.1E+07
1993		4.7E+08	2.1E+08					1.6E+07
1994		1.7E+08	2.7E+08					7.1E+06
1995		2.3E+08	2.3E+08					2.0E+07
1996		3.2E+08	3.6E+08			2.0E+07		1.1E+07
1997		4.3E+08	4.6E+08			2.8E+07		2.1E+08
1998		9.1E+08	6.7E+08			3.6E+07		1.2E+08
1999	9.1E+06	7.7E+08	5.6E+08			2.1E+07		3.0E+08
2000	5.5E+06	3.4E+08	3.4E+08			1.5E+07		1.3E+08
2001		3.4E+08	4.3E+08			2.3E+07		1.0E+08
2002	5.2E+06	4.8E+08	4.5E+08			2.5E+07		5.4E+07
2003	2.7E+06	5.8E+08	4.3E+08			2.2E+07		4.5E+07
2004	7.3E+06	6.1E+08	4.7E+08			2.4E+07		5.8E+07
2005	6.9E+06	4.1E+08	4.4E+08			2.7E+07		5.0E+07
2006	2.6E+06	1.6E+08	2.4E+08			1.1E+07		1.3E+07
Inconel, cold tubes [Bg/m <sup>2</sup> ]								
Year	Fe59	Co58	Co60	Zn65	Cr51	Mn54	Sb122	Sb124
1989		7.0E+06	1.2E+07					8.5E+05
1990		7.3E+08	3.7E+08					2.0E+07
1991		4.1E+08	1.6E+08					3.0E+07
1992		4.5E+08	2.2E+08			1.8E+07		4.0E+07
1993		5.9E+08	2.1E+08					5.3E+07
1994		3.3E+08	2.2E+08					
1995		3.6E+08	1.9E+08					4.2E+07
1996		6.1E+08	3.5E+08			1.4E+07		5.8E+07
1997		1.3E+09	5.3E+08			2.4E+07		3.1E+08
1998		2.3E+09	8.4E+08					4.0E+08
1999	1.4E+07	2.7E+09	7.9E+08			3.1E+07		6.2E+08
2000		9.9E+08	1.9E+08			2.3E+07		1.6E+08
2001		1.1E+09	7.5E+08			5.5E+07		3.5E+08
2002	1.2E+07	1.6E+09	8.2E+08			4.8E+07		1.9E+08
2003	1.3E+07	2.0E+09	9.5E+08			6.0E+07		1.6E+08
2004	1.2E+07	2.0E+09	9.9E+08	2.0E+07		5.7E+07		1.0E+08
2005	1.3E+07	1.2E+09	9.7E+08			6.2E+07	2.4E+08	1.0E+08
2006	6.9E+06	5.0E+08	5.2E+08			2.5E+07		3.8E+07



The above reactor water activities and gamma scanning data have been recalculated to surface enrichment factors  $K_1$  for the different activated corrosion products according to **Eq. 1** and **Eq. 2**, i.e. according to Model 1 assuming that the activity build-up is controlled by the normal operation conditions. The results are presented in **Figure 5**. The corresponding evaluation of  $K_2$  according to **Eq. 3**, i.e. according to Model 2 assuming that the activity build-up is controlled by the shutdown transient, is presented in **Figure 6**. The following observations are made:

- Several nuclides, Fe-59, Co-58, Co-60 and Zn-65, show quite similar and high  $K_1$  factors in spite of quite different half lives. This agreement is not seen in the case of the Model 2 evaluation, which is supporting that the activity build-up of these nuclides is occurring according to Model 1.
- Other nuclides, especially Mn-54 and Sb-124 show lower  $K_1$  values than the above nuclides. The agreement in Model 1 factor between the radioisotopes Sb-122 and Sb-124 with different half lives is poor, but good in the case of Model 2 evaluation. The agreement in the case of Model 2 in the case of the antimony isotopes supports that the activity build-up of these nuclides is mainly controlled by the shutdown transient. On the other hand, the Model 2 antimony factors show a rather large year-by-year variation, indicating that shutdown procedures may play a role in the actual activity build-up. The source of antimony is not precisely known.
- The stainless steel Model 1 factors for the cobalt isotopes are high, about a couple of order higher than the corresponding BWR factors /2/. It can be suspected that the reactor coolant concentrations in stainless steel systems with a large surface-to-volume ratio, e.g. thin sampling lines, will be affected by the large deposition rate. This is further discussed in later sections of the report.
- The Model 1 deposition rate is considerable lower on Inconel SG tubing compared to the stainless steel piping, about an order of magnitude. The effect of temperature is less, with only slightly higher values on the cold-side surfaces compared to the hot-side surfaces.

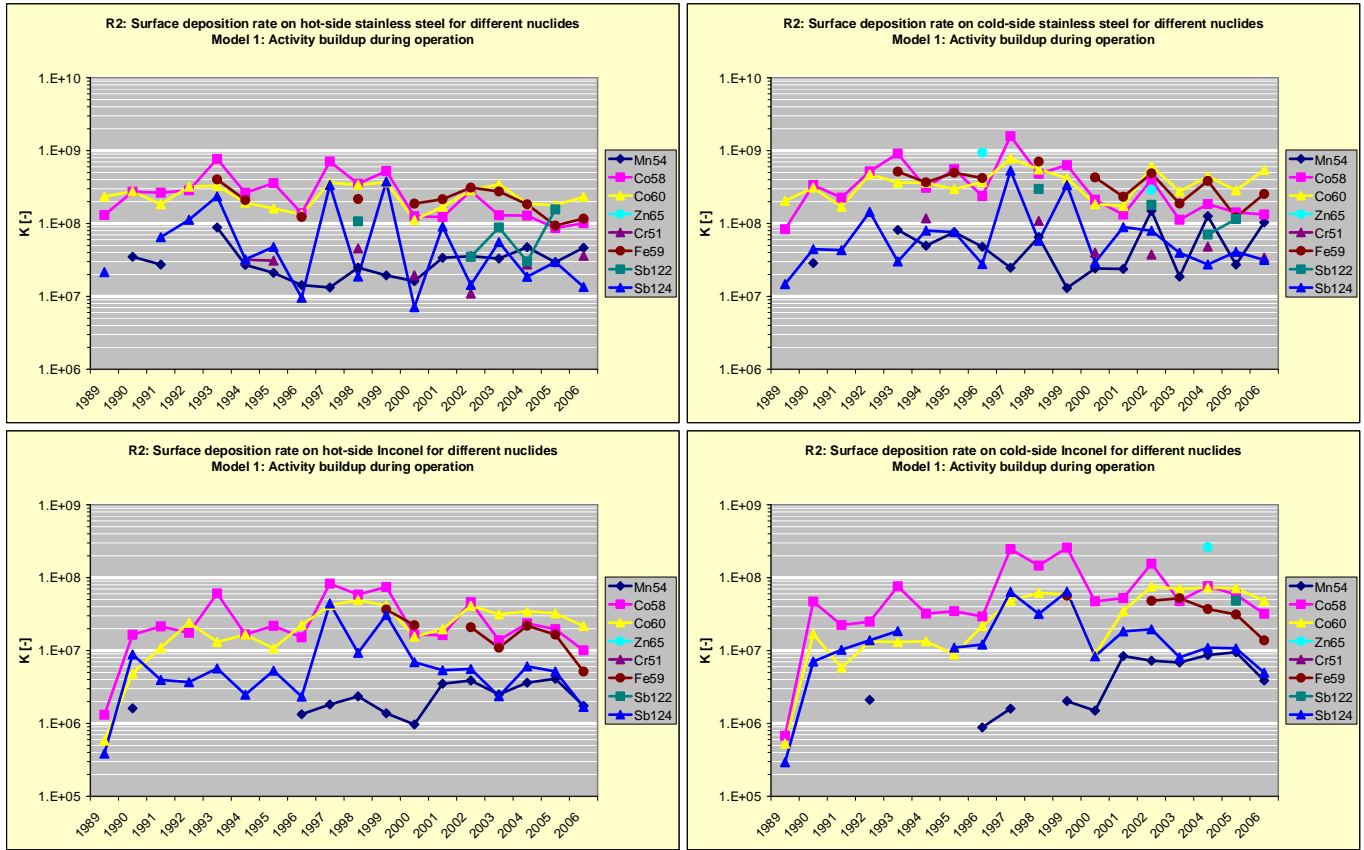


**Figure 5:** Ringhals 2: Normalized surface deposition rates during operation (Model 1) of different activated corrosion products for cold and hot side stainless steel and Inconel (Note: different log scales in the graphs)

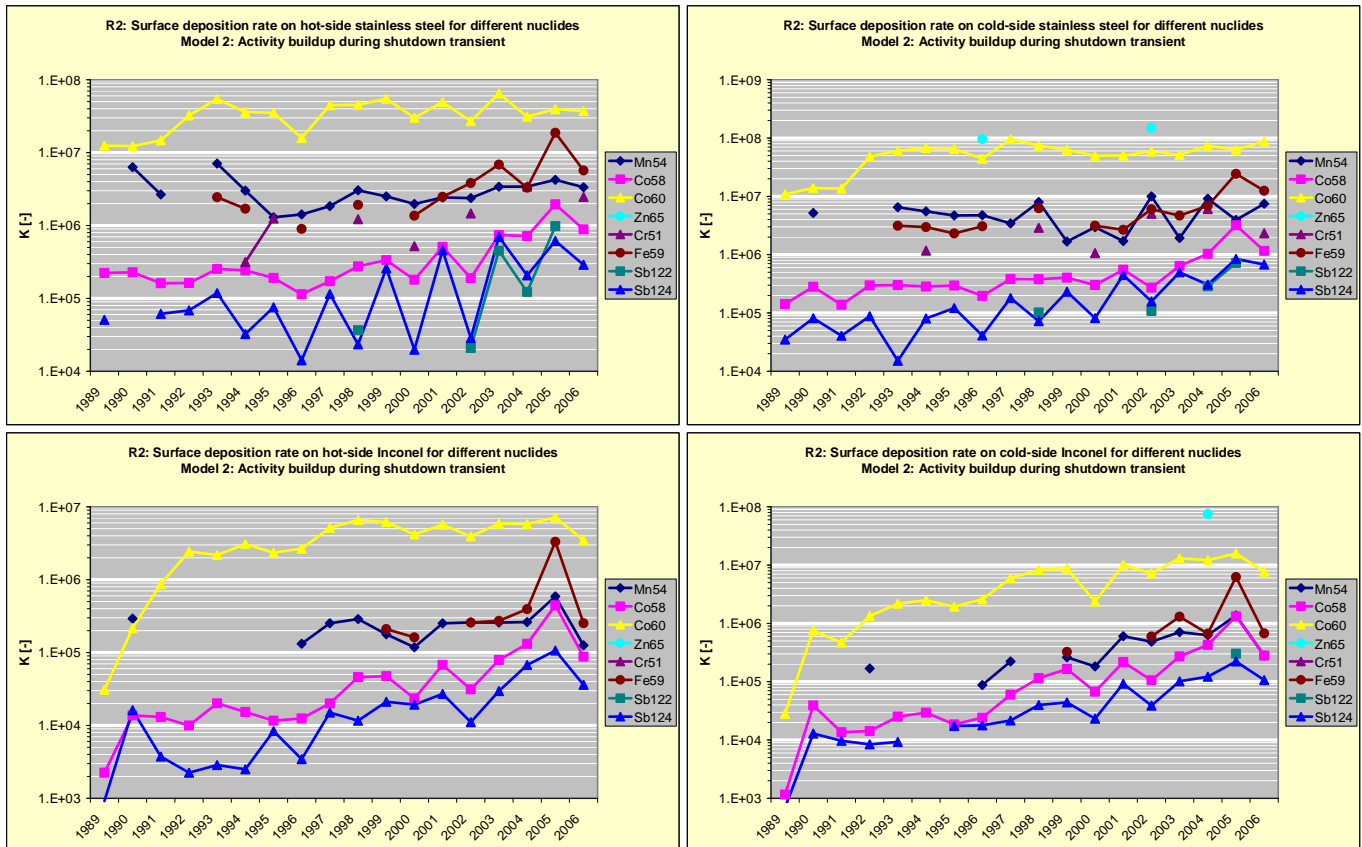


**Figure 6:** Ringhals 2: Normalized surface deposition rates during shutdown transient (Model 2) of different activated corrosion products for cold and hot side stainless steel and Inconel (Note: different log scales in the graphs)

### 2.1.2 Ringhals unit 3 (R3)

R3 started operation in 1981. The reactor water boron, Li and resulting high temperature pH are presented in **Table 6** and **Figure 7**. The measured concentrations of reactor water corrosion products<sup>6</sup> and the evaluation of fuel cycle average values and maximum reactor transient concentrations are presented in **Table 7** and **Figure 8**. The corresponding data for the activated corrosion products are presented **Table 8** and **Figure 9**.

The characteristics of the R3 plant from the water chemistry point of view can be summarised in the following way:

- The SG replacement in 1995 affected the corrosion product balance with initially quite high shutdown transient reactor water Ni. Pre-1995 chemistry data, i.e. during the period with the previous Inconel 600 SGs, are not covered in the present evaluation.
- The pH strategy was as in R2 changed in the fuel cycle 1999-2000 from  $\text{pH}_{300} = 7.2$  to  $\text{pH}_{300} = 7.4$  during most of the cycle (but not at BOC due to the Li restrictions). This was accomplished by increasing the maximum reactor water

<sup>6</sup> The availability of integrated reactor water corrosion product measurements has been much less than in the R2 plant.

Li from 2.2 ppm to 3.5 ppm. A further change was introduced in the fuel cycle 2006-2007 allowing reactor water Li >3.5 ppm to start up the fuel cycle with  $\text{pH}_{300} \approx 7.2$ , see **Figure 7**.

- The introduction of  $\text{pH}_{300} = 7.4$  operation has clearly affected the reactor water chemistry, especially in gradually reduced transients of Ni (**Figure 8**) and Co-58 (**Figure 9**).

**Table 6:** Ringhals 3–Boron, Li and high temperature pH – Annual data in beginning (BLX) and end of cycle (EOC)

Year	Boron [ppm]		Li [ppm]		pH	
	BLX	EOC	BLX	EOC	BLX	EOC
1996				0.5		
1997	930	3	2.2	0.5		7.25
1998	1010	10	2.2	0.7	7.01	7.25
1999	1150	6	2.3	0.7	6.95	7.40
2000	930	3	3.0	0.5	7.20	7.25
2001	950	3	3.3	0.7	7.20	7.40
2002	920	3	3.4	0.7	7.25	7.40
2003	930	3	3.4	0.7	7.22	7.40
2004	1150	15	3.4	0.7	7.12	7.40
2005	1220	4	3.4	0.7	7.10	7.40
2006	1250	17	3.4	0.7	7.10	7.40

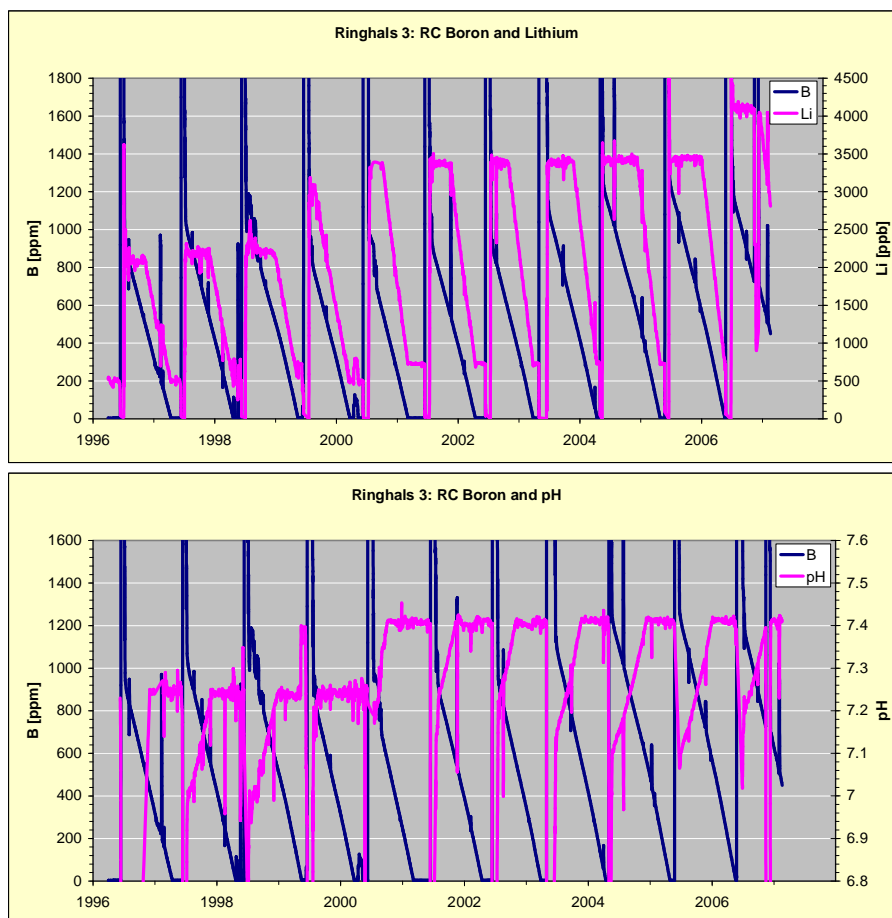


**Figure 7:** Ringhals 3 – Variation of reactor water boron, Li and  $\text{pH}_{300}$

*Table 7: Ringhals 3– Corrosion product reactor water chemistry data – Annual average reactor operation and maximum shutdown transient data*

Year	Fe [ppb]		Ni [ppb]		Co [ppb]		Zn [ppb]		Cr [ppb]		Mn [ppb]		Sb [ppb]	
	Average	Max	Average	Max	Average	Max	Average	Max	Average	Max	Average	Max	Average	Max
1992	1.5E+00	4.5E+02	1.0E-01	2.9E+03	1.5E-02	5.6E-01	2.0E-02	2.0E-02	3.0E-02	2.2E+01	5.0E-02		1.0E-01	
1993	1.5E+00	6.0E+02	1.0E-01	5.2E+03	1.5E-02		2.0E-02	1.3E+02	3.0E-02	1.7E+02	5.0E-02		1.0E-01	
1994	1.5E+00	7.6E+02	1.0E-01	3.8E+03	1.5E-02	4.0E-01	2.0E-02	7.6E+02	3.0E-02	1.8E+01	5.0E-02		1.0E-01	
1995	1.5E+00	6.0E+02	1.0E-01	2.6E+03	1.5E-02		2.0E-02	6.9E+01	3.0E-02	5.9E+01	5.0E-02		1.0E-01	
1996														
1997	1.5E+00	4.3E+02	1.0E-01	9.8E+03	1.5E-02	3.3E+00	2.0E-02	4.4E+01	3.0E-02	4.4E+01	5.0E-02		1.0E-01	
1998	1.5E+00	5.0E+02	1.0E-01	8.2E+03	1.5E-02	1.1E+00	2.0E-02	1.1E+02	3.0E-02	3.8E+01	5.0E-02		1.0E-01	
1999	1.5E+00	6.1E+02	1.0E-01	1.5E+04	1.5E-02	5.0E-01	2.0E-02	1.0E+01	3.0E-02	6.7E+01	5.0E-02		1.0E-01	
2000	1.5E+00		1.0E-01		1.5E-02	1.5E+00	2.0E-02	1.0E+01	3.0E-02	5.9E+01	5.0E-02		1.0E-01	
2001	1.5E+00	5.2E+01	1.0E-01		1.5E-02	1.5E+00	2.0E-02	1.1E+01	3.0E-02	2.8E+01	5.0E-02		1.0E-01	
2002	1.5E+00		1.0E-01		1.5E-02		2.0E-02		3.0E-02		5.0E-02		1.0E-01	

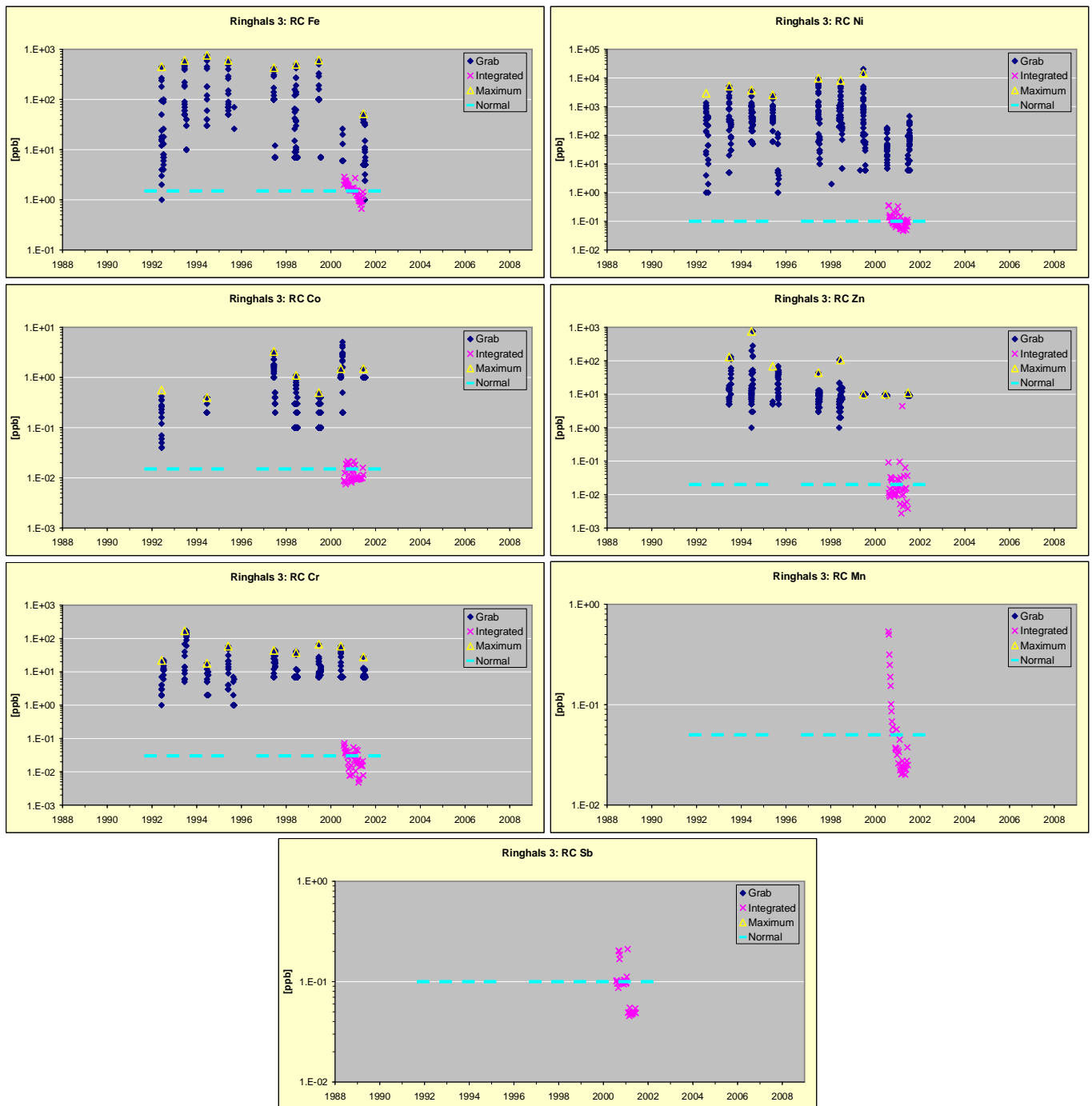


*Figure 8: Ringhals 3 – Variation of corrosion products in reactor water*

*Table 8: Ringhals 3 – Activated corrosion products in reactor water – Annual average reactor operation and maximum shutdown transient data*

Year	Fe59 [Bq/kg]		Co58 [Bq/kg]		Co60 [Bq/kg]		Zn65 [Bq/kg]		Cr51 [Bq/kg]		Mn54 [Bq/kg]		Sb122 [Bq/kg]		Sb124 [Bq/kg]	
	Average	Max	Average	Max	Average	Max	Average	Max	Average	Max	Average	Max	Average	Max	Average	Max
1989	50	8.5E+04	1500	8.3E+07	600	1.2E+06	4		500	1.9E+05	1000	2.0E+05	300	1.9E+06	200	2.0E+06
1990	50	4.6E+04	2000	5.9E+07	600	6.5E+05	4	1.3E+03	500	1.2E+06	1000	1.8E+05	300	1.3E+06	200	1.1E+06
1991	50	7.0E+04	4000	4.8E+07	600	6.0E+05	4	1.1E+03	2000	1.5E+06	750	2.4E+05	300	1.5E+05	200	4.5E+05
1992	50	1.3E+05	1000	2.6E+07	400	3.6E+05	4	1.7E+03	750	3.7E+05	650	3.4E+05	300	1.4E+06	200	7.9E+05
1993	50	2.2E+05	700	1.1E+08	500	8.3E+05	4	1.0E+02	500	1.3E+06	500	4.8E+05	300	2.1E+06	200	1.2E+06
1994	50	2.8E+05	1500	6.7E+07	400	1.1E+06	4	8.9E+02	500	8.6E+05	750	6.2E+05	200	1.2E+06	200	7.3E+05
1995	50	1.6E+05	4000	6.2E+07	400	3.9E+05	4	1.3E+03	1000	1.3E+06	650	3.7E+05	300	1.5E+06	200	7.9E+05
1996	50	1.6E+05	6000	1.4E+08	350	7.6E+05	4	2.1E+03	1000	1.3E+06	500	2.9E+05	500	1.5E+05	200	3.4E+05
1997	50	7.6E+04	10000	1.7E+08	350	5.0E+05	4	3.0E+03	1000	8.2E+05	500	2.0E+05	300	2.1E+05	200	1.5E+05
1998	50	8.8E+04	4000	1.4E+08	300	3.8E+05	4	3.7E+03	1000	1.8E+06	650	2.0E+05	300	6.3E+05	200	2.5E+05
1999	50	2.2E+05	15000	4.0E+08	300	8.2E+05	4	9.7E+03	1000	4.1E+06	650	3.6E+05	300	5.6E+05	200	4.5E+05
2000	50	1.4E+05	5000	7.0E+07	200	2.8E+05	4	2.1E+03	1000	2.0E+06	450	2.9E+05	300		200	2.7E+05
2001	50	1.2E+05	1000	7.4E+07	200	2.6E+05	4	8.8E+02	750	2.4E+05	350	2.9E+05	300		200	5.0E+05
2002	50	8.9E+04	3000	1.4E+08	200	4.6E+05	4	2.7E+03	750	1.4E+06	350	2.4E+05	300	9.5E+04	400	1.8E+06
2003	50	8.8E+04	5000	4.0E+07	250	2.9E+05	4	6.5E+03	750	1.6E+06	350	2.1E+05	500	8.6E+05	400	1.7E+06
2004	100	4.8E+04	3000	7.1E+06	250	1.6E+05	4	8.6E+02	750	2.8E+05	350	1.7E+05	500	1.4E+06	400	8.8E+05
2005	120	3.9E+04	1000	1.0E+07	200	1.7E+05	4	3.1E+03	750	6.7E+05	400	2.1E+05	500	1.9E+06	400	1.2E+06
2006	140	4.7E+04	700	7.9E+06	200	2.0E+05	4	8.1E+02	750	5.0E+05	500	2.6E+05	500	9.9E+05	400	1.0E+06

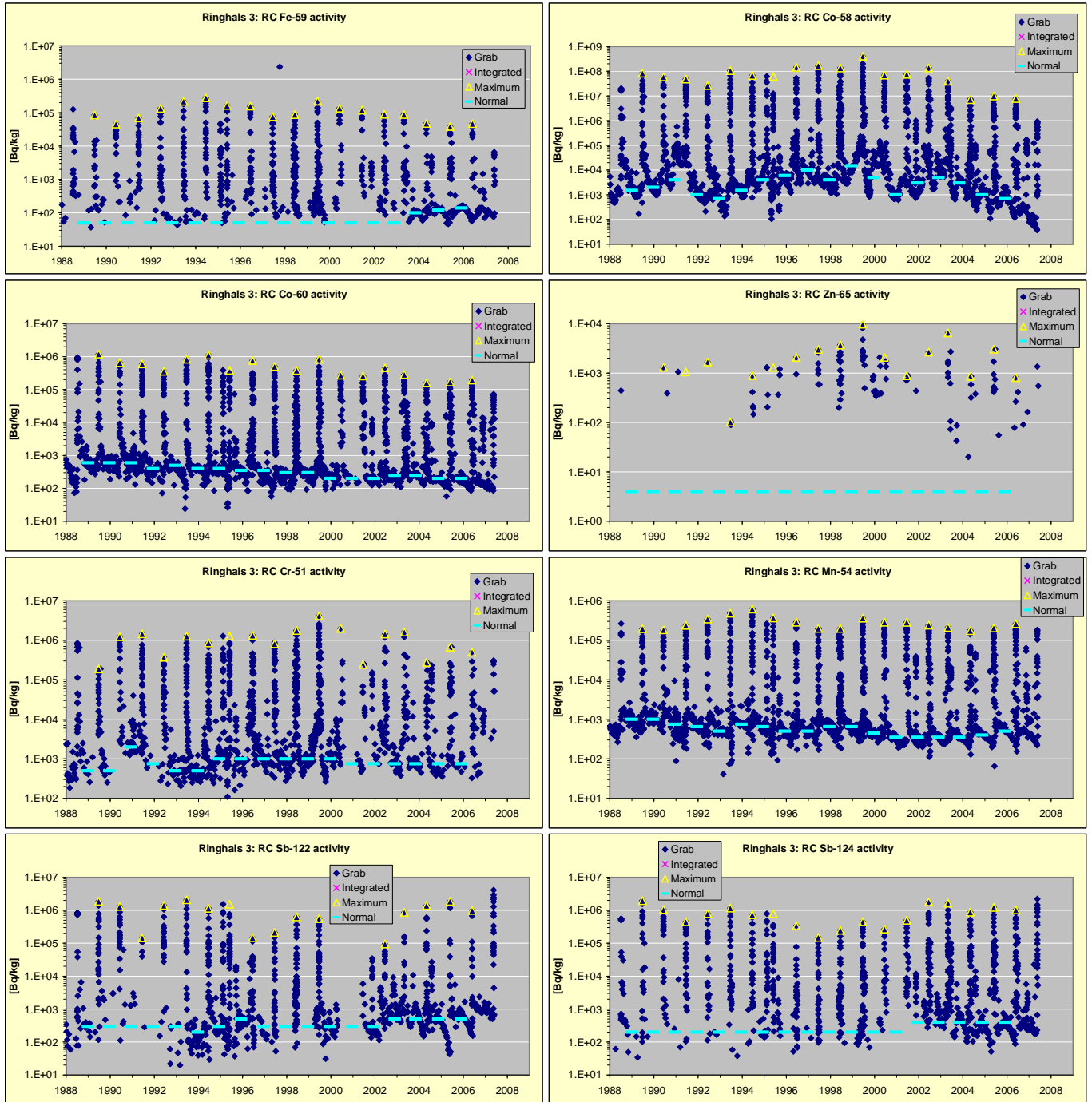


*Figure 9: Ringhals 3 – Variation of activated corrosion products in reactor water*

The results from gamma scanning campaigns during shutdown periods are summarized in **Table 9**. The data are divided into activity on hot-side stainless steel, cold-side stainless steel, hot-side Inconel and cold-side Inconel. The stainless steel data are averaged based on several measurement locations, while the Inconel data are restricted on single measurement locations on the hot and cold side. It has to be also noted that the measurement of activity on the Inconel SG tubing is performed from the outside of the thick SG vessel. The considerable attenuation of photons in the pressure vessel wall reduces the detection limit of some nuclides, especially those with low-energy photons, e.g. Cr-51.

*Table 9: Ringhals 3– Gamma scanning data on hot and cold side stainless steel piping and Inconel SG tubing*

Stainless steel, hot leg [Bg/m <sup>2</sup> ]								
Year	Fe59	Co58	Co60	Zn65	Cr51	Mn54	Sb122	Sb124
1989		1.2E+10	7.3E+09		8.1E+08	4.5E+08		3.6E+07
1990		9.5E+09	5.2E+09		4.2E+08	3.1E+08		
1991	7.2E+07	7.5E+09	5.6E+09		3.6E+08	3.2E+08		1.2E+07
1992	3.5E+07	4.6E+09	4.7E+09			2.9E+08		6.6E+06
1993	8.0E+07	8.4E+09	4.3E+09		3.6E+08	3.8E+08		9.7E+07
1994	1.2E+08	7.5E+09	4.2E+09		2.3E+08	4.1E+08		2.7E+07
1995		7.8E+09	5.2E+09			4.7E+08		4.6E+07
1996	7.6E+07	9.1E+09	1.3E+09		5.0E+08	3.0E+08		
1997	5.7E+07	8.9E+09	1.1E+09		3.0E+08	2.9E+08		
1998	6.7E+07	1.2E+10	1.4E+09		5.5E+08	4.2E+08		7.1E+06
1999	7.2E+07	8.5E+09	1.1E+09		1.3E+09	3.6E+08		9.5E+06
2000	5.2E+07	6.4E+09	1.7E+09			2.4E+08		1.3E+07
2001	4.4E+07	4.7E+09	9.4E+08		5.1E+08	2.5E+08		9.2E+06
2002	5.2E+07	5.7E+09	1.3E+09	1.3E+07	6.4E+08	1.9E+08		4.7E+07
2003	5.1E+07	5.2E+09	1.2E+09		6.7E+08	2.6E+08		3.5E+07
2004	6.3E+07	4.7E+09	1.9E+09			3.0E+08	1.8E+08	1.1E+08
2005	9.5E+07	3.7E+09	1.5E+09		3.4E+08	4.6E+08		4.2E+07
2006	8.6E+07	4.5E+09	2.0E+09	2.5E+07		4.7E+08		1.5E+08
Stainless steel, cold leg [Bg/m <sup>2</sup> ]								
Year	Fe59	Co58	Co60	Zn65	Cr51	Mn54	Sb122	Sb124
1989	6.3E+07	1.1E+10	6.5E+09		1.1E+09	3.3E+08		5.4E+07
1990	1.1E+08	1.1E+10	7.5E+09		1.0E+09	3.7E+08		
1991	1.1E+08	8.0E+09	5.9E+09		6.3E+08	3.4E+08		1.2E+07
1992		3.7E+09	4.0E+09		2.0E+08	2.1E+08		2.1E+07
1993	8.2E+07	6.8E+09	3.6E+09		1.1E+09	2.3E+08		7.7E+07
1994		6.4E+09	4.0E+09		3.3E+08	2.9E+08		2.4E+07
1995		7.6E+09	6.3E+09			3.9E+08		3.1E+07
1996	9.2E+07	8.1E+09	1.0E+09		4.4E+08	2.7E+08		
1997	8.3E+07	8.6E+09	9.4E+08		2.6E+08	3.1E+08		
1998	1.2E+08	1.5E+10	1.5E+09		6.4E+08	5.9E+08		9.5E+06
1999	1.3E+08	1.3E+10	1.3E+09		9.1E+08	7.1E+08		9.6E+06
2000	4.5E+07	7.6E+09	2.9E+09			1.8E+08		1.5E+07
2001	8.8E+07	7.7E+09	1.4E+09		4.6E+08	7.4E+08		2.0E+07
2002	4.6E+07	6.5E+09	2.1E+09			1.7E+08		4.1E+07
2003	1.5E+08	7.5E+09	2.1E+09		1.1E+09	9.1E+08		3.6E+07
2004	7.1E+07	5.1E+09	2.6E+09			2.4E+08		9.1E+07
2005	2.6E+08	5.1E+09	2.8E+09		1.0E+09	1.2E+09		3.1E+08
2006	1.2E+08	4.9E+09	2.6E+09	4.3E+07		3.8E+08		1.3E+08
Inconel, hot tubes [Bg/m <sup>2</sup> ]								
Year	Fe59	Co58	Co60	Zn65	Cr51	Mn54	Sb122	Sb124
1989		1.4E+08	1.5E+08					1.1E+06
1990		4.8E+08	4.4E+08					
1991		1.1E+08	1.5E+08					1.4E+06
1992		4.0E+08	5.7E+08					4.6E+06
1993		7.6E+08	3.3E+08					9.1E+06
1994		2.4E+08	3.2E+08					3.1E+06
1995		1.1E+08	2.1E+08					1.9E+06
1996	6.9E+06	5.5E+08	9.2E+07			1.6E+07		4.4E+05
1997	4.4E+06	7.0E+08	1.3E+08			1.8E+07		
1998	4.1E+06	3.3E+08	7.6E+07			9.0E+06		7.6E+05
1999	7.2E+06	2.5E+08	6.1E+07			6.5E+06		1.4E+06
2000		1.8E+08	6.0E+07			4.2E+06		4.7E+05
2001	2.7E+06	1.3E+08	4.8E+07			4.0E+06		1.8E+06
2002	4.9E+06	1.4E+08	4.8E+07			5.7E+06		5.4E+06
2003	3.7E+06	1.7E+08	5.6E+07		7.5E+09	7.0E+06		1.0E+07
2004	2.8E+06	1.0E+08	5.9E+07			5.7E+06		1.0E+07
2005	2.0E+06	8.8E+07	5.8E+07			7.4E+06		8.4E+06
2006	1.9E+06	7.1E+07	4.6E+07			7.9E+06		8.8E+06
Inconel, cold tubes [Bg/m <sup>2</sup> ]								
Year	Fe59	Co58	Co60	Zn65	Cr51	Mn54	Sb122	Sb124
1989		2.8E+08	1.6E+08					3.8E+06
1990		8.6E+08	4.2E+08					3.2E+06
1991		1.3E+08	9.4E+07					1.6E+06
1992		5.9E+08	4.2E+08					1.0E+07
1993		8.2E+08	3.5E+08			2.5E+07		1.1E+07
1994		7.5E+08	4.7E+08					1.4E+07
1995		2.7E+08	2.3E+08					7.6E+06
1996	2.4E+06	2.3E+08	3.4E+07			3.8E+06		3.9E+05
1997	3.6E+06	5.6E+08	6.3E+07			8.4E+06		8.0E+05
1998	3.2E+06	6.6E+08	7.0E+07			9.0E+06		1.8E+06
1999	2.9E+06	6.4E+08	6.8E+07			1.0E+07		1.9E+06
2000	3.4E+06	6.3E+08	9.7E+07			1.2E+07		4.1E+06
2001	2.1E+06	5.2E+08	9.2E+07			1.2E+07		3.6E+06
2002	3.6E+06	6.2E+08	1.0E+08			1.5E+07		1.1E+07
2003		6.3E+08	1.3E+08		8.1E+09	1.9E+07		8.9E+06
2004		3.1E+08	1.3E+08					9.7E+06
2005	4.4E+06	3.3E+08	1.4E+08			1.8E+07		1.1E+07
2006	4.8E+06	2.7E+08	1.2E+08	3.1E+06		1.6E+07		1.5E+07



The above reactor water activities and gamma scanning data have been recalculated to surface enrichment factors  $K_1$  for the different activated corrosion products according to **Eq. 1** and **Eq. 2**, i.e. according to Model 1 assuming that the activity build-up is controlled by the normal operation conditions. The results are presented in **Figure 10**. The corresponding evaluation of  $K_2$  according to **Eq. 3**, i.e. according to Model 2 assuming that the activity build-up is controlled by the shutdown transient, is presented in **Figure 11**. The observations made for R3 are very similar to those made for R2.

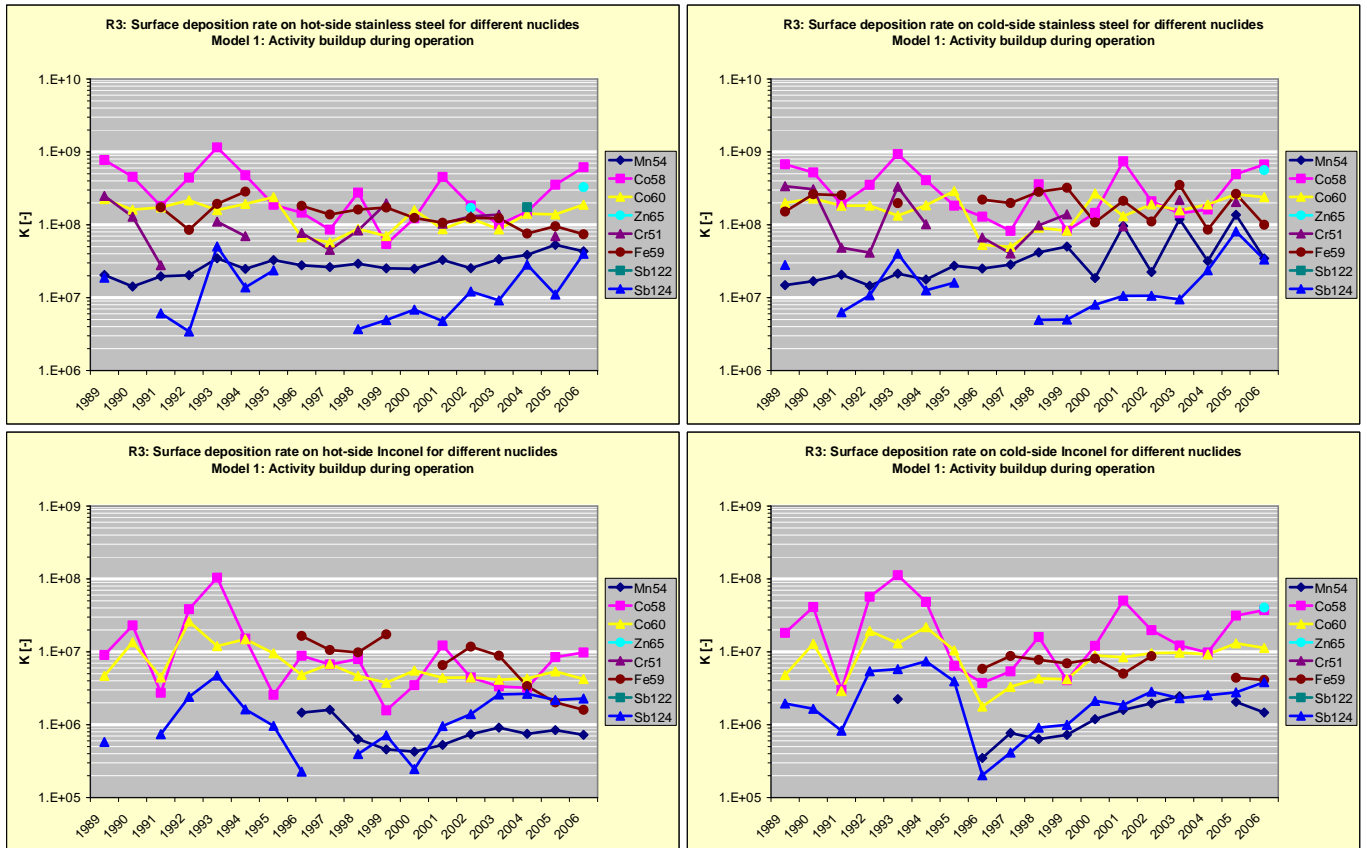


**Figure 10:** Ringhals 3: Normalized surface deposition rates during operation (Model 1) of different activated corrosion products for cold and hot side stainless steel and Inconel (Note: different log scales in the graphs)

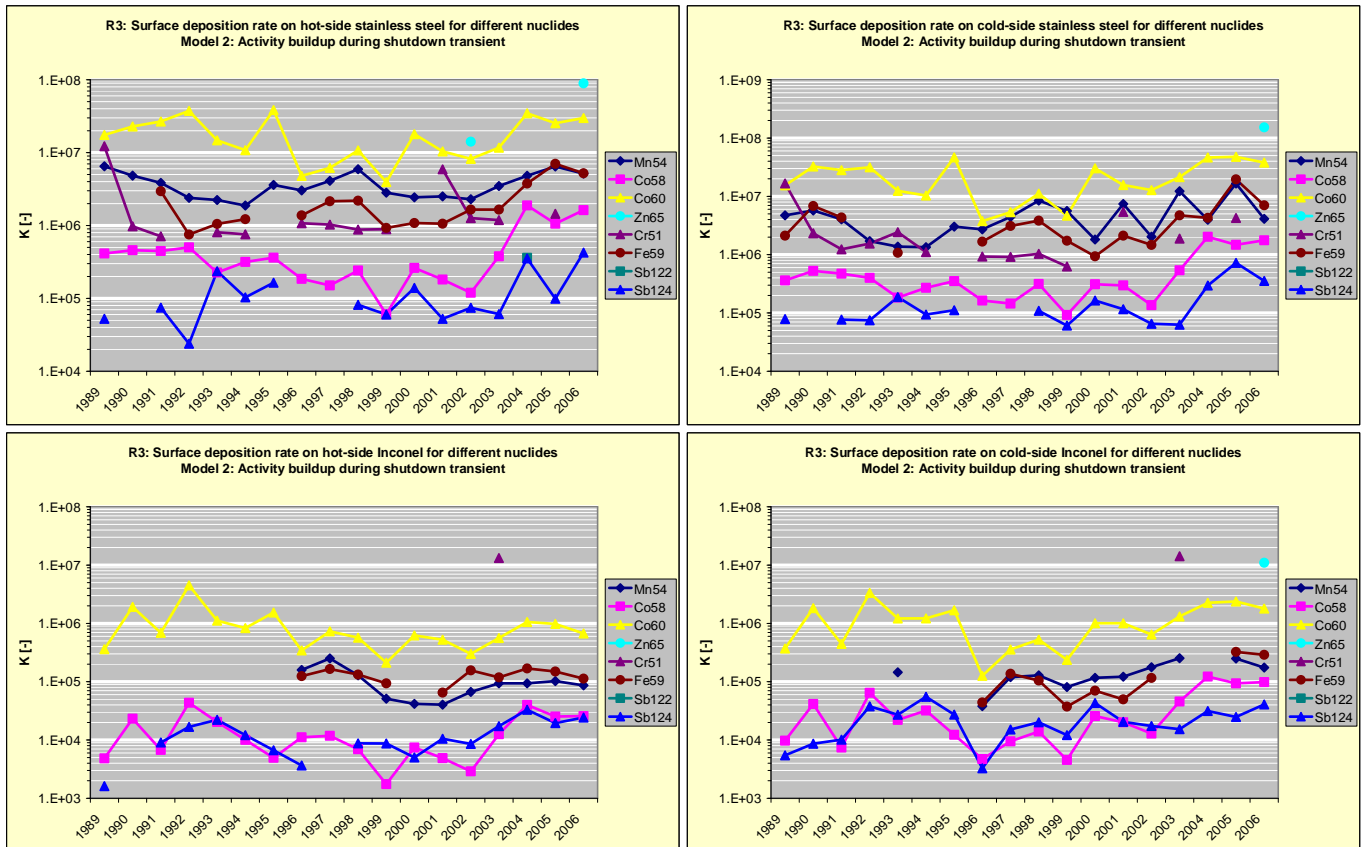


**Figure 11:** Ringhals 3: Normalized surface deposition rates during shutdown transient (Model 2) of different activated corrosion products for cold and hot side stainless steel and Inconel (Note: different log scales in the graphs)

### 2.1.3 Ringhals unit 4 (R4)

R4 is a sister plant to R3 and started operation in 1983. The reactor water boron, Li and resulting high temperature pH are presented in **Table 10** and **Figure 12**. The measured concentrations of reactor water corrosion products and the evaluation of fuel cycle average values and maximum reactor transient concentrations are presented in **Table 11** and **Figure 13**. The corresponding data for the activated corrosion products are presented **Table 12** and **Figure 14**.

The characteristics of the R4 plant from the water chemistry point of view can be summarised in the following way:

- The plant is still operating with the original Inconel 600 SGs, but a replacement is scheduled in 2011.
- The maximum reactor water Li level was increased to 3.5 ppm in R4 during the cycle 1999-2000 as in R2 and R3 but the R4 plant has stayed on a somewhat lower  $\text{pH}_{300} = 7.25$ . The reason for the operation with a lower  $\text{pH}_{300}$  than in R2 and R3 is that an increased pH results in an increase of leakage in the SG tubes (confirmed in a short-term test during the cycle 2005-2006).
- The operation with lower pH than in R2 and R3 affects the reactor water chemistry, especially in maintained rather high transients of Ni (**Figure 13**) and Co-58 (**Figure 14**).

**Table 10:** Ringhals 4–Boron, Li and high temperature – Annual data in beginning (BLX) and end of cycle (EOC)

Year	Boron [ppm]		Li [ppm]		pH	
	BXE	EOC	BXE	EOC	BXE	EOC
1996		3		0.5		
1997	830	3	2.2	0.5		7.25
1998	950	130	2.3	0.7	7.05	7.25
1999	1150	3	2.4	0.5	6.98	7.25
2000	810	100	3.2	0.7	7.23	7.25
2001	620	4	2.8	0.5	7.25	7.25
2002	920	3	3.0	0.5	7.15	7.25
2003	970	20	3.0	0.5	7.12	7.25
2004	1320	27	3.5	0.5	7.07	7.25
2005	1200	3	3.5	0.5	7.12	7.25
2006	1320	4	3.5	0.5	7.08	7.20

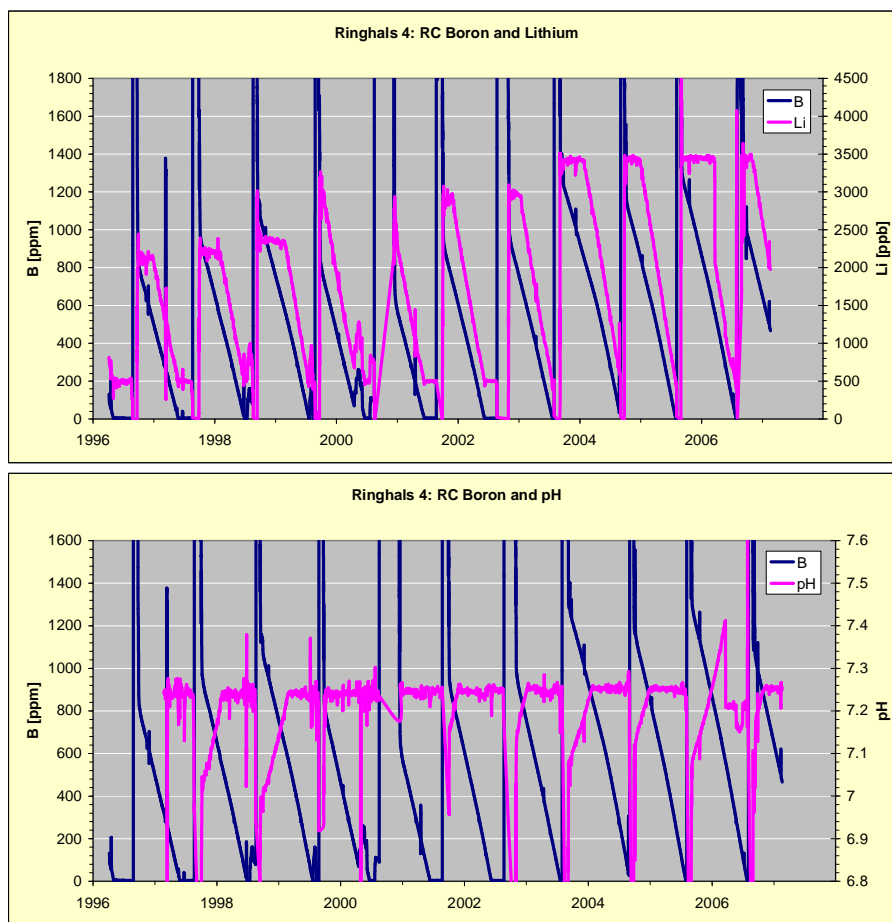


**Figure 12:** Ringhals 4 – Variation of reactor water boron, Li and pH<sub>300</sub>

*Table 11: Ringhals 4– Corrosion product reactor water chemistry data – Annual average reactor operation and maximum shutdown transient data*

Year	Fe [ppb]		Ni [ppb]		Co [ppb]		Zn [ppb]		Cr [ppb]		Mn [ppb]		Sb [ppb]	
	Average	Max	Average	Max	Average	Max	Average	Max	Average	Max	Average	Max	Average	Max
1992	1.5E+00	4.8E+02	7.0E-02	5.5E+03	1.0E-02	9.0E-01	2.0E-02	1.6E+02	1.5E-02	2.4E+01	5.0E-02			
1993	1.5E+00	4.8E+02	7.0E-02	5.5E+03	1.0E-02	9.0E-01	2.0E-02	1.6E+02	1.5E-02	2.4E+01	5.0E-02			
1994	1.5E+00	7.2E+02	7.0E-02	5.2E+03	1.0E-02		2.0E-02	7.2E+01	1.5E-02	1.1E+01	5.0E-02			
1995	1.5E+00	5.3E+02	7.0E-02	3.7E+03	1.0E-02		2.0E-02	3.5E+02	1.5E-02	4.0E+01	5.0E-02			
1996	1.5E+00		7.0E-02		1.0E-02		2.0E-02		1.5E-02		5.0E-02			
1997	1.5E+00	5.3E+02	7.0E-02	5.7E+03	1.0E-02	4.4E+00	2.0E-02	2.0E+01	1.5E-02	3.7E+01	5.0E-02			
1998	1.5E+00	5.0E+02	7.0E-02	5.9E+03	1.0E-02	1.9E+00	2.0E-02	7.6E+01	1.5E-02	4.6E+01	5.0E-02			
1999	1.5E+00	5.0E+02	7.0E-02	8.2E+03	1.0E-02	1.3E+00	2.0E-02	6.7E+01	1.5E-02	3.5E+01	5.0E-02			
2000	1.5E+00		7.0E-02		1.0E-02	1.0E+00	2.0E-02	3.0E+00	1.5E-02		5.0E-02			
2001	1.5E+00		7.0E-02		1.0E-02		2.0E-02		1.5E-02		5.0E-02			
2002	1.0E+00		7.0E-02		1.0E-02		2.0E-02		1.5E-02		5.0E-02			
2003	1.5E+00		7.0E-02		1.0E-02									
2004	1.5E+00		1.2E-01		1.0E-02									
2005	1.2E+00		7.0E-02		1.0E-02									
2006	1.0E+00		7.0E-02		1.0E-02									

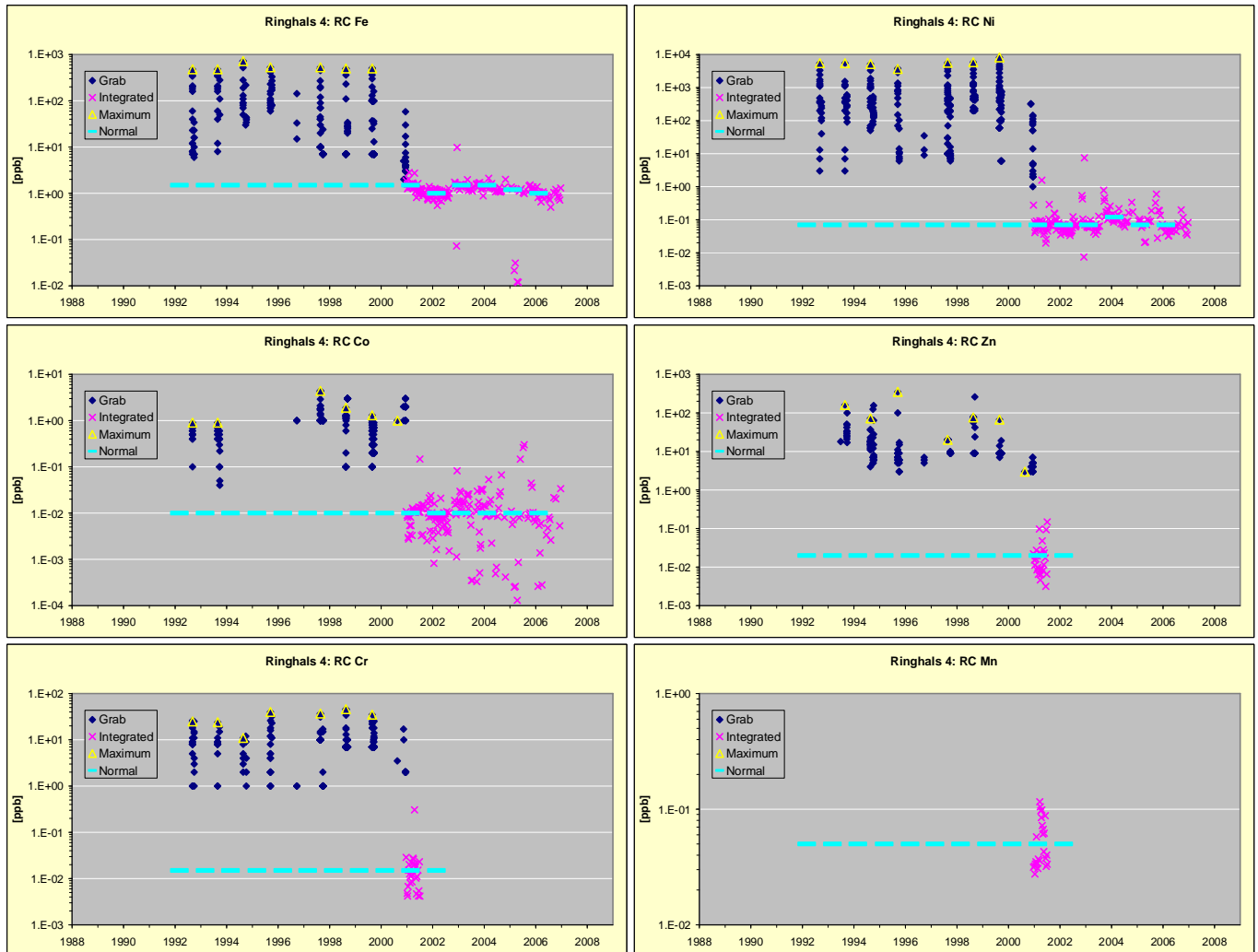


*Figure 13: Ringhals 4 – Variation of corrosion products in reactor water*

*Table 12: Ringhals 4 – Activated corrosion products in reactor water – Annual average reactor operation and maximum shutdown transient data*

Year	Fe59 [Bq/kg]		Co58 [Bq/kg]		Co60 [Bq/kg]		Zn65 [Bq/kg]		Cr51 [Bq/kg]		Mn54 [Bq/kg]		Sb122 [Bq/kg]		Sb124 [Bq/kg]	
	Average	Max	Average	Max	Average	Max	Average	Max	Average	Max	Average	Max	Average	Max	Average	Max
1989	30	8.0E+04	3000	6.7E+07	400	1.1E+06	10		700	3.2E+05	700	2.4E+05	200	2.4E+06	500	1.4E+06
1990	30	1.5E+04	3000	4.8E+07	300	4.4E+05	10	6.9E+03	700	2.7E+05	700	1.9E+05	200	3.5E+06	400	1.9E+06
1991	30	1.4E+05	2000	5.4E+07	200	6.0E+05	10	4.5E+03	700	6.9E+05	400	3.7E+05	200		300	4.6E+05
1992	30	1.3E+05	2000	1.0E+08	281	7.0E+05	10		700	3.5E+05	600	3.1E+05	400	2.9E+06	100	1.1E+06
1993	60	3.7E+05	2500	5.4E+07	267	6.6E+05	10	1.3E+03	650	9.1E+05	677	6.5E+05	100	1.2E+06	150	7.9E+05
1994	70	2.8E+05	1500	9.2E+07	291	6.2E+05	10	1.2E+03	600	7.4E+05	622	4.9E+05	150	1.7E+06	100	1.4E+06
1995	30	2.3E+05	1000	2.6E+07	200	3.0E+05	10	1.4E+03	700	1.4E+06	500	6.4E+05	150	5.4E+06	100	2.3E+06
1996	30	1.6E+05	1500	7.5E+07	203	4.2E+05	10	1.7E+03	650	1.2E+06	350	3.1E+05	400	1.6E+06	100	1.3E+06
1997	30	1.3E+05	1500	8.4E+07	151	4.2E+05	10	6.8E+02	604	6.2E+05	420	3.1E+05	300	2.7E+06	100	2.0E+06
1998	30	1.2E+05	1500	9.5E+07	142	3.7E+05	10	5.2E+02	450	9.0E+05	465	2.6E+05	250	1.6E+06	100	1.4E+06
1999	30	1.5E+05	2000	1.3E+08	155	4.3E+05	10	3.1E+03	300	5.5E+05	491	2.8E+05	150	2.5E+06	100	1.3E+06
2000	30	3.9E+04	2000	3.1E+07	133	1.5E+05	10		300		336	1.3E+05	200		100	5.2E+05
2001	30	8.0E+04	1000	7.5E+07	128	2.3E+05	10	4.1E+02	300	3.0E+05	250	2.5E+05	300		100	1.7E+06
2002	30	9.8E+04	1500	8.8E+07	96	2.8E+05	10	9.8E+02	300	2.2E+05	300	2.7E+05	200	1.2E+06	100	1.0E+06
2003	30	1.0E+05	1648	1.3E+08	146	3.0E+05	10		300	1.5E+05	400	2.3E+05	200		100	1.9E+06
2004	50	3.2E+05	3000	1.6E+08	162	4.5E+05	10		600	1.8E+05	400	2.8E+05	250		100	1.5E+06
2005	50	1.0E+05	3500	2.2E+08	150	5.0E+05	10		600	5.5E+05	400	3.1E+05	250		100	1.5E+06
2006	70	1.1E+05	3500	2.4E+08	150	5.6E+05	10		600	4.0E+05	400	3.9E+05	250		100	1.2E+06

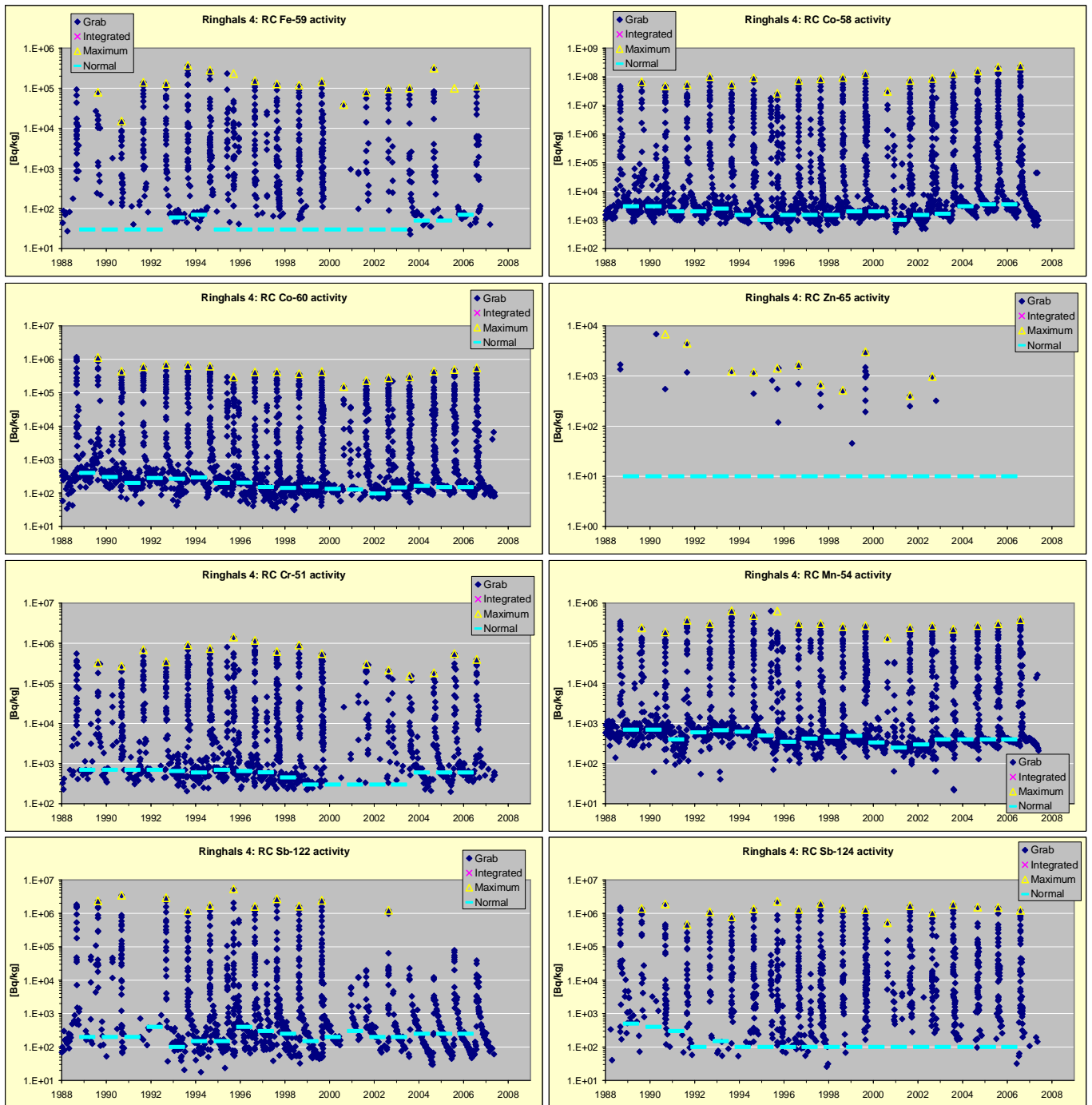


*Figure 14: Ringhals 4 – Variation of activated corrosion products in reactor water*

The results from gamma scanning campaigns during shutdown periods are summarized in **Table 13**. The data are divided into activity on hot-side stainless steel, cold-side stainless steel, hot-side Inconel and cold-side Inconel. The stainless steel data are averaged based on several measurement locations, while the Inconel data are restricted on single measurement locations on the hot and cold side. It has to be also noted that the measurement of activity on the Inconel SG tubing is performed from the outside of the thick SG vessel. The considerable attenuation of photons in the pressure vessel wall reduces the detection limit of some nuclides, especially those with low-energy photons, e.g. Cr-51.

*Table 13: Ringhals 4– Gamma scanning data on hot and cold side stainless steel piping and Inconel SG tubing*

Stainless steel, hot leg [Bg/m <sup>2</sup> ]								
Year	Fe59	Co58	Co60	Zn65	Cr51	Mn54	Sb122	Sb124
1989		8.2E+09	3.7E+09			3.8E+08		1.7E+07
1990		8.2E+09	3.3E+09			3.6E+08		
1991	7.8E+07	1.4E+10	3.1E+09			4.0E+08		2.1E+07
1992	9.3E+07	6.6E+09	2.3E+09			3.0E+08		
1993	5.4E+07	8.2E+09	2.6E+09		3.4E+08	3.2E+08		3.9E+07
1994	1.1E+08	9.4E+09	2.6E+09		1.9E+09	3.7E+08		5.4E+07
1995	3.6E+07	5.9E+09	2.3E+09		3.9E+08	2.3E+08		3.8E+07
1996	5.9E+07	6.0E+09	2.2E+09		2.8E+09	2.4E+08		4.4E+07
1997	6.9E+07	6.0E+09	1.9E+09		3.1E+08	2.1E+08		5.0E+07
1998	4.9E+07	8.4E+09	2.3E+09		5.9E+08	2.8E+08		5.6E+07
1999	6.2E+07	1.1E+10	1.5E+09		5.0E+08	2.4E+08	1.8E+08	4.0E+07
2000	3.1E+07	6.2E+09	1.3E+09	1.9E+07	3.6E+08	1.9E+08		5.4E+07
2001	4.8E+07	2.5E+09	8.1E+08			7.9E+07		5.0E+07
2002	5.2E+07	6.3E+09	8.0E+08		3.2E+08	1.5E+08		2.3E+07
2003	4.5E+07	6.2E+09	7.6E+08		7.9E+08	1.5E+08	1.1E+08	4.4E+07
2004	4.4E+07	5.9E+09	7.1E+08		4.3E+08	1.3E+08		2.4E+07
2005	6.3E+07	6.2E+09	7.5E+08		3.5E+08	1.5E+08		3.3E+07
2006	4.3E+07	4.4E+09	5.5E+08			9.7E+07		1.5E+07
Stainless steel, cold leg [Bg/m <sup>2</sup> ]								
Year	Fe59	Co58	Co60	Zn65	Cr51	Mn54	Sb122	Sb124
1989		7.7E+09	3.6E+09		3.7E+08	3.1E+08		9.3E+06
1990		6.5E+09	2.9E+09			2.4E+08		
1991	5.5E+07	1.1E+10	2.9E+09		3.6E+08	2.6E+08		2.1E+07
1992		6.6E+09	2.5E+09			2.0E+08		
1993	6.4E+07	7.3E+09	2.5E+09		7.3E+08	2.7E+08		3.1E+07
1994	9.8E+07	5.6E+09	2.5E+09		1.4E+09	2.5E+08		4.9E+07
1995		4.7E+09	2.8E+09		4.6E+08	2.4E+08		3.9E+07
1996	2.2E+07	5.0E+09	2.6E+09		5.2E+08	2.3E+08		4.0E+07
1997	5.2E+07	5.0E+09	1.9E+09		3.3E+08	2.3E+08		5.3E+07
1998	4.1E+07	7.4E+09	2.1E+09		3.2E+08	2.2E+08		4.3E+07
1999	3.7E+07	7.3E+09	1.9E+09		2.9E+08	2.0E+08	2.3E+08	3.6E+07
2000	4.2E+07	4.9E+09	1.8E+09	3.7E+06	3.4E+08	1.8E+08		5.0E+07
2001	1.6E+07	1.4E+09	4.6E+08			3.2E+07		2.7E+07
2002	1.3E+07	5.7E+09	9.7E+08			1.2E+08		1.2E+07
2003	4.7E+07	5.9E+09	1.0E+09		7.7E+08	1.4E+08	1.3E+08	5.0E+07
2004	3.2E+07	5.6E+09	7.9E+08		6.2E+08	1.2E+08		2.8E+07
2005	4.2E+07	7.0E+09	8.2E+08		4.1E+08	1.3E+08		3.7E+07
2006	4.1E+07	5.8E+09	7.1E+08			1.2E+08		2.4E+07
Inconel, hot tubes [Bg/m <sup>2</sup> ]								
Year	Fe59	Co58	Co60	Zn65	Cr51	Mn54	Sb122	Sb124
1989		9.7E+07	6.7E+07					6.1E+05
1990		4.0E+08	2.5E+08					
1991		6.4E+08	3.0E+08					
1992		4.4E+08	2.5E+08					3.6E+06
1993		4.7E+08	2.7E+08					4.6E+06
1994		5.2E+08	2.7E+08					5.2E+06
1995		2.3E+08	2.0E+08			1.1E+07		4.0E+06
1996	4.8E+06	3.0E+08	1.9E+08			9.3E+06		5.0E+06
1997	4.1E+06	2.6E+08	1.6E+08			6.3E+06		4.5E+06
1998	2.4E+06	2.5E+08	1.2E+08			3.5E+06		3.2E+06
1999	3.1E+06	2.7E+08	1.0E+08			3.2E+06		1.8E+06
2000		1.1E+08	5.6E+07					2.2E+06
2001		1.2E+08	5.4E+07					2.7E+06
2002		1.2E+08	4.4E+07					1.5E+06
2003	2.8E+06	2.6E+08	7.6E+07			3.1E+06		3.3E+06
2004	1.8E+06	2.0E+08	4.4E+07			2.2E+06		1.4E+06
2005	3.4E+06	3.5E+08	6.4E+07			3.4E+06		2.6E+06
2006	3.1E+06	4.6E+08	6.1E+07			4.8E+06		1.9E+06
Inconel, cold tubes [Bg/m <sup>2</sup> ]								
Year	Fe59	Co58	Co60	Zn65	Cr51	Mn54	Sb122	Sb124
1989		1.5E+08	5.9E+07					3.5E+06
1990		8.1E+08	1.5E+08			1.9E+07		
1991		6.6E+08	1.5E+08					5.1E+06
1992		5.8E+08	1.5E+08					9.8E+06
1993	5.8E+06	4.4E+08	1.4E+08					1.2E+07
1994	5.4E+06	7.4E+08	2.0E+08					2.0E+07
1995		6.5E+08	2.4E+08					2.8E+07
1996	4.1E+06	7.9E+08	2.4E+08			1.3E+07		2.3E+07
1997	4.8E+06	7.9E+08	2.3E+08			1.2E+07		2.1E+07
1998	4.7E+06	1.1E+09	2.4E+08			8.7E+06		1.9E+07
1999	6.0E+06	1.7E+09	2.6E+08			1.3E+07		1.9E+07
2000	3.5E+06	7.9E+08	2.1E+08			7.8E+06		2.0E+07
2001	3.1E+06	8.0E+08	1.6E+08			7.5E+06		2.2E+07
2002	4.3E+06	1.3E+09	1.9E+08			8.4E+06		1.5E+07
2003	5.7E+06	1.4E+09	1.7E+08			1.1E+07		2.1E+07
2004	6.2E+06	2.0E+09	1.7E+08			1.1E+07		1.7E+07
2005	6.4E+06	2.0E+09	1.7E+08			1.3E+07		1.9E+07
2006	6.5E+06	2.6E+09	1.7E+08			1.5E+07		1.5E+07

The above reactor water activities and gamma scanning data have been recalculated to surface enrichment factors  $K_1$  for the different activated corrosion products according to **Eq. 1** and **Eq. 2**, i.e. according to Model 1 assuming that the activity build-up is controlled by the normal operation conditions. The results are presented in **Figure 15**. The corresponding evaluation of  $K_2$  according to **Eq. 3**, i.e. according to Model 2 assuming that the activity build-up is controlled by the shutdown transient, is presented in **Figure 16**. The observations made for R4 are very similar to those made for R2 and R3.

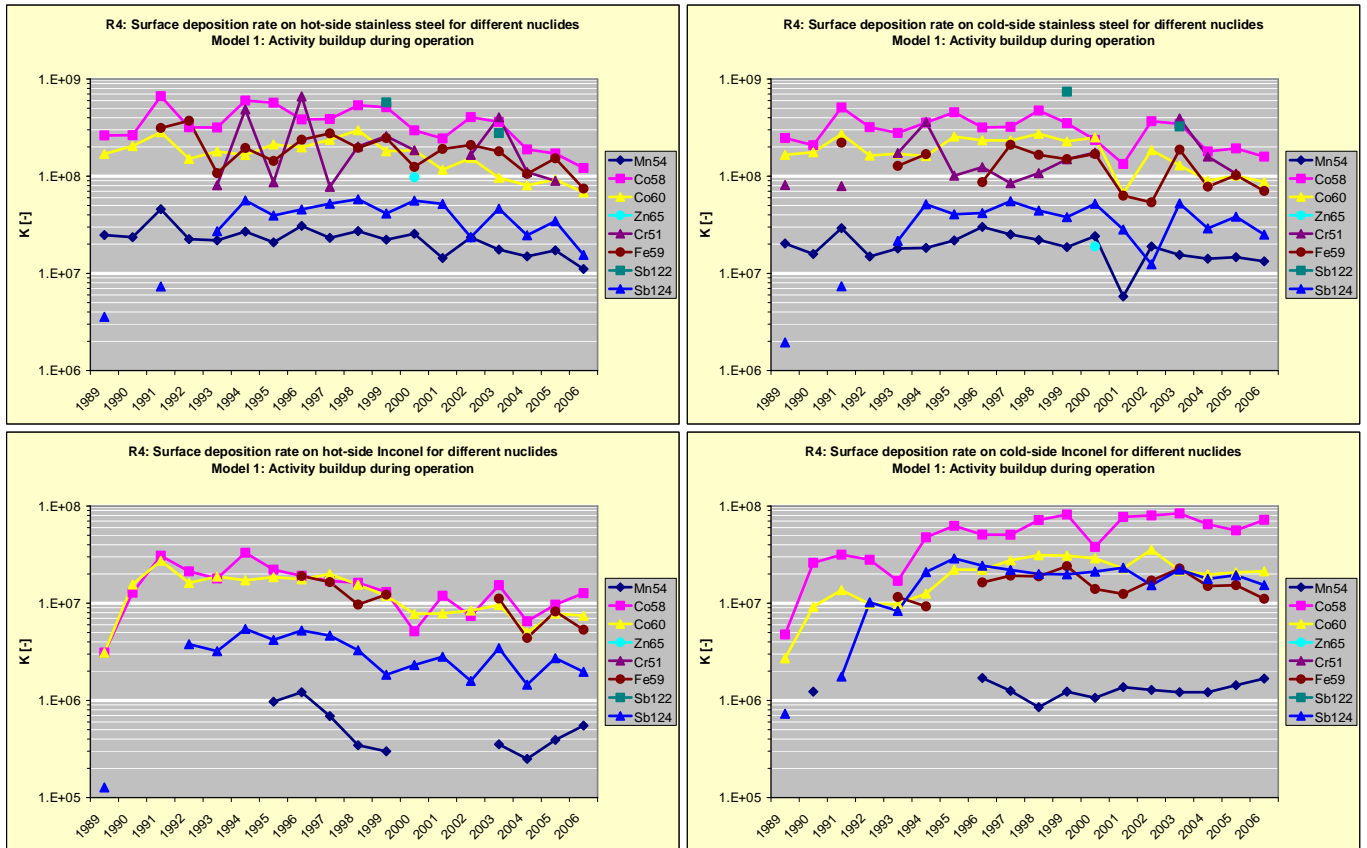


**Figure 15:** Ringhals 4: Normalized surface deposition rates during operation (Model 1) of different activated corrosion products for cold and hot side stainless steel and Inconel (Note: different log scales in the graphs)



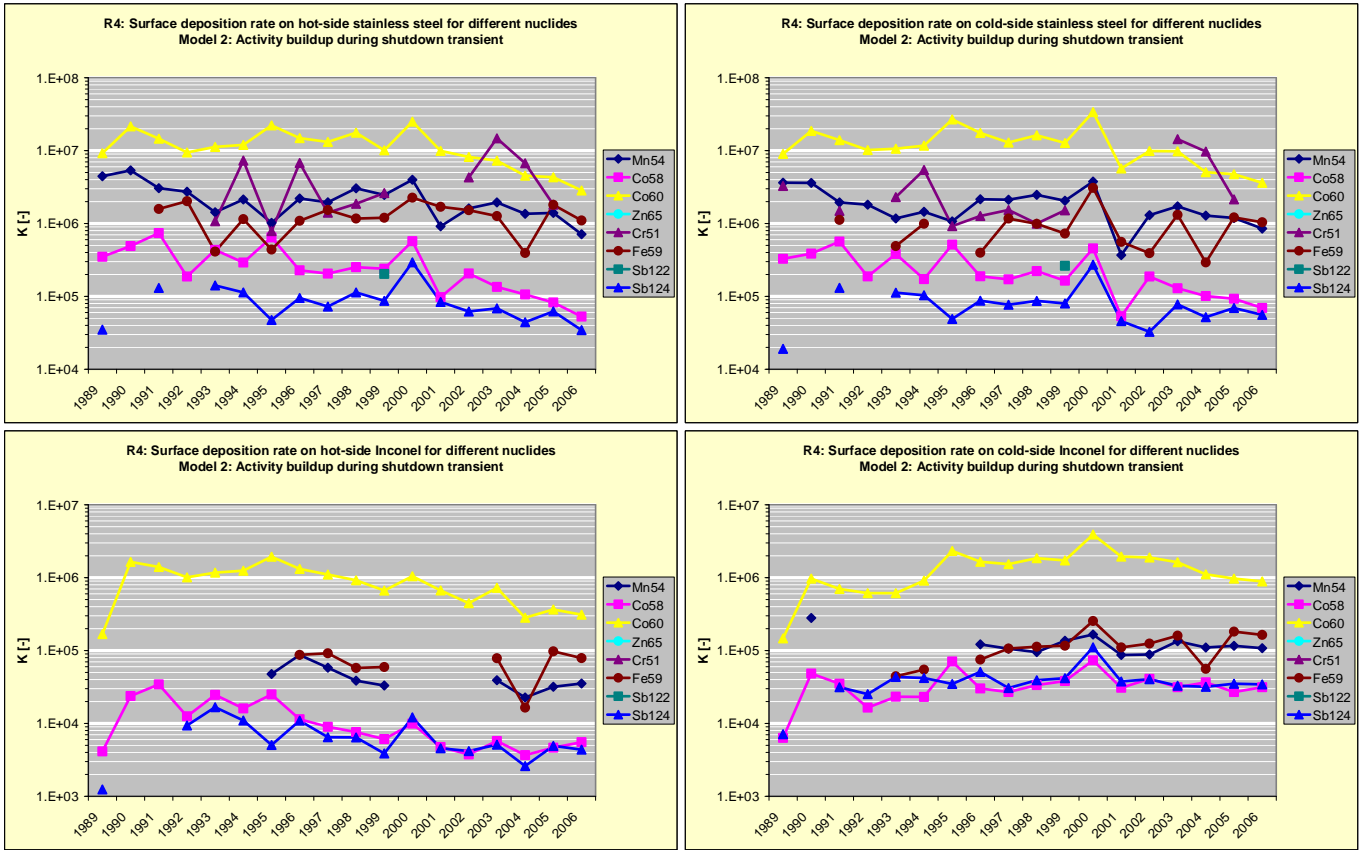


**Figure 16:** Ringhals 4: Normalized surface deposition rates during shutdown transient (Model 2) of different activated corrosion products for cold and hot side stainless steel and Inconel (Note: different log scales in the graphs)

## 2.2 WWER plants

### 2.2.1 Loviisa unit 1 (LO1)

LO1 started operation in 1977. The reactor water boron, Li, K,  $\text{NH}_3$  and pH are presented in **Figure 17**. The high temperature pH is mainly controlled with addition of KOH in contrast to the  ${}^7\text{LiOH}$  addition used in the western type of PWRs. The  $\text{pH}_{300}$  is typically controlled to be 7.1 – 7.2. The measured concentrations of reactor water corrosion products are presented in **Figure 18**<sup>7</sup>. Note that the type of integrated sampling performed in the Ringhals PWRs is not applied in the Loviisa WWERs, which means that normal operation levels are normally below the detection level with the exception of Fe. The measured data for the activated corrosion products, including evaluated normal operation averages and transient maximum values, are presented **Table 14** and **Figure 19**.

The characteristics of the LO1 plant from the water chemistry point of view can be summarised in the following way:

- The corrosion product balance is characterized by stainless steel SG tubes and primary piping. This is a difference compared to the Ringhals PWRs which have a large Inconel area in SG tubing. The dominance of stainless steel in the WWERs means that the corrosion product Ni:Fe ratio stays close to or below the spinel ratio 1:2, while in the Ringhals PWRs this ratio shows excess of Ni.
- Another difference compared to the Ringhals PWRs is the way to control pH. Less restrictions on reactor water K compared to Li allows the WWERs to operate on more stable high temperature pH levels, especially during the beginning of the fuel cycle.
- Inflow of antimony and silver to the primary circuit results in considerable production of antimony (Sb-122, Sb-124) and silver (Ag-110m) activation products. As a matter of fact the nuclide Sb-124 dominates the radiation fields in the plant during outage conditions.
- A change of measured normal operation reactor water activity levels is seen after the 2004 outage. Plant personnel suspected that this change may predominantly be due to a rebuilding of the sampling system during the outage.

---

<sup>7</sup> The data for both the corrosion and activated corrosion products are split up on "Soluble" fraction and "Total", the difference being in the insoluble form. The insoluble form is determined by filtering the sample through a 0.47  $\mu\text{m}$  membrane.

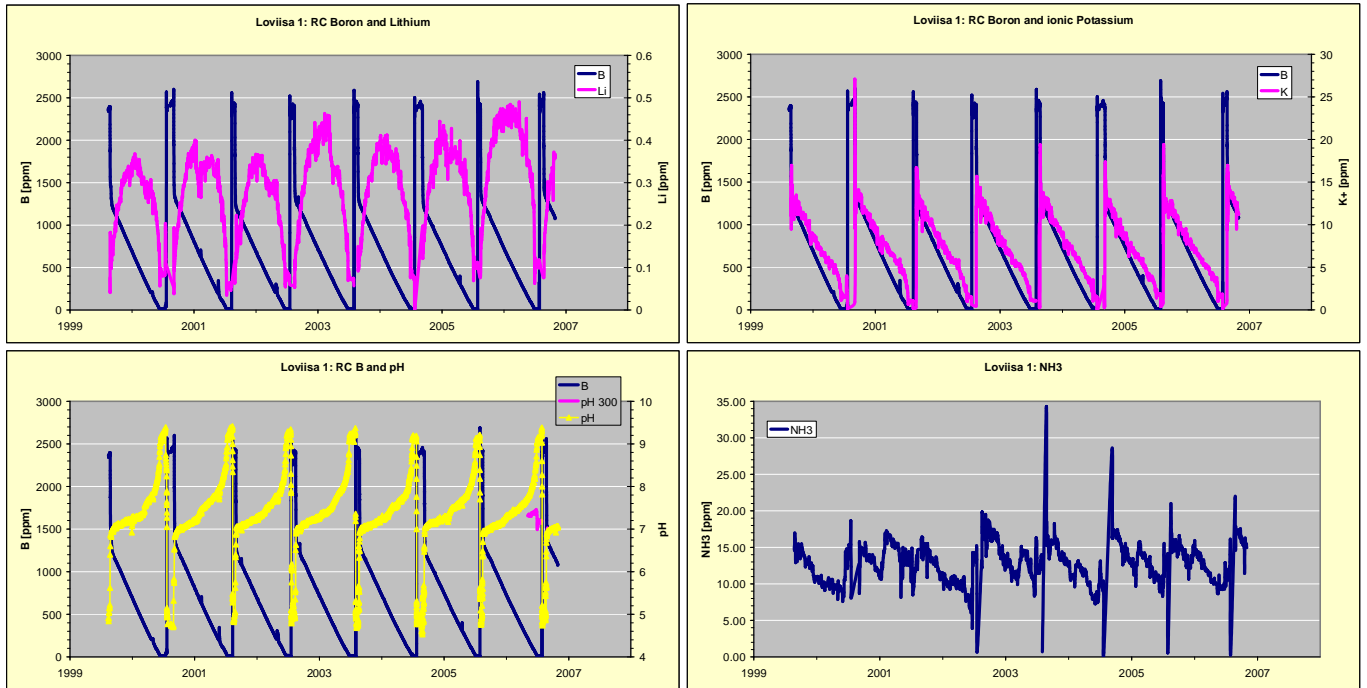


*Figure 17: Loviisa 1 – Variation of reactor water B, Li, K, NH<sub>3</sub> and pH*

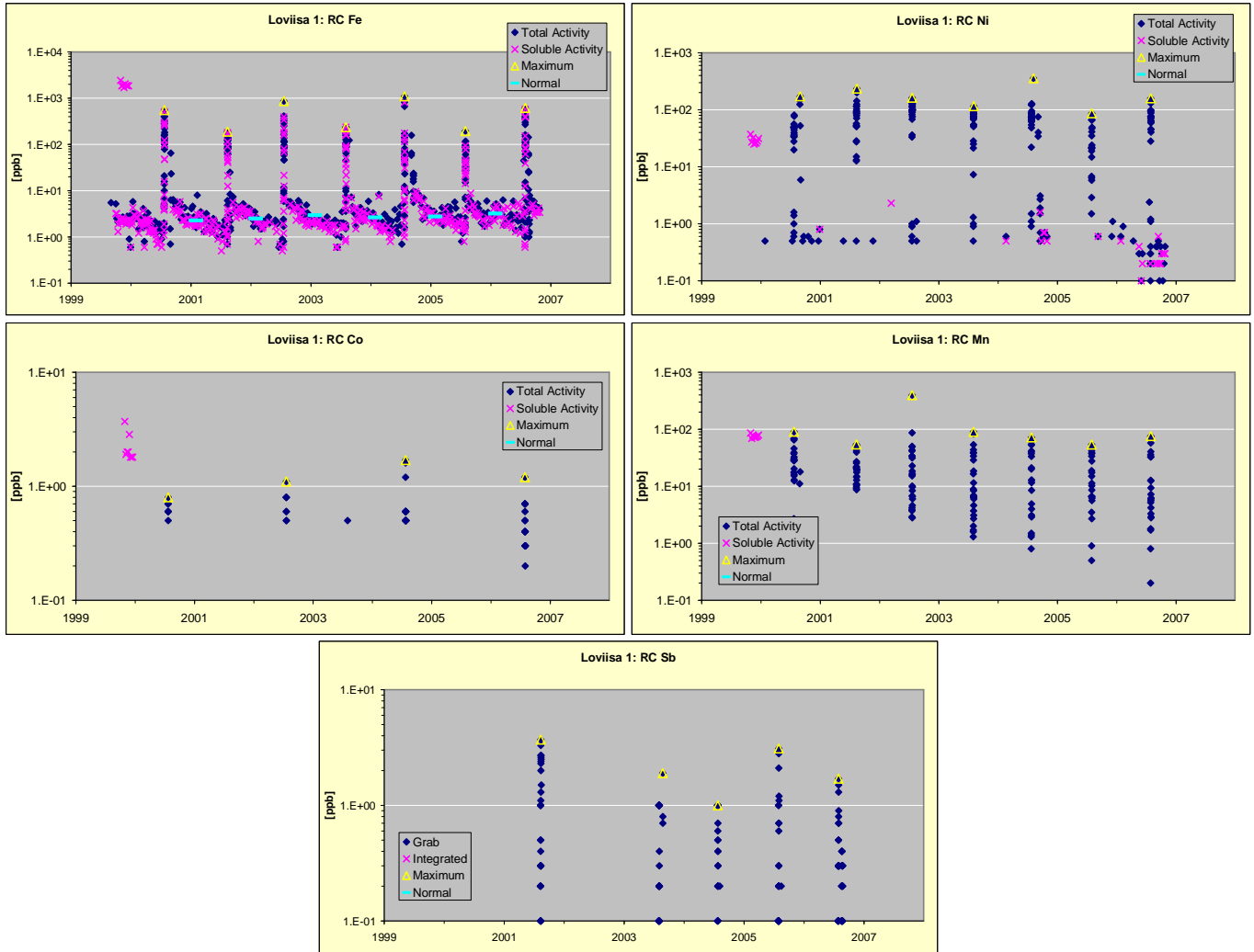
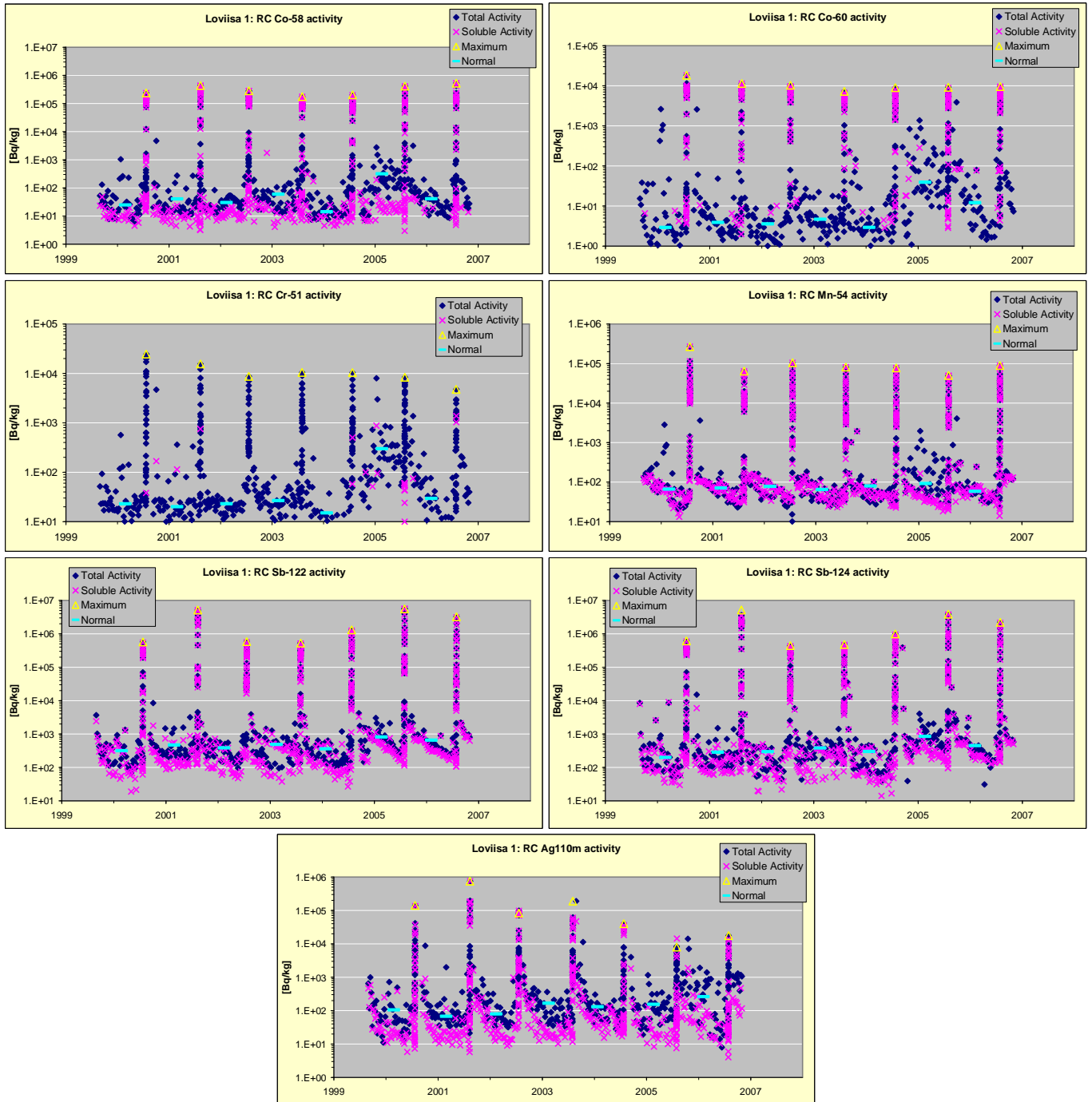


Figure 18: Loviisa 1 – Variation of corrosion products in reactor water

Table 14: Loviisa 1 – Activated corrosion products in reactor water – Annual average reactor operation and maximum shutdown transient data

Fuel Cycle	Co58 [Bq/kg]		Co60 [Bq/kg]		Cr51 [Bq/kg]		Mn54 [Bq/kg]		Sb122 [Bq/kg]		Sb124 [Bq/kg]		Ag110m [Bq/kg]	
	Average	Max	Average	Max	Average	Max	Average	Max	Average	Max	Average	Max	Average	Max
1999/2000	25	2.37E+05	3	1.83E+04	23	2.46E+04	67	2.68E+05	318	5.73E+05	200	6.17E+05	105	1.41E+05
2000/2001	41	4.38E+05	4	1.14E+04	20	1.56E+04	71	6.44E+04	471	5.17E+06	285	5.17E+06	68	7.53E+05
2001/2002	30	2.83E+05	4	1.03E+04	23	8.74E+03	78	1.05E+05	386	5.85E+05	297	4.45E+05	80	8.34E+04
2002/2003	60	1.76E+05	5	7.24E+03	27	1.05E+04	65	8.15E+04	488	5.27E+05	384	4.80E+05	167	1.89E+05
2003/2004	14	2.03E+05	3	8.95E+03	15	1.04E+04	80	7.77E+04	361	1.31E+06	300	9.93E+05	131	4.02E+04
2004/2005	317	4.14E+05	39	9.15E+03	300	8.36E+03	92	5.02E+04	816	5.57E+06	853	3.87E+06	155	7.99E+03
2005/2006	41	5.27E+05	12	9.56E+03	30	4.78E+03	59	8.94E+04	656	3.24E+06	450	2.21E+06	263	1.77E+04



*Figure 19: Loviisa 1 – Variation of activated corrosion products in reactor water*

The results from gamma scanning campaigns during shutdown periods are summarized in **Table 15**. The data are divided into activity on hot-side stainless steel piping, cold-side stainless steel piping, hot-side stainless steel SG tubing and cold-side stainless steel SG tubing. It shall be noted, that the measurement of activity on the SG tubing is performed from the outside of the thick SG vessel. The considerable attenuation of photons in the pressure vessel wall reduces the detection limit of some nuclides, especially those with low-energy photons, e.g. Cr-51.

**Table 15: Loviisa 1 – Gamma scanning data on hot and cold side stainless steel piping and SG hot and cold side stainless steel tubing**

Stainless steel, hot leg [Bg/m <sup>2</sup> ]										
Year	Co-60	Co-58	Mn-54	Ag-110m	Sb-124	Nb-95	Fe-59	Sb-122	Zr-95	Cr-51
1992	3.95E+08	3.73E+08	6.53E+07	5.23E+07	6.86E+08	3.80E+07	4.45E+07	7.86E+08		
1993	3.28E+08	2.97E+08	7.63E+07	2.74E+07	3.46E+08	3.63E+07	2.46E+07	6.87E+08	1.38E+07	
1994	3.50E+08	3.23E+08	9.13E+07	3.31E+07	2.81E+08	3.98E+07	3.08E+07	5.75E+08	1.60E+07	
1995	2.96E+08	3.29E+08	6.79E+07	3.17E+07	5.44E+08	3.67E+07	2.62E+07	9.73E+08	4.30E+06	9.95E+06
1996	2.75E+08	3.30E+08	5.90E+07	2.01E+07	6.39E+08	4.14E+07	2.53E+07	1.15E+09	1.70E+07	9.83E+06
1997	2.61E+08	3.87E+08	6.10E+07	2.98E+07	5.41E+08	4.66E+07	2.14E+07	9.69E+08	1.34E+07	9.91E+07
1998	2.35E+08	3.10E+08	5.74E+07	3.86E+07	4.95E+08	4.38E+07	2.08E+07	7.50E+08	1.69E+07	6.68E+07
1999	2.19E+08	3.60E+08	5.59E+07	5.64E+07	4.38E+08	4.22E+07	2.30E+07	5.14E+08	1.69E+07	9.78E+07
2000	2.07E+08	3.24E+08	4.87E+07	7.93E+07	5.99E+08	4.67E+07	1.98E+07	8.14E+08	1.74E+07	8.84E+07
2001	2.05E+08	4.39E+08	4.74E+07	6.60E+07	5.80E+08	4.89E+07	2.38E+07	9.75E+08	2.16E+07	1.03E+08
2002	2.09E+08	5.70E+08	4.75E+07	6.26E+07	5.57E+08	5.55E+07	2.46E+07	8.60E+08	2.60E+07	3.96E+08
2003	1.96E+08	5.46E+08	4.91E+07	4.16E+07	5.62E+08	5.74E+07	2.35E+07	8.78E+08	2.69E+07	2.45E+08
2004	1.83E+08	4.98E+08	4.59E+07	4.40E+07	6.95E+08	4.80E+07	1.87E+07	1.27E+09	1.27E+09	3.27E+08
2005	1.70E+08	4.97E+08	3.96E+07	3.44E+07	4.73E+08	4.15E+07	2.10E+07	8.67E+08	1.93E+07	2.96E+08
2006	1.71E+08	5.74E+08	4.42E+07	3.36E+07	7.57E+08	4.86E+07	2.38E+07	1.34E+09	2.52E+07	2.17E+08
2007	1.54E+08	5.46E+08	4.05E+07	1.87E+07	6.60E+08	5.20E+07	2.04E+07	1.15E+09	3.06E+07	
Stainless steel, cold leg [Bg/m <sup>2</sup> ]										
Year	Co-60	Co-58	Mn-54	Ag-110m	Sb-124	Nb-95	Fe-59	Sb-122	Zr-95	Cr-51
1992	4.38E+08	3.11E+08	5.29E+07	4.04E+07	4.38E+08	3.07E+07	6.07E+07	6.38E+08		
1993	3.00E+08	3.34E+08	6.18E+07	3.43E+07	3.27E+08	3.02E+07	2.31E+07	5.55E+08		
1994	3.01E+08	3.61E+08	6.45E+07	3.56E+07	2.20E+08	2.61E+07	2.51E+07	4.48E+08		
1995	2.91E+08	4.64E+08	5.96E+07	3.69E+07	4.22E+08	3.11E+07	3.12E+07	7.65E+08		
1996	2.60E+08	3.82E+08	4.63E+07	2.14E+07	4.98E+08	3.17E+07	2.58E+07	8.95E+08	8.79E+06	
1997	2.45E+08	3.59E+08	4.33E+07	2.17E+07	4.43E+08	3.43E+07	2.12E+07	8.21E+08	6.30E+06	8.87E+07
1998	2.17E+08	2.94E+08	3.78E+07	2.51E+07	3.37E+08	3.03E+07	1.90E+07	5.08E+08	9.08E+06	7.65E+07
1999	2.27E+08	3.43E+08	3.71E+07	8.34E+07	3.35E+08	3.00E+07	2.28E+07	3.97E+08	6.63E+06	8.10E+07
2000	1.97E+08	3.01E+08	3.23E+07	1.05E+08	3.48E+08	2.67E+07	1.89E+07	5.02E+08	5.50E+06	5.95E+07
2001	2.01E+08	3.36E+08	2.81E+07	1.22E+08	3.73E+08	2.96E+07	1.84E+07	6.55E+08	3.60E+06	5.68E+07
2002	1.95E+08	4.25E+08	2.73E+07	6.34E+07	2.77E+08	2.88E+07	2.11E+07	4.45E+08	1.56E+07	3.75E+08
2003	1.87E+08	4.11E+08	2.99E+07	6.49E+07	3.78E+08	2.42E+07	1.94E+07	6.15E+08	8.58E+06	2.93E+08
2004	1.77E+08	3.87E+08	2.91E+07	5.09E+07	4.36E+08	2.31E+07	2.19E+07	8.22E+08	1.16E+07	3.09E+08
2005	1.63E+08	3.74E+08	2.47E+07	3.76E+07	3.61E+08	1.81E+07	1.77E+07	6.52E+08	6.00E+06	3.03E+08
2006	1.71E+08	4.47E+08	2.79E+07	3.94E+07	4.90E+08	2.26E+07	1.72E+07	8.90E+08	1.18E+07	1.24E+08
2007	1.30E+08	4.75E+08	2.70E+07	2.15E+07	4.44E+08	2.46E+07	1.43E+07	7.53E+08	5.90E+06	
SG stainless steel tubes, hot side [Bg/m <sup>2</sup> ]										
Year	Co-60	Co-58	Mn-54	Ag-110m	Sb-124	Nb-95	Fe-59	Sb-122	Zr-95	Cr-51
1996	1.22E+08	1.37E+08	6.96E+07	1.93E+07	2.43E+08		1.77E+07	5.62E+08		
1997	1.13E+08	1.33E+08	3.11E+07	2.30E+07	2.80E+08		1.19E+07	5.80E+08		
1998	1.23E+08	1.30E+08	3.05E+07	1.67E+07	3.10E+08	7.80E+06	9.74E+06	5.02E+08		
1999	1.11E+08	1.17E+08	2.95E+07	6.52E+07	2.73E+08	1.00E+07	9.77E+06	4.28E+08	1.00E+07	
2000	9.18E+07	9.95E+07	4.93E+07	2.28E+07	2.38E+08	1.37E+07	1.67E+07	2.71E+08		
2001	1.06E+08	1.08E+08	4.85E+07	1.72E+07	2.63E+08	8.67E+06	1.59E+07	5.78E+08		
2002	9.84E+07	1.36E+08	2.24E+07	2.97E+07	2.31E+08	9.28E+06	7.04E+06	4.21E+08	3.11E+06	
2003	1.08E+08	1.66E+08	2.83E+07	7.31E+07	3.68E+08	1.11E+07	9.18E+06	5.53E+08		
2004	1.01E+08	1.64E+08	2.64E+07	2.14E+07	3.14E+08	1.14E+07	1.43E+07	5.88E+08		
2005	8.10E+07	1.20E+08	4.60E+07	3.35E+07	2.71E+08	6.00E+06	1.30E+07	4.64E+08		
2006	7.15E+07	1.31E+08	1.88E+07	1.16E+07	2.37E+08	6.63E+06	6.80E+06	3.65E+08		
2007	7.05E+07	1.37E+08	1.70E+07	9.60E+06	2.36E+08	6.80E+06	5.40E+06	4.08E+08	2.70E+06	
SG stainless steel tubes, cold side [Bg/m <sup>2</sup> ]										
Year	Co-60	Co-58	Mn-54	Ag-110m	Sb-124	Nb-95	Fe-59	Sb-122	Zr-95	Cr-51
1996	3.05E+07	4.08E+07			1.86E+07			4.30E+07		
1997	2.93E+07	5.65E+07	7.45E+06		1.49E+07	6.10E+06		3.09E+07		
1998	3.77E+07	4.97E+07			1.97E+07	9.60E+06	3.25E+06	3.18E+07		
1999	3.51E+07	4.34E+07	3.74E+06	3.06E+05	1.35E+07	2.67E+06	4.97E+06	2.11E+07		
2000	3.63E+07	3.99E+07			1.61E+07	2.19E+07	1.28E+07	2.49E+07		
2001	3.51E+07	4.63E+07			9.94E+06	2.40E+07	7.25E+06	5.27E+07		
2002	3.76E+07	5.18E+07	3.17E+06	1.29E+07	1.74E+07	8.77E+06	2.31E+06	3.16E+07		
2003	2.56E+07	5.40E+07			1.08E+07	2.66E+07	5.83E+06	3.99E+07		
2004	3.65E+07	8.55E+07			9.40E+06	1.96E+07	1.20E+07	3.67E+07		
2005	3.00E+07	5.80E+07			2.80E+07	2.60E+07	9.00E+06	4.45E+07		
2006	2.28E+07	6.67E+07	2.83E+06	2.95E+06	1.75E+07	8.42E+06	3.06E+06	2.99E+07		
2007	2.10E+07	5.00E+07	2.00E+06	3.00E+06	2.10E+07	5.60E+06	1.60E+06	2.64E+07	3.50E+06	

The above reactor water activities and gamma scanning data have been recalculated to surface enrichment factors  $K_1$  for the different activated corrosion products according to **Eq. 1** and **Eq. 2**, i.e. according to Model 1 assuming that the activity build-up is controlled by the normal operation conditions. The results are presented in **Figure 20**. The corresponding evaluation of  $K_2$  according to **Eq. 3**, i.e. according to Model 2 assuming that the activity build-up is controlled by the shutdown transient, is presented in **Figure 21**. The following observations are made:

- Several nuclides, Co-58, Co-60, Cr-51 and Zn-65, show quite similar and high  $K_1$  factors in spite of quite different half lives. This agreement is not seen in the

case of the Model 2 evaluation, which is supporting that the activity build-up of these nuclides is occurring according to Model 1.

- Other nuclides, especially Mn-54, Sb-124 and Ag-110m show lower  $K_1$  values than the above nuclides. The agreement in Model 1 factor between the radioisotopes Sb-122 and Sb-124 with different half lives is poor, but good in the case of Model 2 evaluation. The agreement in the case of Model 2 for the antimony isotopes supports that the activity build-up of these nuclides is mainly controlled by the shutdown transient. On the other hand, the Model 2 antimony factors show a rather large year-by-year variation, indicating that shutdown procedures may play a role in the actual activity build-up.
- The stainless steel Model 1 factors for the cobalt isotopes are high, similar as the Ringhals PWR factors but about a couple of order higher than the corresponding BWR factors [2]. It can be suspected that the reactor coolant concentrations in stainless steel systems with a large surface-to-volume ratio, e.g. thin sampling lines, will be affected by the large deposition rate. This is further discussed in later sections of the report.
- The Model 1 deposition rate is somewhat lower on stainless steel SG tubing compared to the stainless steel piping, but considerable higher than on the Inconel tubing in the Ringhals PWRs. The effect of temperature is rather small, with a tendency of somewhat lower deposition on the cold side of the SG tubing especially for Sb-124.

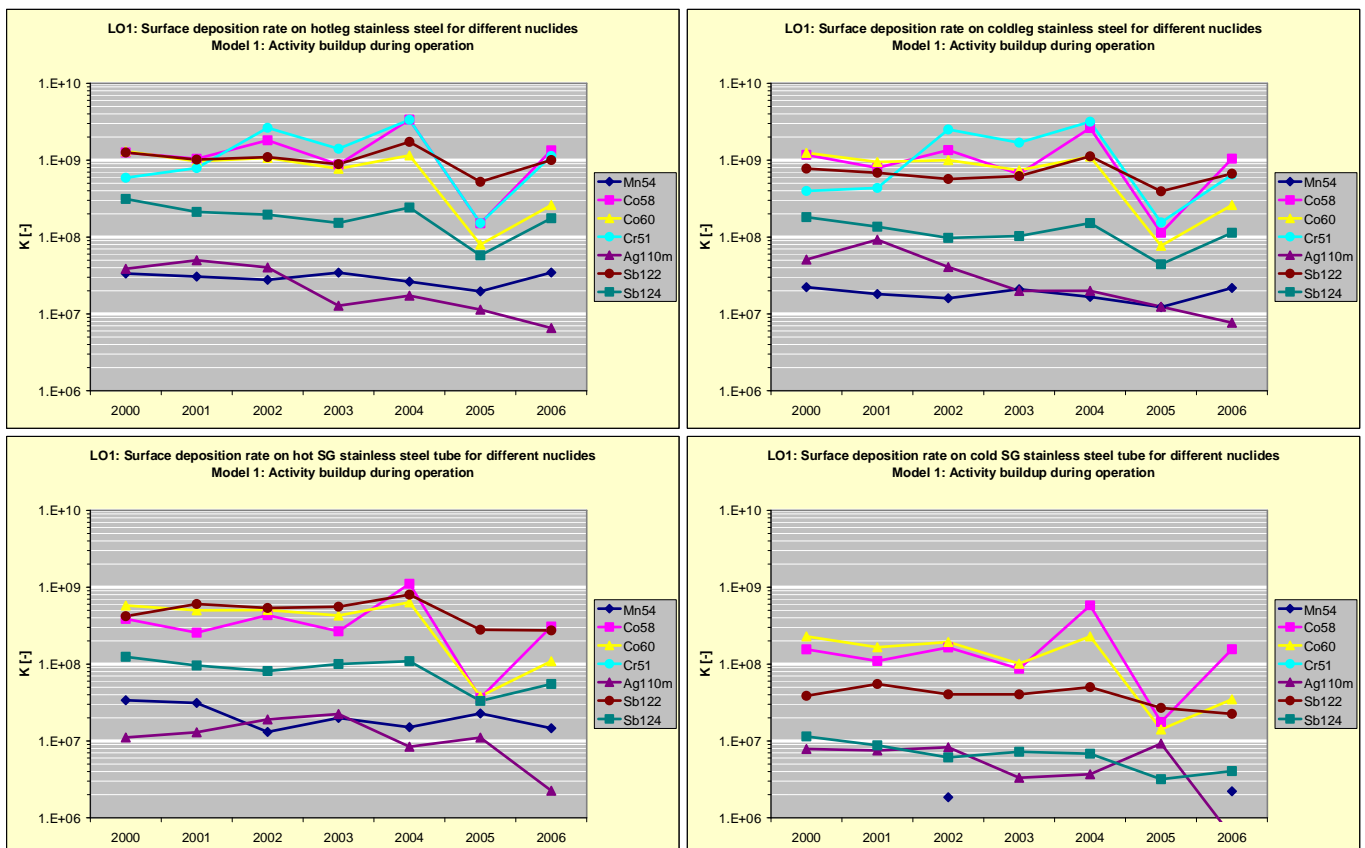


*Figure 20: Loviisa 1: Normalized surface deposition rates during operation (Model 1) of different activated corrosion products for cold and hot side stainless steel piping and SG tubes*

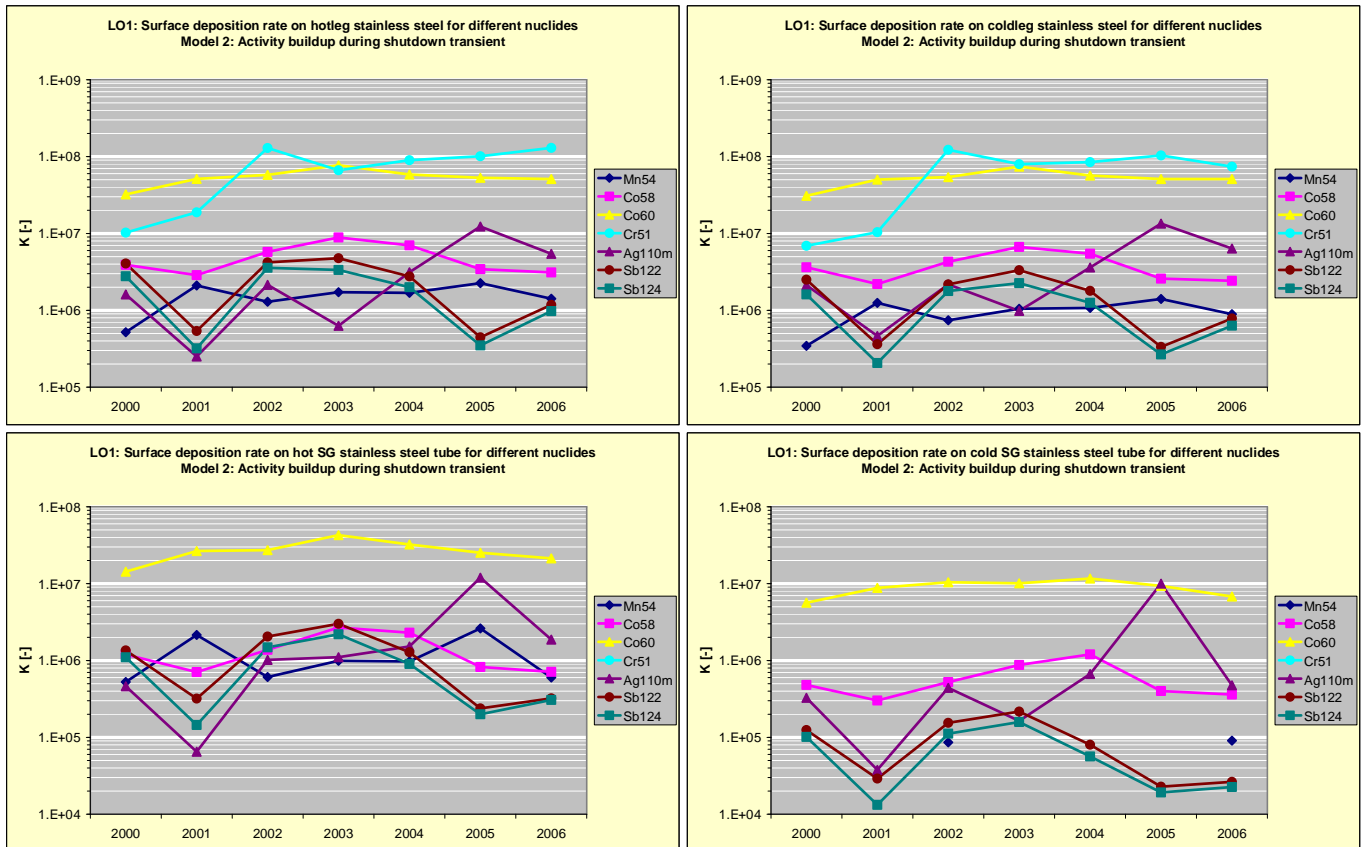


**Figure 21:** Loviisa 1: Normalized surface deposition rates during shutdown transient (Model 2) of different activated corrosion products for cold and hot side stainless steel piping and SG tubes  
(Note: different log scales in the graphs)

### 2.2.2 Loviisa unit 2 (LO2)

LO2 started operation in 1981. The reactor water boron, Li, K,  $\text{NH}_3$  and pH are presented in **Figure 22**. The high temperature pH is mainly controlled with addition of KOH as in LO1. The measured concentrations of reactor water corrosion products are presented in **Figure 23**. Note that the type of integrated sampling performed in the Ringhals PWRs is not applied in the Loviisa WWERs, which means that normal operation levels are normally below the detection level with the exception of Fe. The measured data for the activated corrosion products, including evaluated normal operation averages and transient maximum values, are presented **Table 16** and **Figure 24**.

The characteristics of the LO2 plant from the water chemistry point of view are quite similar to the LO1 plant and can be summarised in the following way:

- The corrosion product balance is characterized by stainless steel SG tubes and primary piping. This is a difference compared to the Ringhals PWRs which have a large Inconel area in SG tubing. The dominance of stainless steel in the WWERs means that the corrosion product Ni:Fe ratio stays close to or below the spinel ratio 1:2, while in the Ringhals PWRs this ratio shows excess of Ni.
- Another difference compared to the Ringhals PWRs is the way to control pH. Less restrictions on reactor water K compared to Li allows the WWERs to operate on more stable high temperature pH levels, especially during the beginning of the fuel cycle.



- Inflow of antimony and silver to the primary circuit results in considerable production of antimony (Sb-122, Sb-124) and silver (Ag-110m) activation products. As a matter of fact the nuclide Sb-124 dominates the radiation fields in the plant during outage conditions.
- A change of measured normal operation reactor water activity levels is seen after the 2002 outage. Plant personnel suspected that this change may predominantly be due to a rebuilding of the sampling system during the outage.

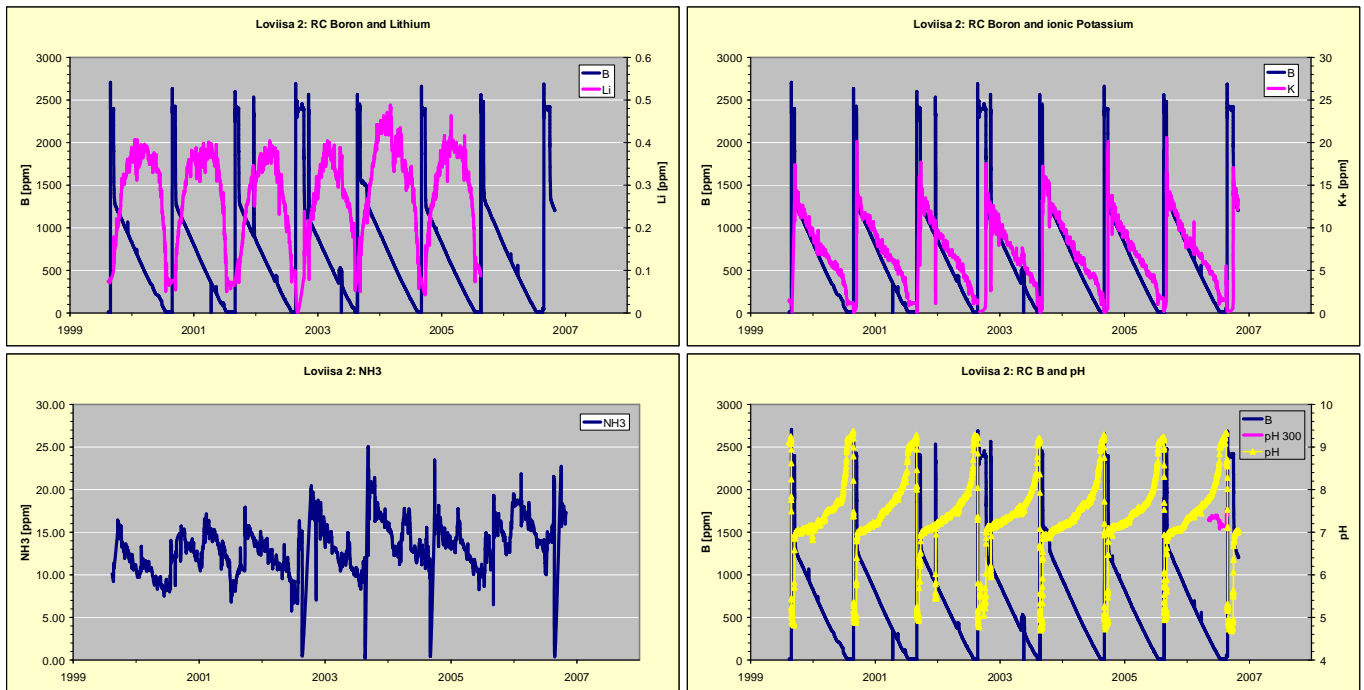


*Figure 22: Loviisa 2 – Variation of reactor water B, Li, K, NH<sub>3</sub> and pH*

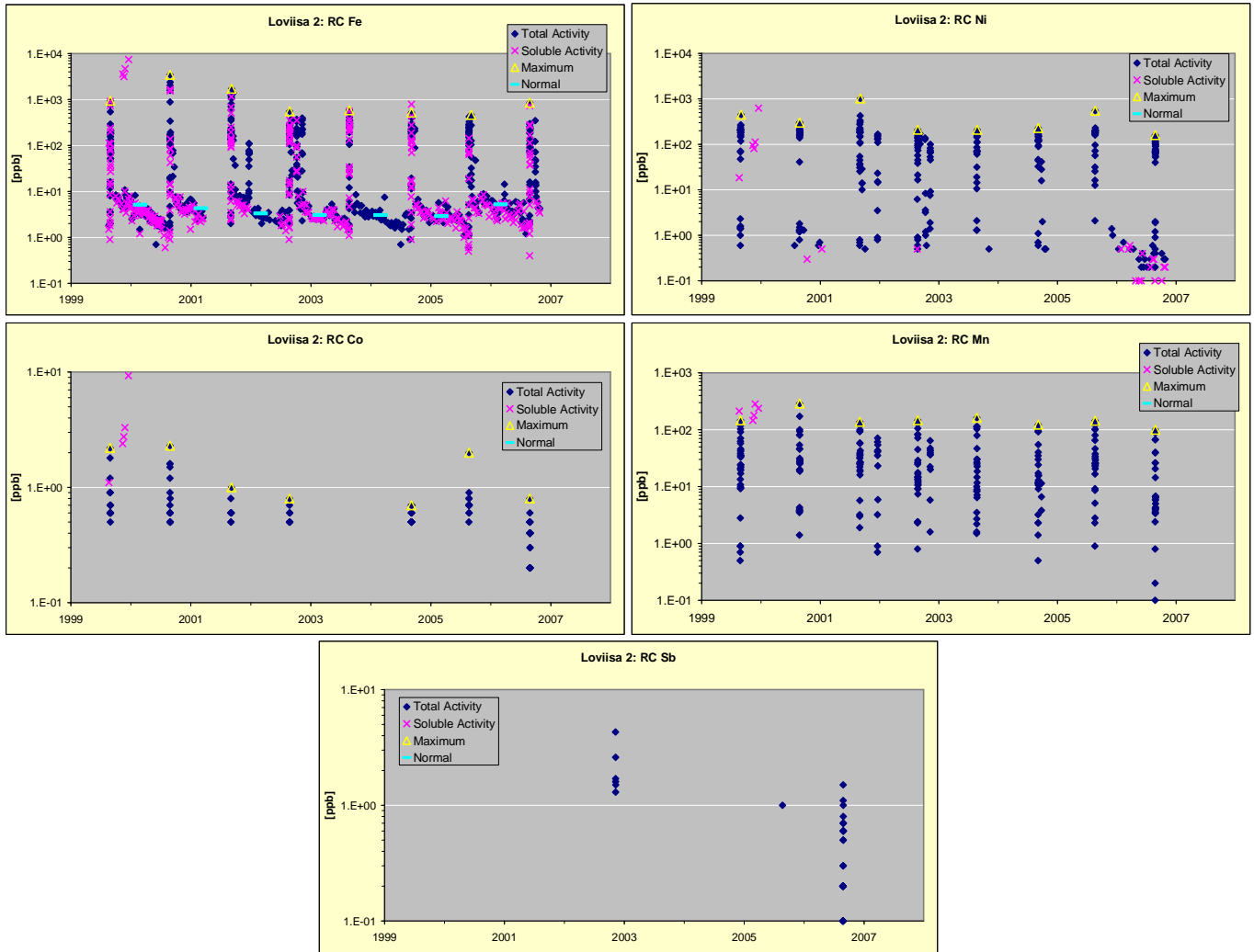


*Figure 23: Loviisa 2 – Variation of corrosion products in reactor water*

*Table 16: Loviisa 2 – Activated corrosion products in reactor water – Annual average reactor operation and maximum shutdown transient data*

Fuel Cycle	Co58 [Bq/kg]		Co60 [Bq/kg]		Cr51 [Bq/kg]		Mn54 [Bq/kg]		Sb122 [Bq/kg]		Sb124 [Bq/kg]		Ag110m [Bq/kg]	
	Average	Max	Average	Max	Average	Max	Average	Max	Average	Max	Average	Max	Average	Max
1999/2000	60	7.83E+05	20	2.71E+04	47	5.64E+04	114	2.63E+05	515	5.44E+05	500	3.59E+05	10	7.87E+03
2000/2001	72	6.11E+05	16	2.60E+04	72	4.86E+04	178	1.96E+05	392	4.45E+05	400	3.37E+05	22	2.78E+03
2001/2002	166	4.82E+05	60	1.24E+04	120	5.96E+03	423	1.64E+05	300	3.56E+05	200	2.33E+05	17	8.01E+03
2002/2003	275	6.66E+05	120	1.17E+04	168	1.09E+04	961	1.09E+05	709	8.47E+05	1768	4.91E+05	234	1.83E+04
2003/2004	698	3.17E+05	179	1.19E+04	635	2.07E+04	355	1.19E+05	949	1.66E+05	2900	1.45E+05	123	2.27E+03
2004/2005	256	3.21E+05	119	1.44E+04	224	3.09E+04	238	1.03E+05	327	5.41E+05	786	4.85E+05	143	1.04E+04
2005/2006	375	2.80E+05	79	8.97E+03	151	8.37E+03	255	1.08E+05	458	1.05E+06	1716	1.12E+06	446	2.55E+03

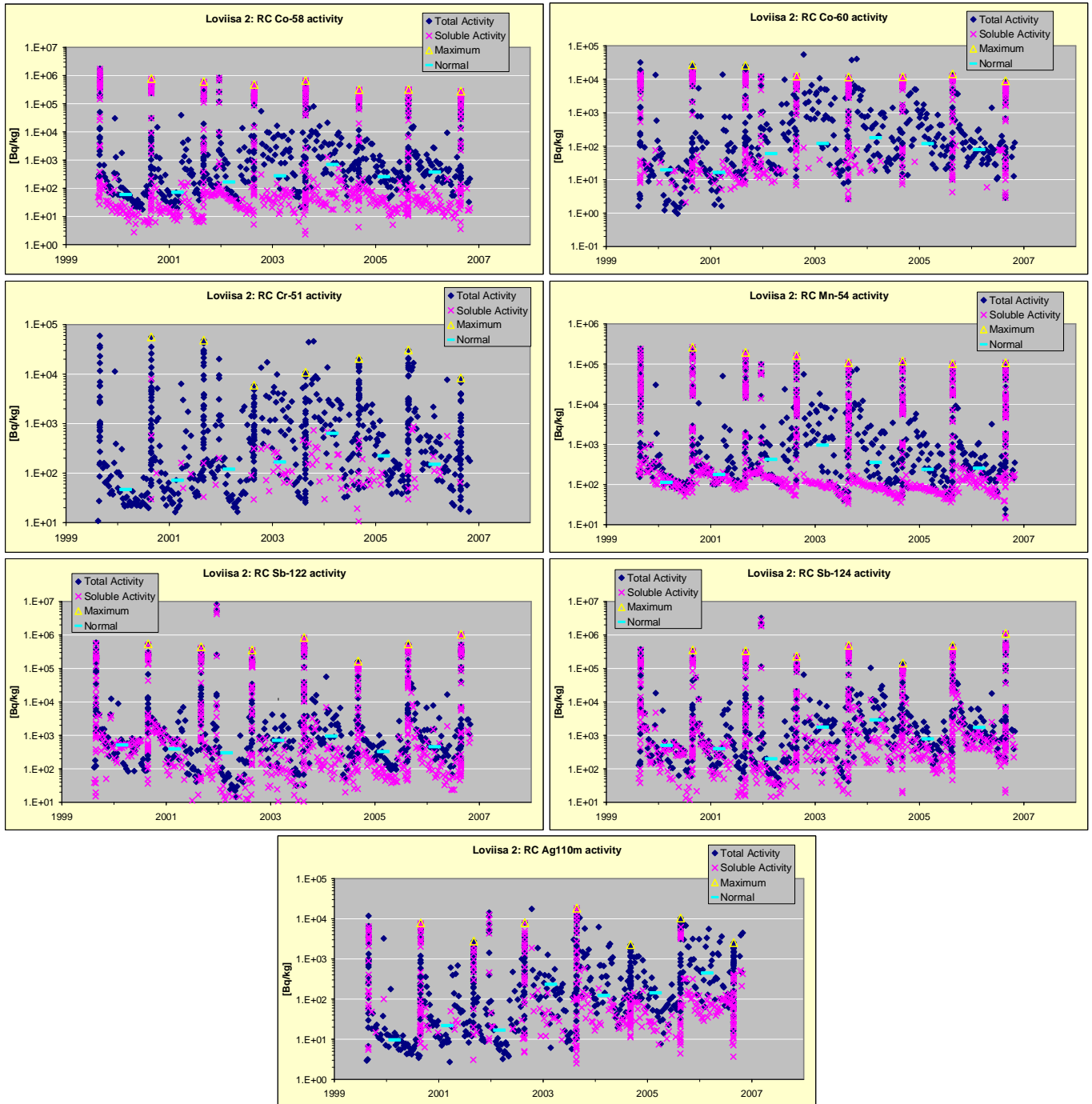


**Figure 24:** Loviisa 2 – Variation of activated corrosion products in reactor water

The results from gamma scanning campaigns during shutdown periods are summarized in **Table 17**. The data are divided into activity on hot-side stainless steel piping, cold-side stainless steel piping, hot-side stainless steel SG tubing and cold-side stainless steel SG tubing. It shall be noted, that the measurement of activity on the SG tubing is performed from the outside of the thick SG vessel. The considerable attenuation of photons in the pressure vessel wall reduces the detection limit of some nuclides, especially those with low-energy photons, e.g. Cr-51.

**Table 17:** Loviisa 2 – Gamma scanning data on hot and cold side stainless steel piping and SG hot and cold side stainless steel tubing

Stainless steel, hot leg [Bg/m <sup>2</sup> ]										
Year	Co-60	Co-58	Mn-54	Ag-110m	Sb-124	Nb-95	Fe-59	Sb-122	Zr-95	Cr-51
1993	1.0E+09	3.4E+08	2.6E+08	5.2E+07	4.0E+08	3.2E+07	5.7E+07	9.1E+08		
1994	4.8E+08	1.6E+08	1.1E+08	5.4E+07	1.7E+08	1.5E+07	2.6E+07	7.3E+08	1.6E+07	
1995	1.7E+08	1.7E+09	3.2E+08		1.2E+07	5.2E+08	1.8E+08		3.4E+08	
1996	3.7E+08	9.5E+08	5.0E+08	2.6E+06	9.1E+06	7.9E+07	1.8E+08		4.3E+07	2.8E+08
1997	4.3E+08	5.5E+08	4.0E+08		2.6E+07	5.1E+07	8.1E+07	5.6E+07	2.8E+07	
1998	6.6E+08	1.0E+09	3.9E+08		1.6E+08	6.9E+07	9.1E+07	2.6E+08	4.2E+07	
1999	5.6E+08	6.9E+08	1.7E+08	8.1E+06	2.0E+08	8.0E+07	3.3E+07	3.1E+08	4.4E+07	3.4E+08
2000	5.2E+08	4.9E+08	9.9E+07	1.0E+07	2.6E+08	8.4E+07	4.3E+07	4.6E+08	4.5E+07	4.8E+08
2001	5.2E+08	5.7E+08	8.7E+07	1.5E+07	2.2E+08	9.4E+07	6.6E+07	3.8E+08	5.7E+07	3.1E+08
2002	5.0E+08	4.4E+08	6.6E+07	1.2E+07	4.3E+08	7.9E+07	3.7E+07	8.0E+08	4.6E+07	1.6E+08
2003	4.9E+08	6.5E+08	5.2E+07	1.5E+07	2.6E+08	6.2E+07	3.0E+07	5.3E+08	3.4E+07	4.5E+08
2004	4.4E+08	3.8E+08	3.6E+07	1.5E+07	2.7E+08	6.9E+07	1.8E+07	4.8E+08	4.0E+07	3.1E+08
2005	4.0E+08	5.4E+08	3.5E+07	1.7E+07	3.8E+08	5.9E+07	2.3E+07	6.5E+08	2.3E+07	1.4E+08
2006	4.0E+08	4.1E+08	3.3E+07	1.4E+07	2.5E+08	4.6E+07	1.6E+07	3.1E+08	2.0E+07	9.7E+07
2007	3.6E+08	3.3E+08	2.9E+07	2.3E+07	3.9E+08	5.4E+07	2.1E+07	6.6E+08	2.9E+07	8.6E+07
Stainless steel, cold leg [Bg/m <sup>2</sup> ]										
Year	Co-60	Co-58	Mn-54	Ag-110m	Sb-124	Nb-95	Fe-59	Sb-122	Zr-95	Cr-51
1993	2.9E+09	9.6E+08	5.1E+08	1.8E+08	9.5E+08	5.2E+07	1.0E+08	1.7E+09		
1994	1.5E+09	4.6E+08	2.4E+08	6.8E+07	5.0E+08	2.3E+07	5.6E+07	1.9E+09		
1995	2.5E+08	5.2E+08	1.1E+08	8.6E+06	7.0E+06	2.0E+07	2.3E+07	3.7E+07	9.3E+06	
1996	2.2E+08	3.8E+08	2.0E+08	1.2E+07	2.1E+07	1.2E+07	2.2E+07	6.0E+07		3.1E+08
1997	1.6E+08	3.6E+08	1.8E+08	1.4E+07	5.9E+07	1.5E+07	1.3E+07	1.8E+08		
1998	2.1E+08	5.4E+08	1.5E+08	1.8E+07	1.4E+08	1.9E+07	1.9E+07	2.8E+08	1.8E+07	2.3E+08
1999	1.9E+08	3.3E+08	6.5E+07	1.4E+07	1.4E+08	1.4E+07	1.2E+07	2.3E+08	3.0E+06	2.5E+08
2000	2.1E+08	2.2E+08	5.5E+07	1.5E+07	2.3E+08	1.9E+07	1.5E+07	4.0E+08		1.9E+08
2001	2.2E+08	2.4E+08	5.9E+07	1.7E+07	2.1E+08	1.8E+07	1.1E+07	3.4E+08		3.3E+08
2002	2.4E+08	2.4E+08	5.8E+07	2.4E+07	3.1E+08	1.8E+07	1.1E+07	5.8E+08		5.6E+07
2003	2.6E+08	2.6E+08	3.5E+07	1.9E+07	3.2E+08	2.1E+07	1.7E+07	6.9E+08	1.5E+07	2.5E+08
2004	2.1E+08	2.5E+08	3.1E+07	1.7E+07	4.2E+08	2.0E+07	1.1E+07	7.1E+08	1.2E+07	2.5E+08
2005	1.6E+08	2.6E+08	2.6E+07	3.8E+07	4.6E+08	1.8E+07	1.3E+07	7.7E+08	9.9E+06	5.9E+07
2006	2.3E+08	2.5E+08	3.6E+07	2.1E+07	5.2E+08	1.9E+07	1.3E+07	5.7E+08	8.5E+06	6.6E+07
2007	2.0E+08	2.5E+08	3.2E+07	2.5E+07	3.9E+08	1.8E+07	1.4E+07	6.1E+08	1.1E+07	6.8E+07
SG stainless steel tubes, hot side [Bg/m <sup>2</sup> ]										
Year	Co-60	Co-58	Mn-54	Ag-110m	Sb-124	Nb-95	Fe-59	Sb-122	Zr-95	Cr-51
1996	7.9E+07	3.7E+08	1.6E+08		1.7E+07		4.3E+07			
1997	1.5E+08	3.3E+08	1.8E+08	9.0E+06		1.5E+07	2.8E+07			
1998	1.5E+08	3.1E+08	1.2E+08		5.4E+07		1.6E+07			
1999	1.3E+08	2.4E+08	6.1E+07		8.7E+07	1.8E+07	1.2E+07	1.7E+08		
2000	9.4E+07	1.2E+08	3.6E+07		1.1E+08	1.1E+07	1.1E+07	1.3E+08		
2001	9.4E+07	1.2E+08	3.6E+07		1.1E+08	1.1E+07	1.1E+07	1.3E+08		
2002	9.4E+07	9.8E+07	2.4E+07		1.1E+08	1.5E+07	9.2E+06	1.2E+08		
2003	1.1E+08	1.1E+08	3.5E+07		1.3E+08	1.5E+07	6.9E+06	1.9E+08		
2004	9.8E+07	1.4E+08	1.6E+07	5.6E+07	3.0E+08	1.5E+07	8.3E+06	4.3E+08		
2005	8.7E+07	1.1E+08	1.7E+07	1.6E+07	1.7E+08	8.3E+06	6.9E+06	3.1E+08	5.3E+06	
2006	8.1E+07	8.6E+07	1.5E+07	8.9E+06	1.8E+08	7.4E+06	4.4E+06	1.8E+08		
2007	7.0E+07	8.4E+07	1.3E+07	1.2E+07	1.3E+08	9.3E+06	4.3E+06	2.7E+08		
SG stainless steel tubes, cold side [Bg/m <sup>2</sup> ]										
Year	Co-60	Co-58	Mn-54	Ag-110m	Sb-124	Nb-95	Fe-59	Sb-122	Zr-95	Cr-51
1996	4.7E+07	2.3E+08	1.0E+08	0.0E+00	4.7E+07		1.1E+07			
1997	6.0E+07	2.1E+08	1.0E+08	1.0E+07	8.6E+07		8.6E+06			
1998	6.7E+07	2.9E+08	6.5E+07	9.4E+06	1.3E+08		6.5E+06			
1999	5.8E+07	2.0E+08	3.8E+07	2.5E+07	1.9E+08			2.4E+08		
2000	6.7E+07	1.3E+08	3.1E+07	3.8E+07	2.5E+08	8.9E+06	7.8E+06	4.0E+08		
2001	6.7E+07	1.3E+08	3.1E+07	3.8E+07	2.5E+08	8.9E+06	7.8E+06	4.0E+08	2.6E+07	
2002	8.0E+07	1.1E+08	2.1E+07	6.6E+07	2.4E+08	1.1E+07		4.4E+08		
2003	8.1E+07	1.0E+08	1.9E+07	6.6E+07	2.9E+08	9.7E+06		4.9E+08		
2004	9.3E+07	8.9E+07	2.0E+07		1.8E+08			2.7E+08		
2005	9.1E+07	1.5E+08	1.8E+07	3.8E+07	3.6E+08	1.0E+07	6.0E+06	5.0E+08		
2006	8.3E+07	1.2E+08	1.5E+07	5.4E+07	3.2E+08	6.3E+06	4.2E+06	3.0E+08		
2007	7.1E+07	1.2E+08	1.6E+07	4.5E+07	2.6E+08	8.2E+06	4.9E+06	4.1E+08		

The above reactor water activities and gamma scanning data have been recalculated to surface enrichment factors  $K_1$  for the different activated corrosion products according to **Eq. 1** and **Eq. 2**, i.e. according to Model 1 assuming that the activity build-up is controlled by the normal operation conditions. The results are presented in **Figure 25**. The corresponding evaluation of  $K_2$  according to **Eq. 3**, i.e. according to Model 2 assuming that the activity build-up is controlled by the shutdown transient, is presented in **Figure 26**. The observations made are very close to that of the sister plant LO1:

- Several nuclides, Co-58, Co-60, Cr-51 and Zn-65, show quite similar and high  $K_1$  factors in spite of quite different half lives. This agreement is not seen in the case of the Model 2 evaluation, which is supporting that the activity build-up of these nuclides is occurring according to Model 1.

- Other nuclides, especially Mn-54, Sb-124 and Ag-110m show lower  $K_1$  values than the above nuclides. The agreement in Model 1 factor between the radioisotopes Sb-122 and Sb-124 with different half lives is poor, but good in the case of Model 2 evaluation. The agreement in the case of Model 2 for the antimony isotopes supports that the activity build-up of these nuclides is mainly controlled by the shutdown transient. On the other hand, the Model 2 antimony factors show a rather large year-by-year variation, indicating that shutdown procedures may play a role in the actual activity build-up.
- The stainless steel Model 1 factors for the cobalt isotopes are high, similar as the Ringhals PWR factors but about a couple of order higher than the corresponding BWR factors [2]. It can be suspected that the reactor coolant concentrations in stainless steel systems with a large surface-to-volume ratio, e.g. thin sampling lines, will be affected by the large deposition rate. This is further discussed in later sections of the report.
- The Model 1 deposition rate is somewhat lower on stainless steel SG tubing compared to the stainless steel piping, but considerable higher than on the Inconel tubing in the Ringhals PWRs. The effect of temperature rather small, with a tendency of somewhat lower deposition on the cold side of the SG tubing.

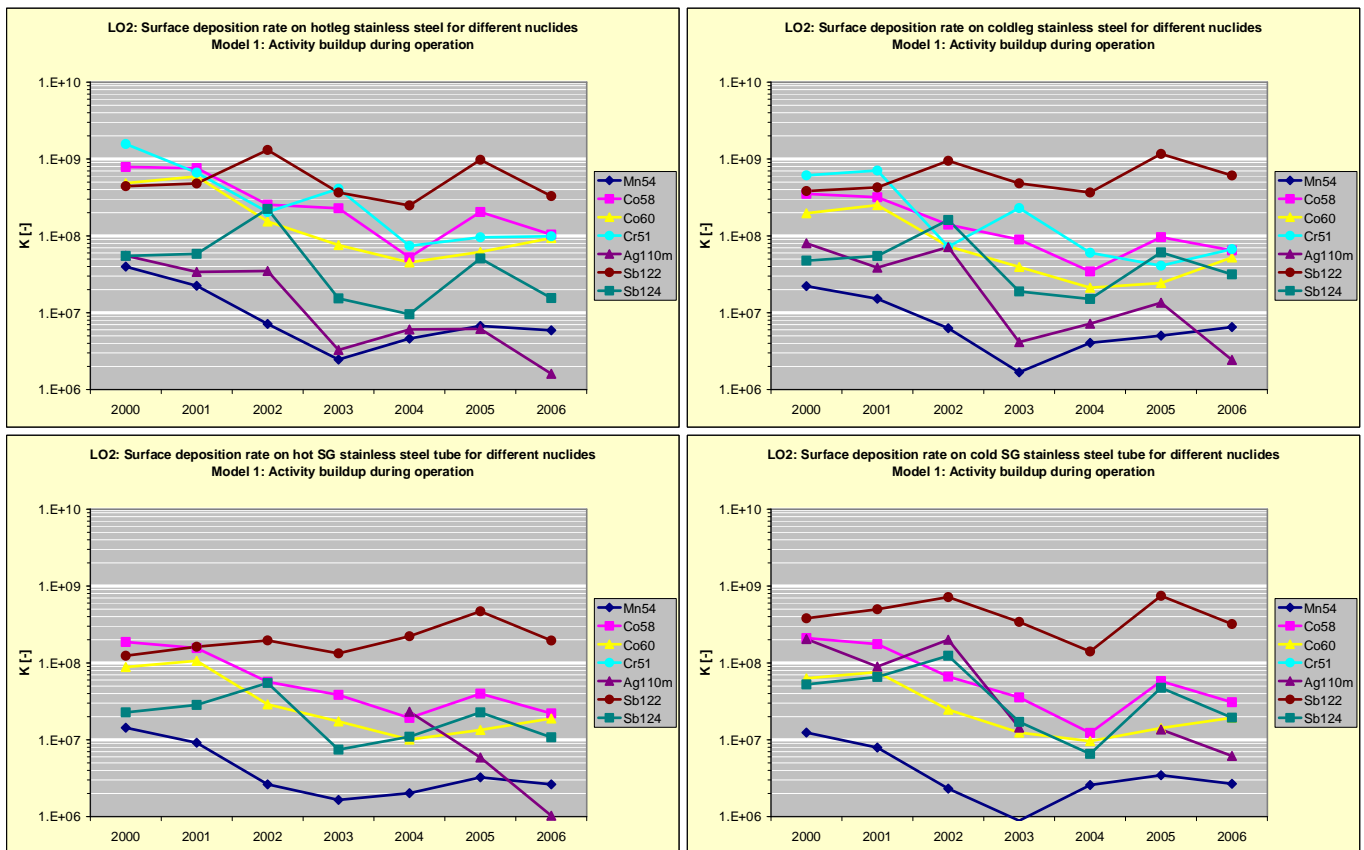


*Figure 25: Loviisa 2: Normalized surface deposition rates during operation (Model 1) of different activated corrosion products for cold and hot side stainless steel piping and SG tubes*

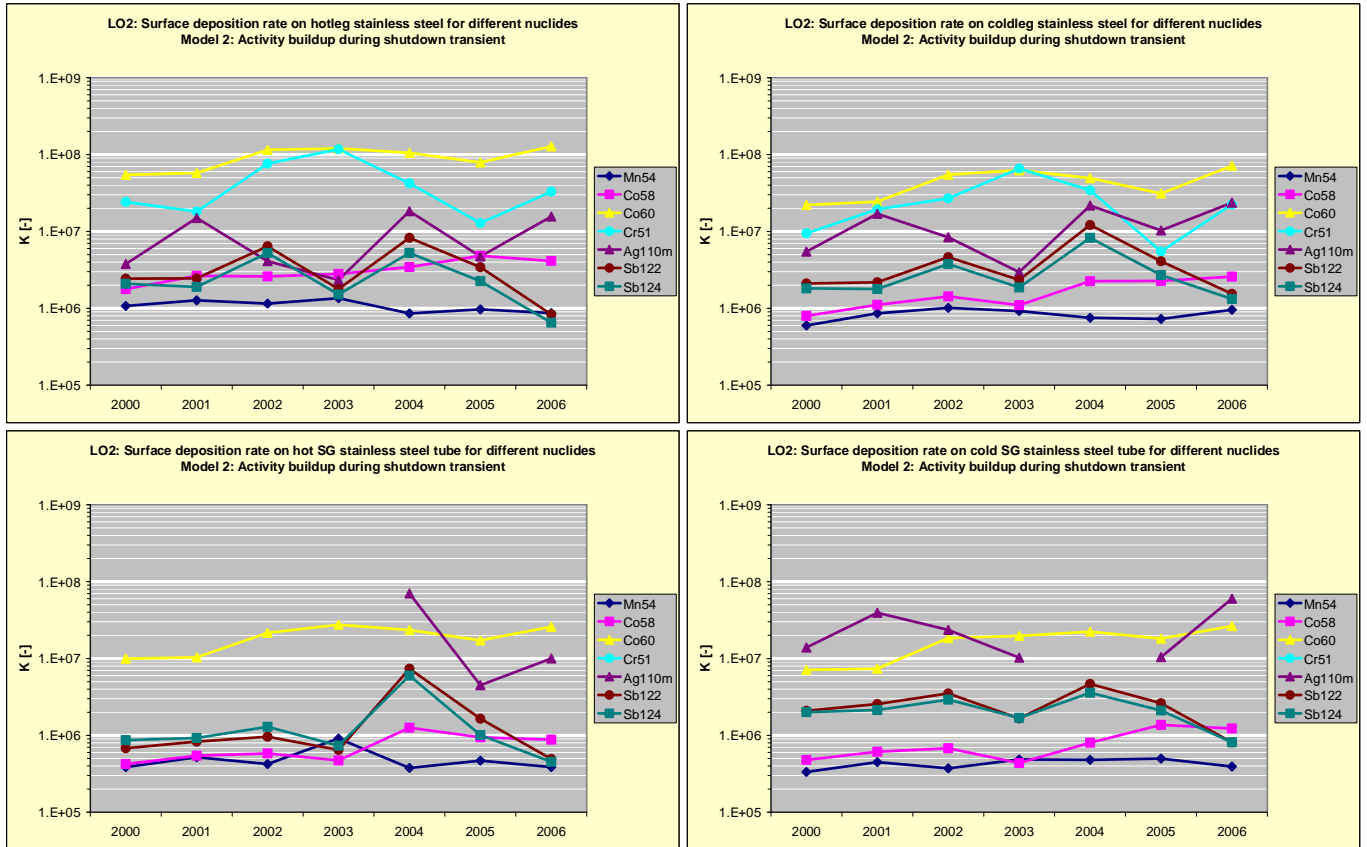


**Figure 26:** Loviisa 2: Normalized surface deposition rates during shutdown transient (Model 2) of different activated corrosion products for cold and hot side stainless steel piping and SG tubes

The LO2 primary recirculation system was decontaminated in 1994. The pre-decontamination radiation levels in LO2 were quite high, and considerably higher than the LO1 levels, see **Figure 27**. The LO2 radiation levels after the decontamination have stayed on a low level comparable to the LO1 conditions. The reasons for the high radiation buildup in the LO2 have been addressed in several investigations, but no firm conclusion was reached. The present evaluation is restricted to the post-decontamination conditions in LO2. It might be worth mentioning that the overall decontamination campaign in LO2 was not a complete success as some sludge from the decontamination was remaining in the coolant and deposited on the fuel rods.

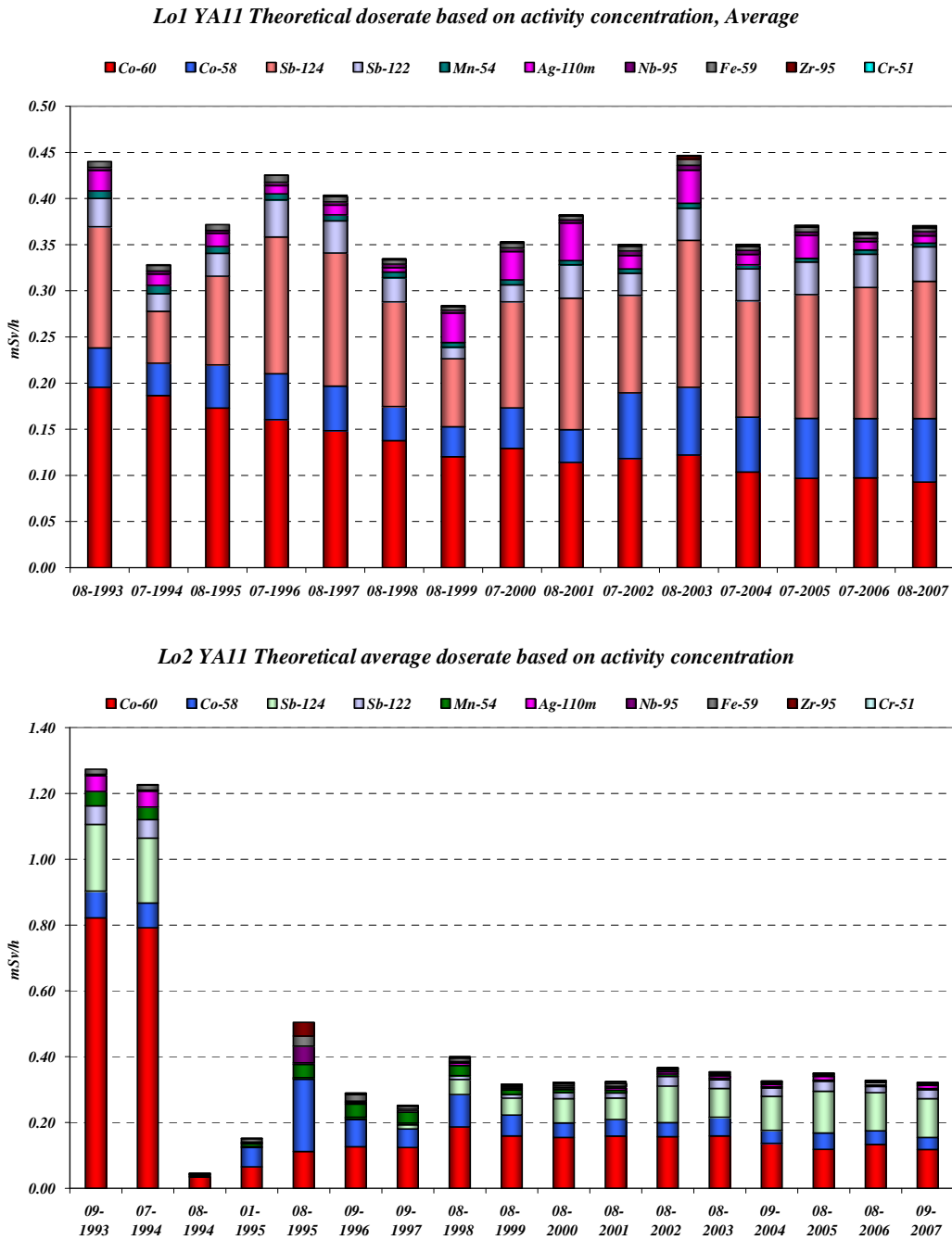


**Figure 27:** Loviisa 1 & 2: Measured radionuclide contribution to dose rates on primary piping (average hot and cold leg), Note: decontamination in LO2 in 1994

## 3 Analysis

### 3.1 Plant comparison

#### 3.1.1 Co-58 and Co-60

It was concluded in the previous chapter that the activity build-up of the cobalt isotopes Co-58 and Co-60 both are controlled by the normal operation conditions, i.e. according to Model 1 (Eq. 2). These nuclides also show quite similar performance as some other nuclides, e.g. Fe-59 and Zn-65. A comparison of the Co-58 Model 1 deposition rates for the five different reactors and the four different measurement locations are shown in **Figure 28**. The corresponding comparison for the nuclide Co-60 is presented in **Figure 29**.

The data show some scattering. An obvious reason for the scattering is problem to accurately determine the base line reactor water activity level during operation.

No obvious difference is seen between the reactors for the stainless steel piping. On the other hand, a difference is seen in the case of SG tubes between the plants with Inconel and stainless steel tubes with lower deposition rates in the former. A lower activity build-up on the Inconel tubes compared to the stainless steel tubes is expected due to considerable thinner oxide layers formed on the Inconel tubes. On the other hand, the deposition rate on the SG stainless steel tubes is notably lower than the corresponding deposition rate on the stainless steel piping. It is obvious that differences between the oxide layers formed on different stainless steel surfaces exist. The observed difference between the Loviisa stainless steel primary piping and SG tubes may be that the latter originally had a better surface finish.

A considerable difference is also seen for the  $K_1$  factors for the Loviisa plants. A closer analysis of the reason for this difference shows that it is the difference in measured reactor water activity in the plants that mainly contributes and not the surface activity. As mentioned earlier sampling systems have been rebuilt in the plants, but during different years. It may not be excluded that the observed difference to a large degree is affected by the impact of the sampling systems.

A closer comparison of the Co-58 and Co-60 deposition rates indicate that the latter are somewhat lower. This is in line with an expected influence of the effect of different half lives of the nuclides on the sampling efficiency. This matter will be further discussed later in the report.



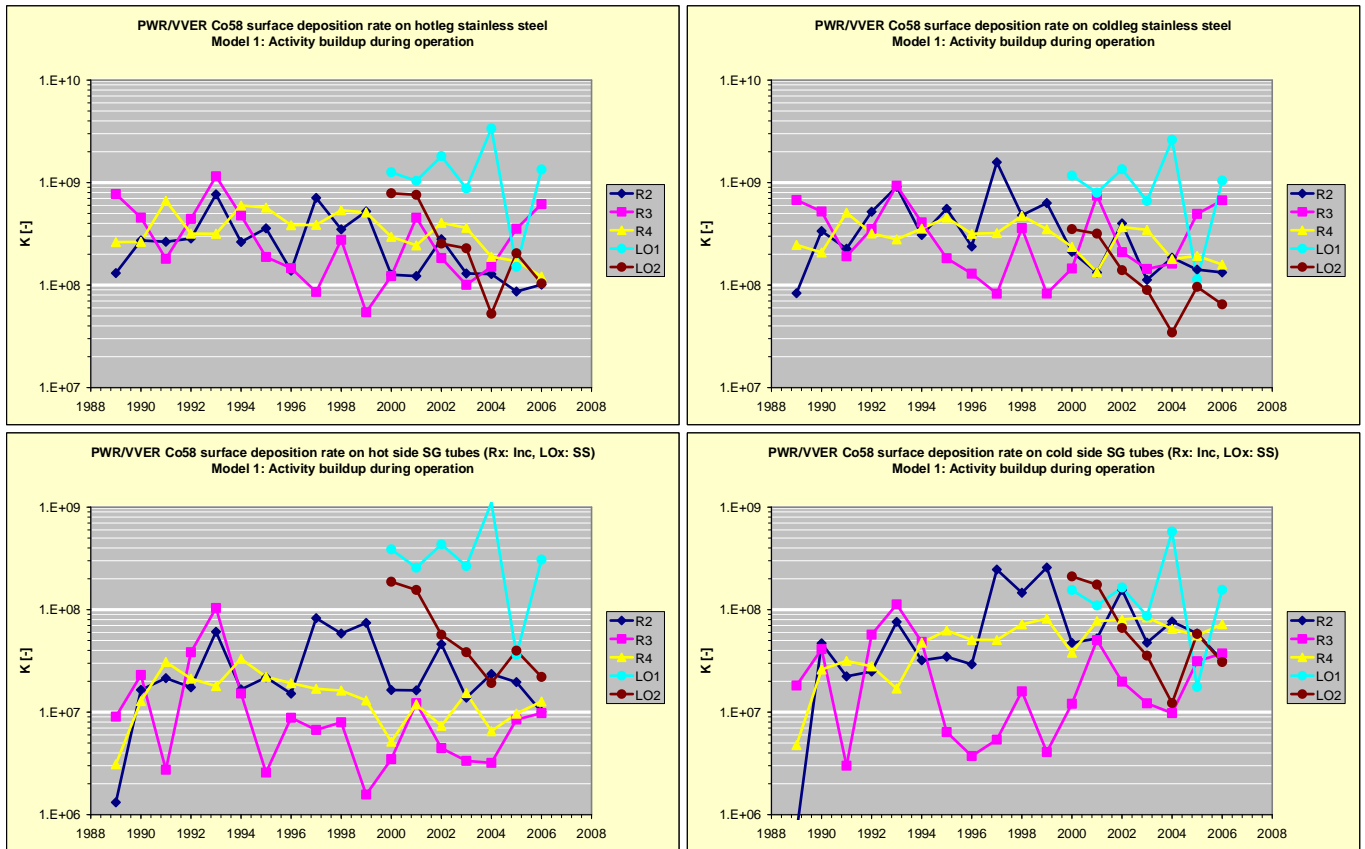


**Figure 28:** Co-58: Normalized surface deposition rates during operation (Model 1) of different activated corrosion products for cold and hot side stainless steel piping and SG tubes (Ringhals: Inconel, Loviisa: stainless steel)

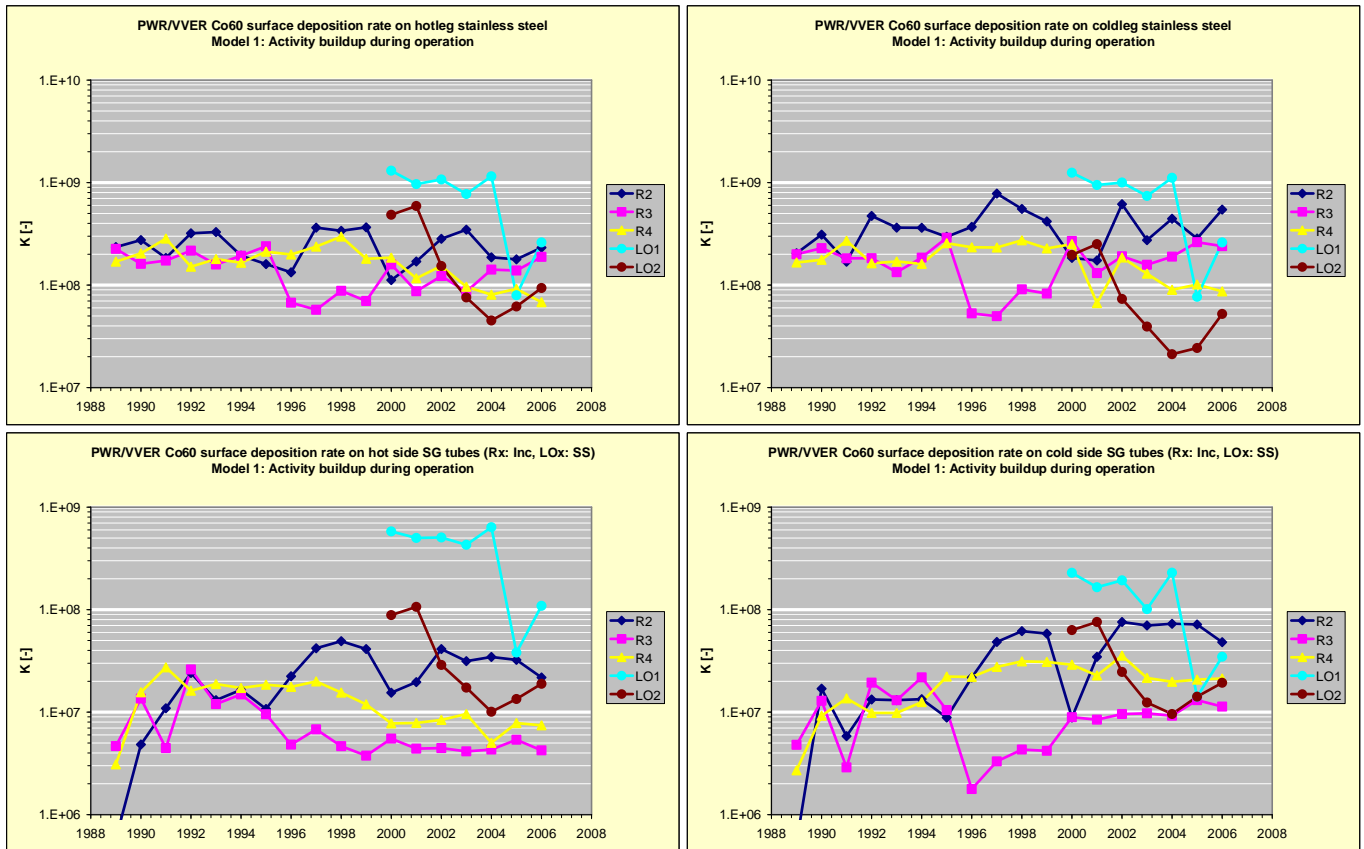


**Figure 29:** Co-60: Normalized surface deposition rates during operation (Model 1) of different activated corrosion products for cold and hot side stainless steel piping and SG tubes (Ringhals: Inconel, Loviisa: stainless steel)

### 3.1.2 Mn-54

A corresponding comparison of Model 1 deposition rates for Mn-54 is presented in **Figure 30**. The deposition rate for the Mn-54 nuclide is about an order of magnitude lower than the corresponding rate for the cobalt isotopes. The same qualitative differences are seen for different materials, with the lowest deposition rate on the SG Inconel tubing.

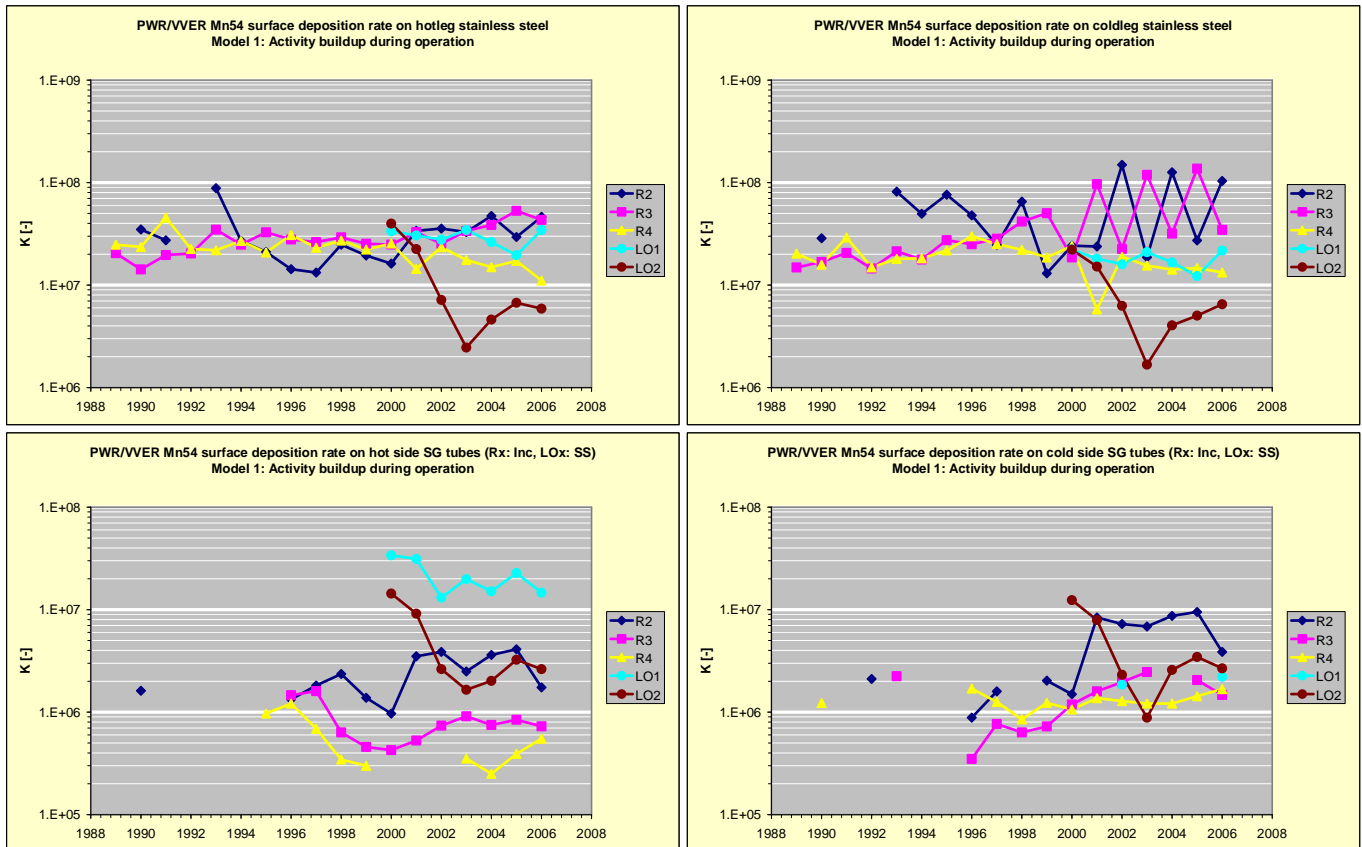


**Figure 30:** Mn-54: Normalized surface deposition rates during operation (Model 1) of different activated corrosion products for cold and hot side stainless steel piping and SG tubes (Ringhals: Inconel, Loviisa: stainless steel)

### 3.1.3 Sb-122 and Sb-124

The activity build-up of the antimony isotopes are found to correlate to the shutdown transient, i.e. follow the Model 2 (Eq. 3). The Model 2 evaluation for Sb-122 is summarized in Figure 31, and the corresponding evaluation for the more long-lived Sb-124 is presented in Figure 32. There is some lack of data for the short-lived Sb-122, especially for Inconel SG tubing, so the analysis is focused on the Sb-124 nuclide. A significant difference is seen between the Ringhals PWRs and Loviisa WWERs, with a considerable higher deposition rate during the transient in the WWERs. On the other hand, a rather large difference is also seen between the Loviisa plants cold side values. It was observed in the BWR evaluation that the deposition of Sb-124 was much effected by the Ni:Fe ratio, which may also play a role in the PWRs and WWERs. Another possible factor influencing this activity build-up is the actual shutdown procedures applied in the different types of plants. A considerable pH variation is occurring during the shutdown process, and this variation may be different in the WWER plants due to a different way to control pH compared to the PWR plants. An in-depth study of the shutdown procedures may identify methods to reduce the Sb-124 activity build-up in association with reactor shutdowns.

A similar difference between stainless steel and Inconel surfaces is also found for the Sb-124 nuclide. Note also that the LO1 and LO2 plants show a large difference for the location cold side SG tubes. In Loviisa the main source of antimony is most likely the main circulation pump gaskets. The sources of antimony in the Ringhals PWRs are not accurately known.

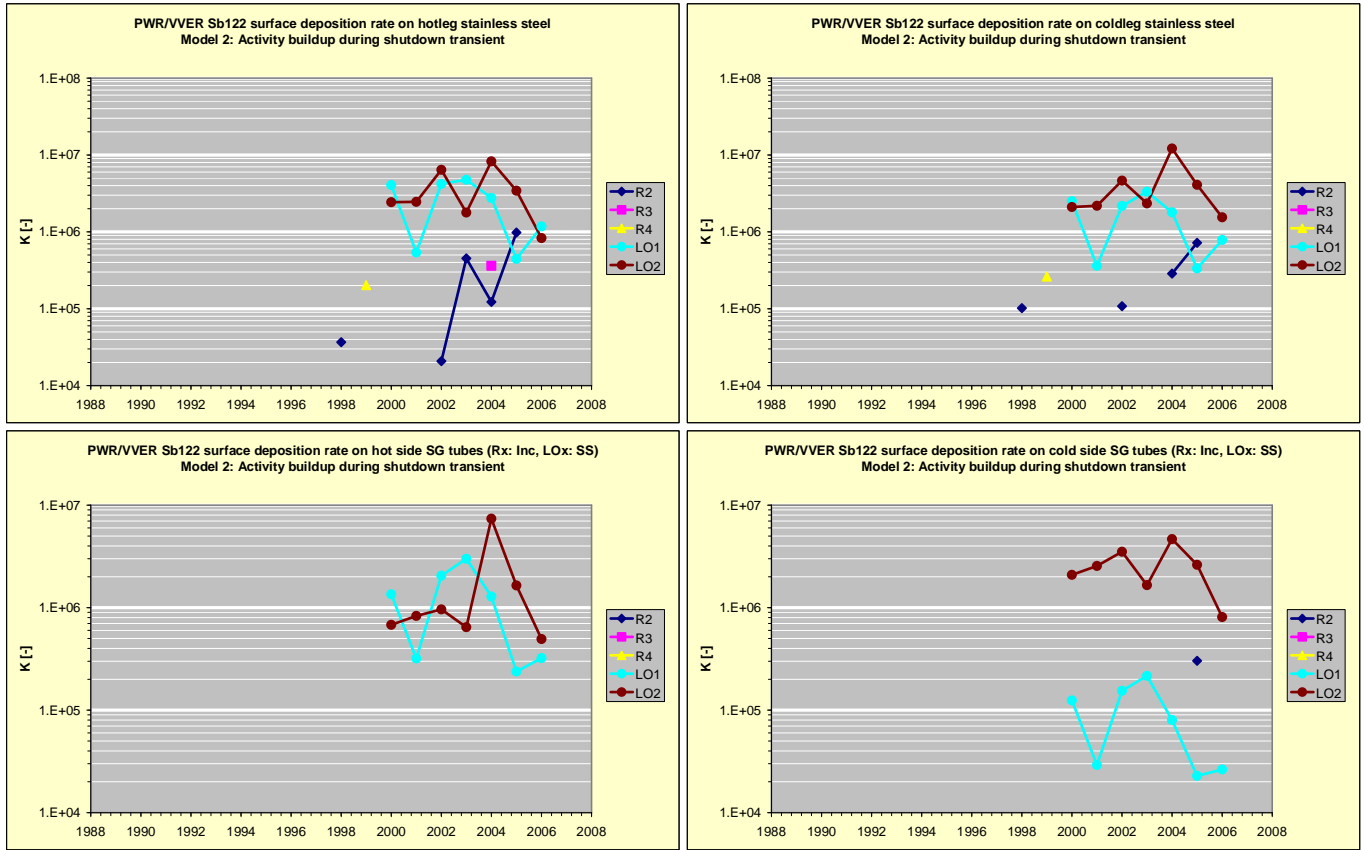


**Figure 31:** Sb-122: Normalized surface deposition rates during shutdown transient (Model 2) of different activated corrosion products for cold and hot side stainless steel piping and SG tubes (Ringhals: Inconel, Loviisa: stainless steel)

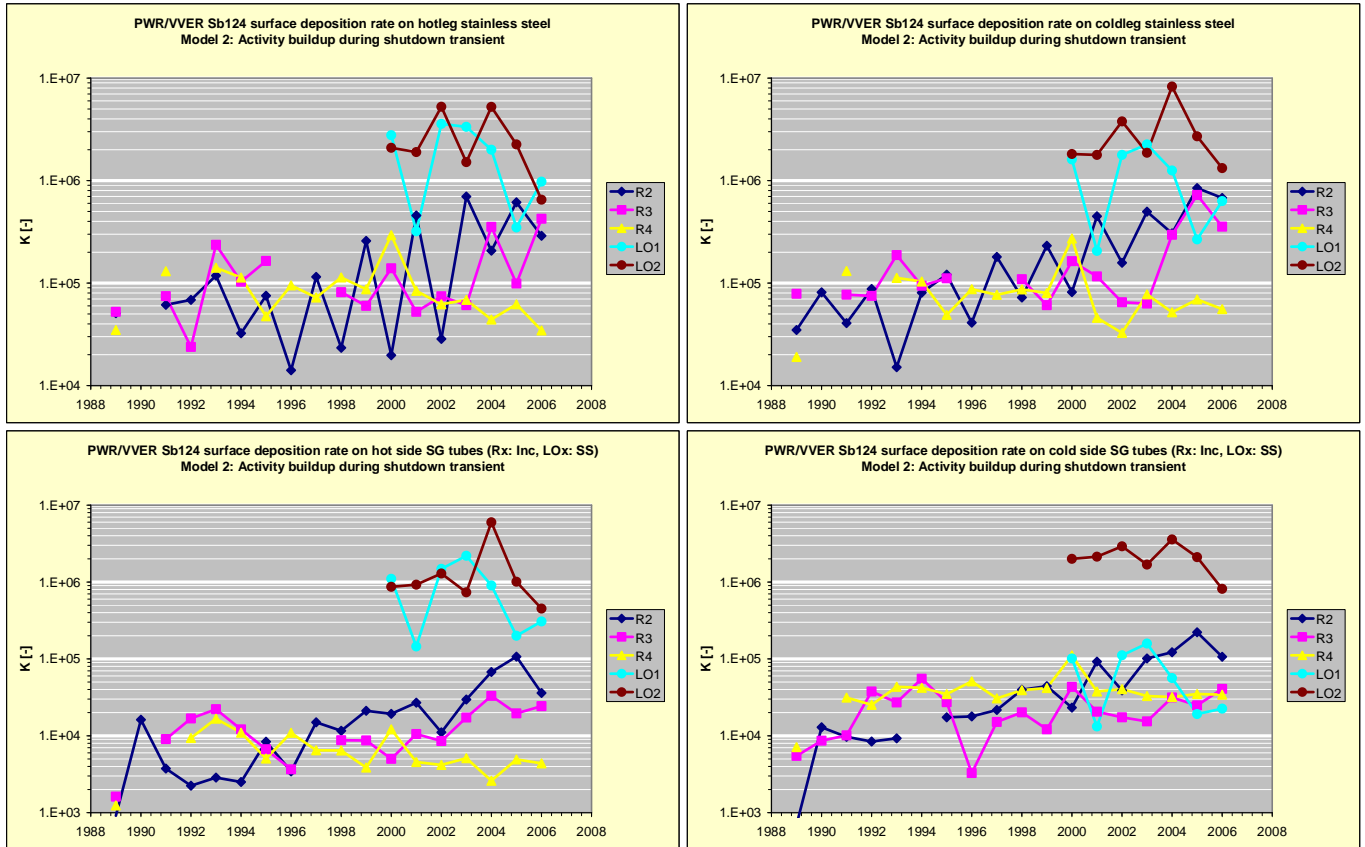


**Figure 32:** Sb-124: Normalized surface deposition rates during shutdown transient (Model 2) of different activated corrosion products for cold and hot side stainless steel piping and SG tubes (Ringhals: Inconel, Loviisa: stainless steel)

### 3.2 Influence of sampling system design

The main systems in R3 and R4 are schematically illustrated in **Figure 33**. The reactor water activity is historically measured via a sampling line connected to the hot-leg upstream of the SGs. This hot sampling line is exposing a relatively large surface area to the coolant. The following data are valid for the R3 and R4 plants:

Sampling line inner diameter: 6 mm  
 Sampling line length upstream of cooler: approx. 100 m  
 Sampling line material: stainless steel  
 Sampling line flow rate: ca 80 g/s  
 Sampling line temperature: 320°C ÷ 280°C just upstream of cooler

If the activity build-up inside the hot sampling line is assumed to follow *Eq. 2*, the following variation of water activity along the sampling line is expected:

$$\text{Eq. 4} \quad \frac{C_w(l)}{C_w(0)} = \exp\left(-\frac{\pi l d}{F} \cdot \rho \cdot \sqrt{\lambda D} \cdot K_1\right)$$

where:

$C(l)$  – Water activity [Bq/kg] at sampling line position “ $l$ ” [m]

$d$  – Sampling line inner diameter [=0.006 m]

$F$  – Sampling line flow rate [=0.08 kg/s]

$\lambda$  – Decay constant for the nuclide [ $s^{-1}$ ]

$\rho$  – Assumed density for oxide layer [ $=3500 \text{ kg m}^{-3}$ ]

$D$  – Assumed average diffusion rate in oxide layer [ $=10^{-18} \text{ m}^2 \text{ s}^{-1}$ ]

The above relation is plotted for four different values of  $K_1$  and five different nuclides with different half lives in **Figure 34**. The reduction of activity along the line is considerable, at least for  $K_1 \approx 1 \cdot 10^8$  and for nuclides with not too long half lives. It means that the earlier evaluations of  $K_1$  factors in this report in several cases is biased, and as a matter of fact have been performed with too low reactor water activity levels which in turn has resulted in an over-prediction of the  $K_1$  value.

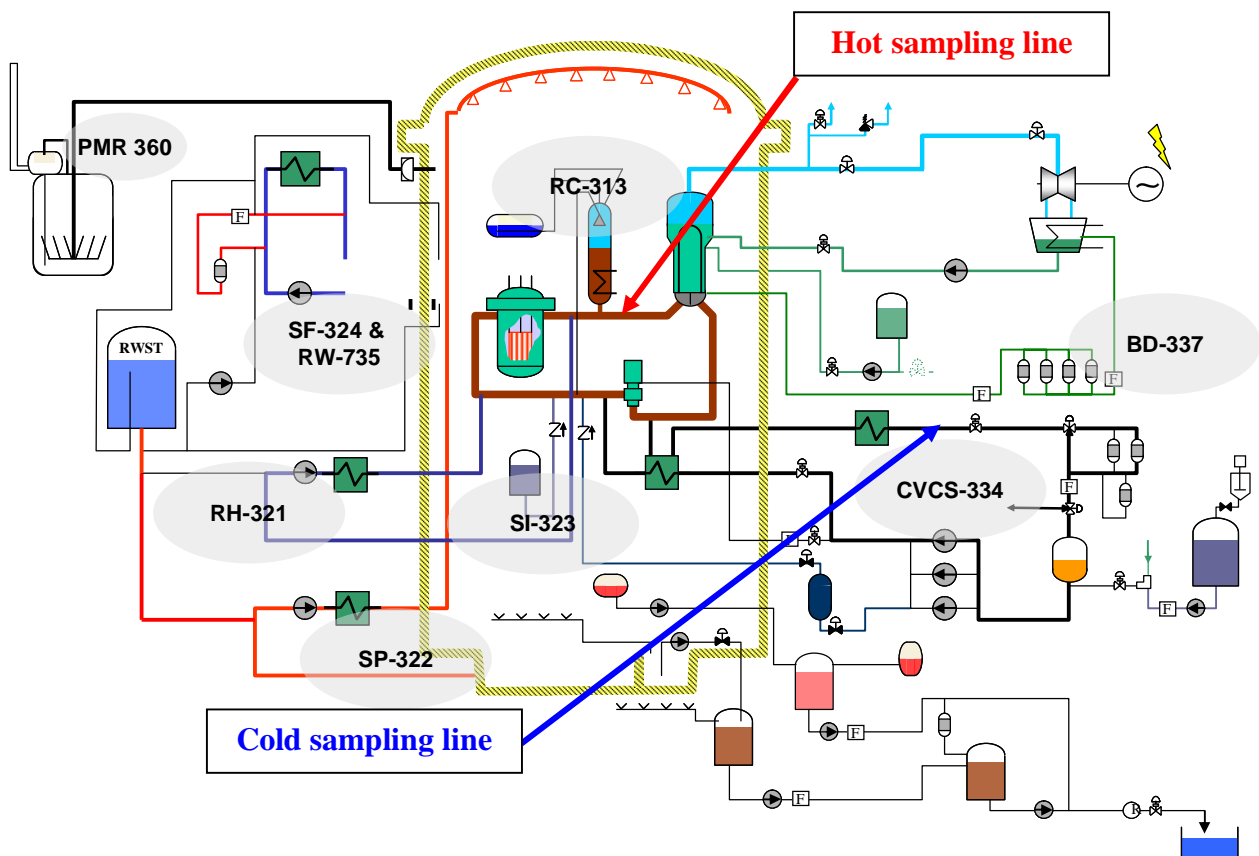


*Figure 33: Ringhals 3 & 4: Locations for hot and cold sampling lines*

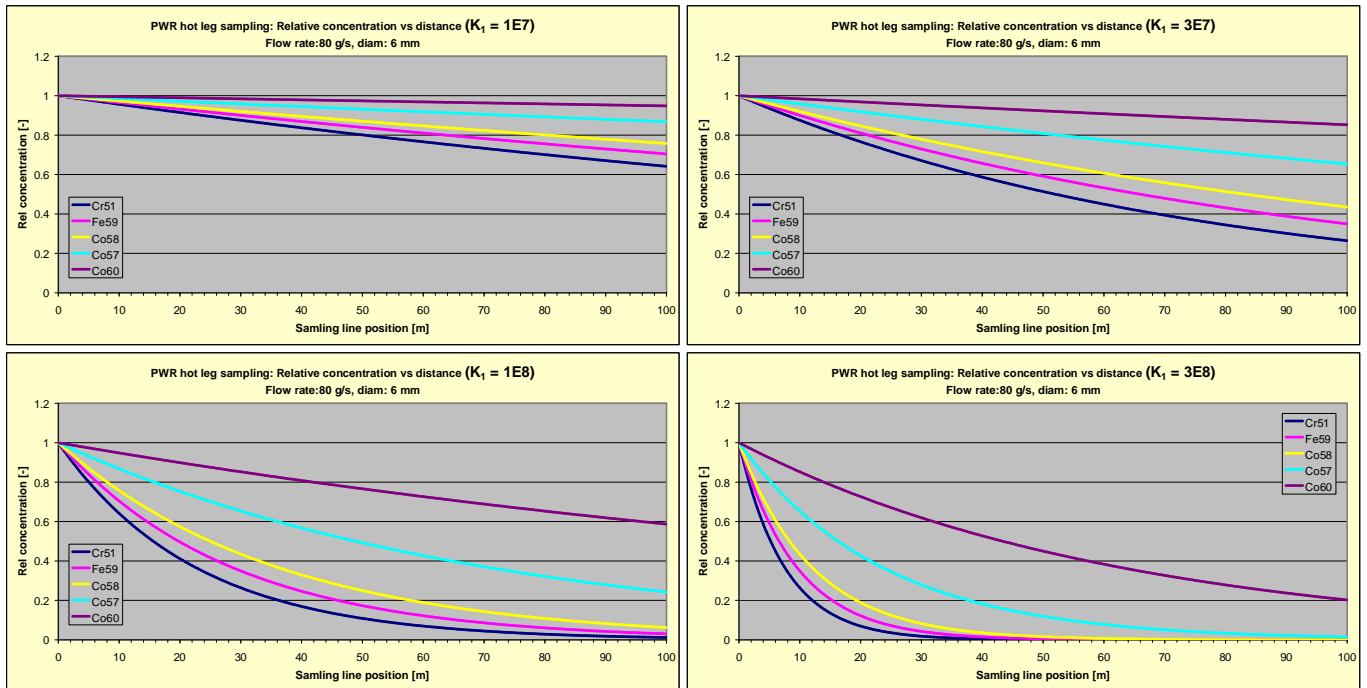


**Figure 34:** Simulation of hot sampling line influence on water activity concentration for four different Model 1 deposition rates ( $K_1 = 1E7, 3E7, 1E8$  and  $3E8$ ) for five different activated corrosion products with different half lives (Cr-51: 27.7 d, Fe-59: 45.1 d, Co-58: 70.8 d, Co-57: 271.8 d, Co-60: 5.27 y)

An alternate position to monitor reactor water activity exists; in the CVCS just upstream of the cleanup unit, see **Figure 33**. The water to the CVCS is taken from one cold-leg downstream of the SGs, and cooled down to about 46°C in a regenerative heat exchanger plus a cooler in series. The relatively high flow rate and large pipes, and a rather quick cooling of the water mean that only a small reduction of water activity is expected before the cleanup. A cold sampling line is connected to the piping upstream of the cleanup unit, and no significant activity buildup is expected in that sampling line due to the low temperature. The reactor water activity sampled in that location is expected to be closer to the activity concentration in the primary loop compared to the water sampled in the hot line. Any reason to expect an enrichment of activity in the sampling lines compared to the reactor water concentration has not been identified and is therefore excluded.

Until recently activity measurements have not regularly been performed in the cold sampling line. A rebuilding of the sampling systems in R3 and R4 has been performed, introducing improved methods for integrated sampling in both sampling locations. As a result of that the activity concentration measurements based on integrated sampling has been performed in both locations in R4 during two cycles and in R3 during the most recent cycle. Those activity measurements are compared in **Figure 35** and **Figure 36**. The results clearly show that a considerable consumption is occurring for certain nuclides in the hot sampling line, e.g. Co-58, while other nuclides are more unaffected, e.g. Mn-54. The results indicate an influence of half life of the nuclide, which is in line with the prediction according to **Eq. 4**. Results for other nuclides are not so easily understood; especially the rather large observed effect on the antimony and silver isotopes. It is known that these nuclides have a tendency to accumulate in coolers, and it can be expected that the sampling system coolers are especially effective in that respect because of a large surface area in relation to the flow rate.

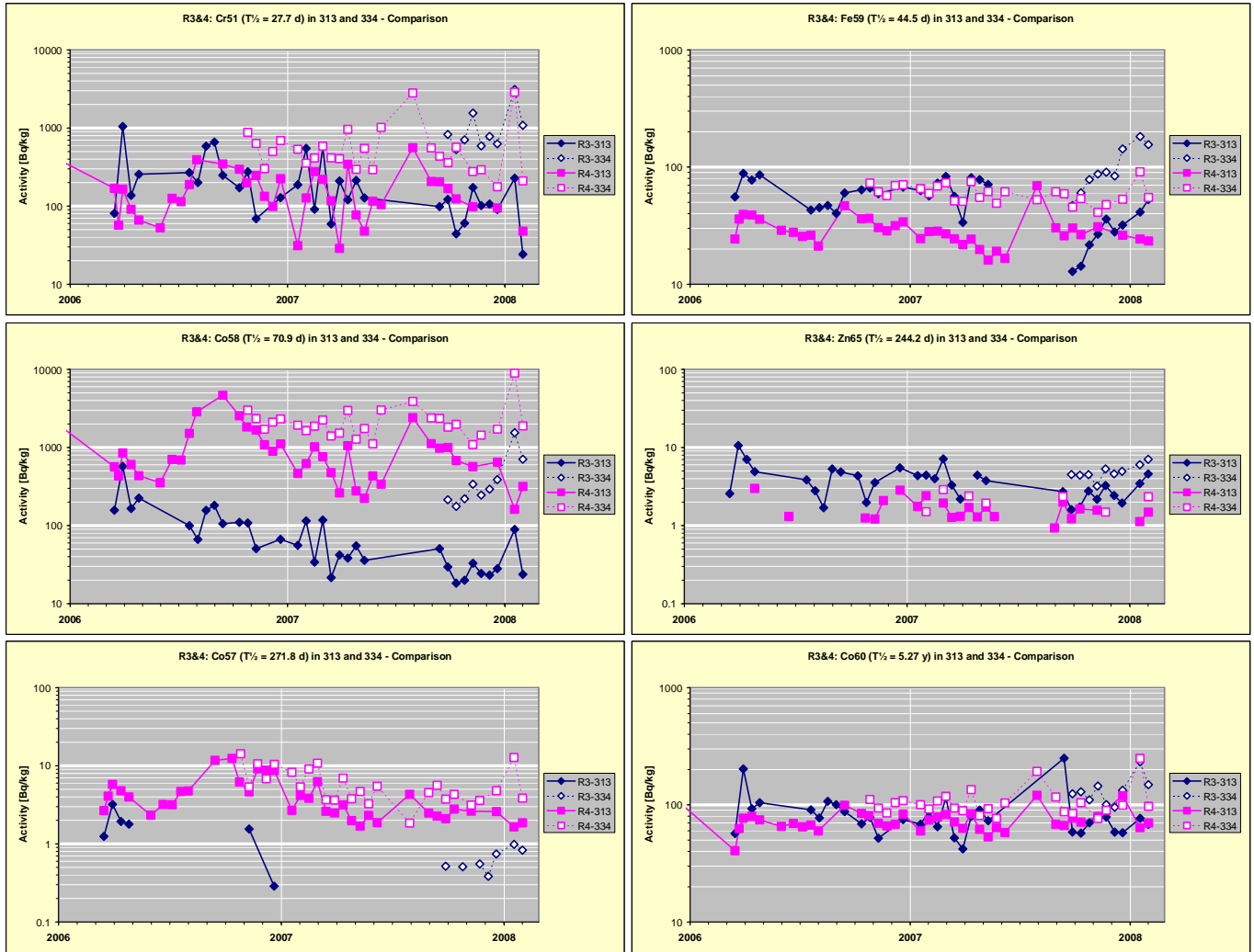


*Figure 35: R3 and R4: Cr-51, Fe-59, Co-58, Zn-65, Co-57 and Co-60 - Comparison of reactor water activity sampling via hot (313) and cold (334) sampling lines*



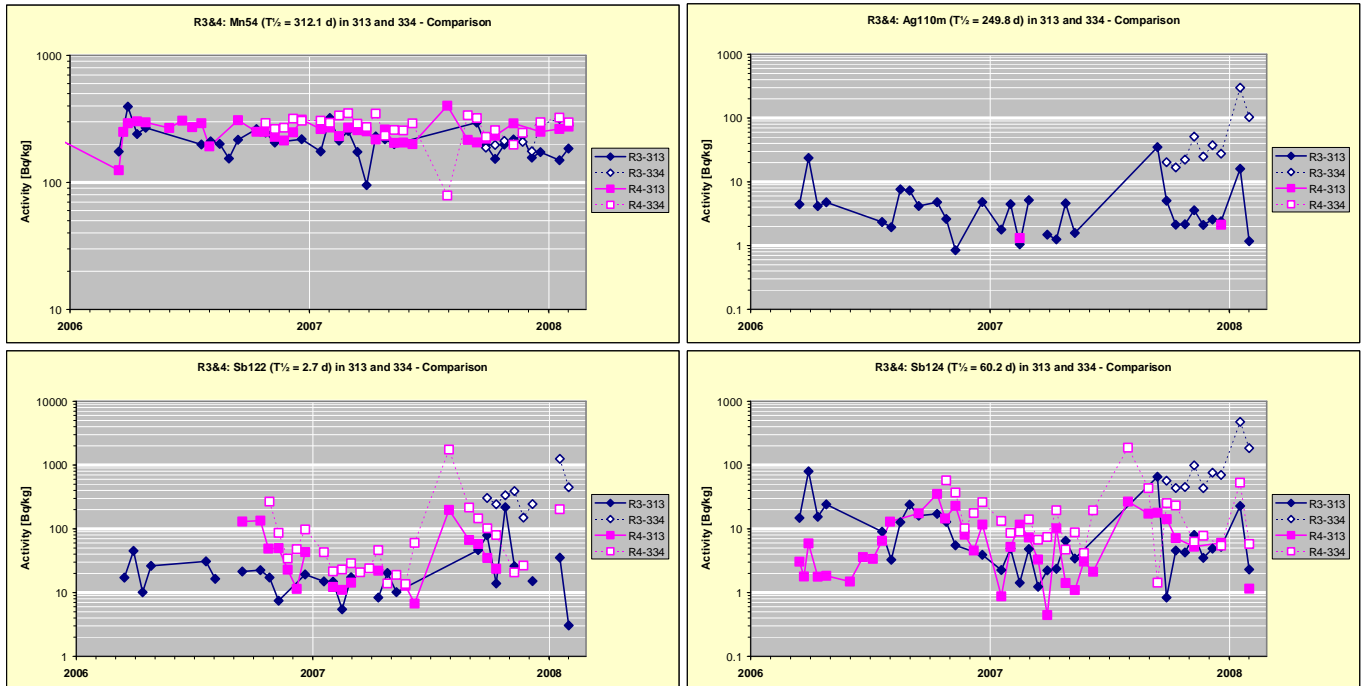


**Figure 36:** R3 and R4: Mn-54, Ag-110m, Sb-122 and Sb-124 - Comparison of reactor water activity sampling via hot (313) and cold (334) sampling lines

The results of the measurements in **Figure 35** and **Figure 36** are summarized in **Figure 37** as a function of the decay constant for each nuclide. A significant difference is seen between the R3 and R4 plants with higher deposition rates in the latter. An influence of half life is also evident with a larger effect for the short-lived nuclides.

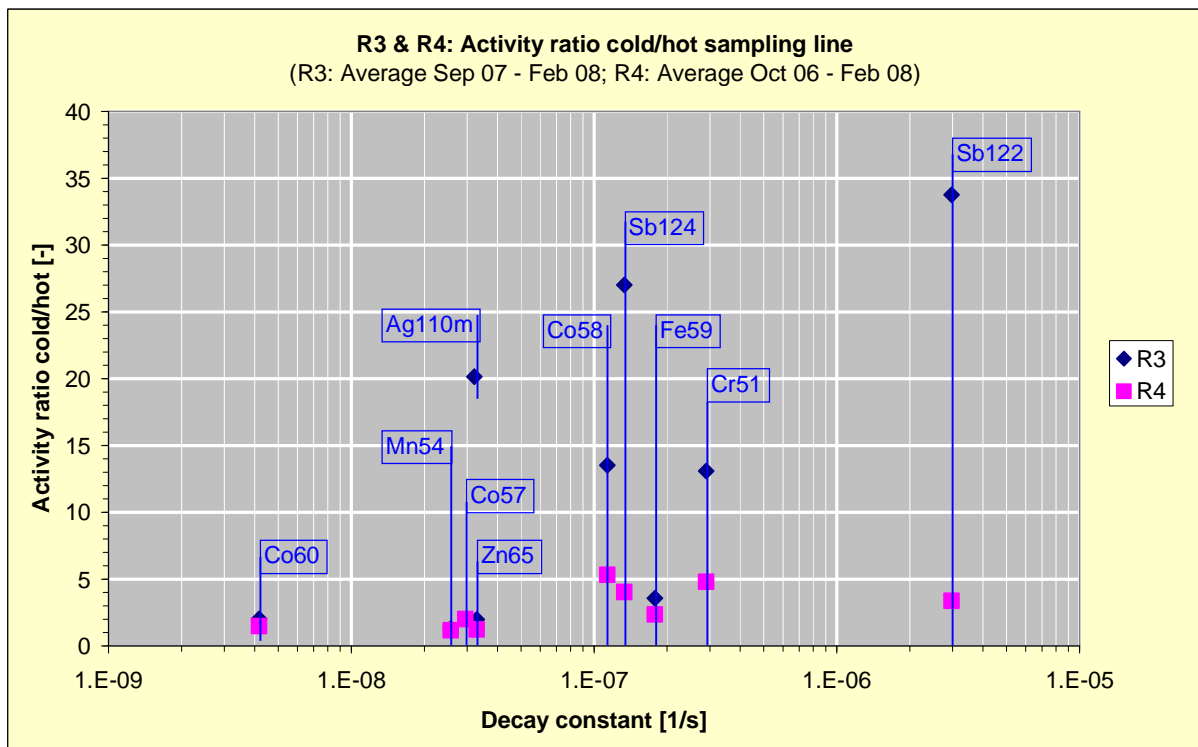


**Figure 37:** R3 & R4: Average activity ratio between cold and hot sampling lines for different nuclides

The above relation **Eq. 4** can be reformulated to show estimated deposition factor  $K_1$  for different nuclides based on the observed ratio between water activity in the cold and hot sampling line:

$$\text{Eq. 5} \quad K_1 = \frac{F \cdot \ln\left(\frac{C_w(0)}{C_w(l)}\right)}{\pi d l \cdot \rho \cdot \sqrt{\lambda D}}$$

The above relation is plotted for different nuclides in **Figure 38** for a hot sampling line with operation conditions typical for the R3 and R4 plants.

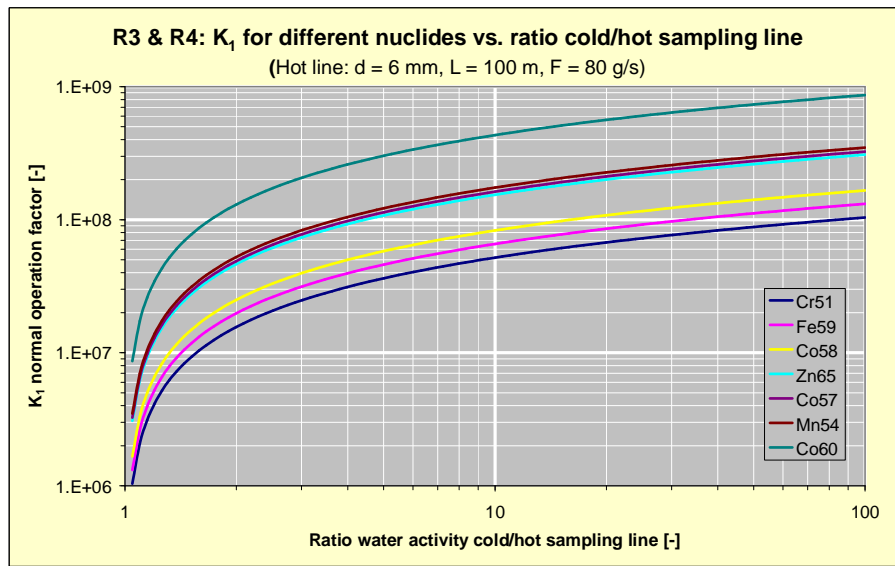


**Figure 38:** R3 & R4: Calculated relation between ratio water activity cold/hot sample line and normal operation deposition rate  $K_1$  for different nuclides

If observed cold/hot sampling ratios according to **Figure 37** are combined with the calculated curves according to **Figure 38** the following  $K_1$  factors are obtained:

- R3:

○ Cr-51:	$C_{\text{cold}}/C_{\text{hot}} = 13.1$	à	$K_1 = 5.8 \cdot 10^7$
Fe-59:	$C_{\text{cold}}/C_{\text{hot}} = 3.6$	à	$K_1 = 3.7 \cdot 10^7$
Co-58:	$C_{\text{cold}}/C_{\text{hot}} = 13.5$	à	$K_1 = 9.4 \cdot 10^7$
Zn-65:	$C_{\text{cold}}/C_{\text{hot}} = 2.0$	à	$K_1 = 4.6 \cdot 10^7$
Mn-54:	$C_{\text{cold}}/C_{\text{hot}} = 1.3$	à	$K_1 = 2.0 \cdot 10^7$
Co-60:	$C_{\text{cold}}/C_{\text{hot}} = 2.0$	à	$K_1 = 1.3 \cdot 10^8$

- R4:

○ Cr-51:	$C_{\text{cold}}/C_{\text{hot}} = 4.8$	à	$K_1 = 3.5 \cdot 10^7$
Fe-59:	$C_{\text{cold}}/C_{\text{hot}} = 2.35$	à	$K_1 = 2.4 \cdot 10^7$
Co-58:	$C_{\text{cold}}/C_{\text{hot}} = 5.3$	à	$K_1 = 6.0 \cdot 10^7$
Zn-65:	$C_{\text{cold}}/C_{\text{hot}} = 1.23$	à	$K_1 = 1.4 \cdot 10^7$
Co-57:	$C_{\text{cold}}/C_{\text{hot}} = 2.0$	à	$K_1 = 4.9 \cdot 10^7$
Mn-54:	$C_{\text{cold}}/C_{\text{hot}} = 1.17$	à	$K_1 = 1.2 \cdot 10^7$
Co-60:	$C_{\text{cold}}/C_{\text{hot}} = 1.49$	à	$K_1 = 7.5 \cdot 10^7$

The above results show a rather good agreement for comparable radioisotopes, e.g. Co-57, Co-58 and Co-60, in the same plant, but indicate somewhat different conditions in the two plants. The above  $K_1$  factors are probably closer to the true values than the earlier based only on activity concentrations measured in the hot sampling lines.

### 3.3 Corrosion release from Inconel

The removal of Ni and Co-58 from the reactor water is followed at the annual exposures in the Ringhals PWR plants. The annual removal of Ni in the R3 plant is shown in **Figure 39**, and the removal of Co-58 activity is presented in **Figure 40**. The corresponding data for the R4 PWR plant are shown in **Figure 42** and **Figure 43**. The plants display a quite different behaviour during recent years, with a considerable reduction in the R3 case but constant or slightly increasing levels in the R4 plant. The main differences between these plants are:

- R3: New SGs with Inconel 690 tubes installed 1995. High temperature pH was changed from 7.24 to 7.4 around year 2000.
- R4: Old SGs with Inconel 600 tubes are maintained. The plant has stayed on a high temperature pH of 7.24 during recent years.

The measured R3 data indicates a considerable effect of an increase of high temperature pH from 7.24 to 7.4, with a reduction of the corrosion release of Ni with almost an order of magnitude. Similar behaviour is experienced in the R2 plant. An evaluation of the Co-58 activity in relation to the amount of Ni indicates a specific activity close to what is expected if the reactor transient originates from the fuel crud. The observed difference in amount of fuel crud Ni has certainly a large effect on radiation fields, with a reducing trend in the R3 plant, **Figure 41**, but an increasing trend in the R4 plant, **Figure 44**.

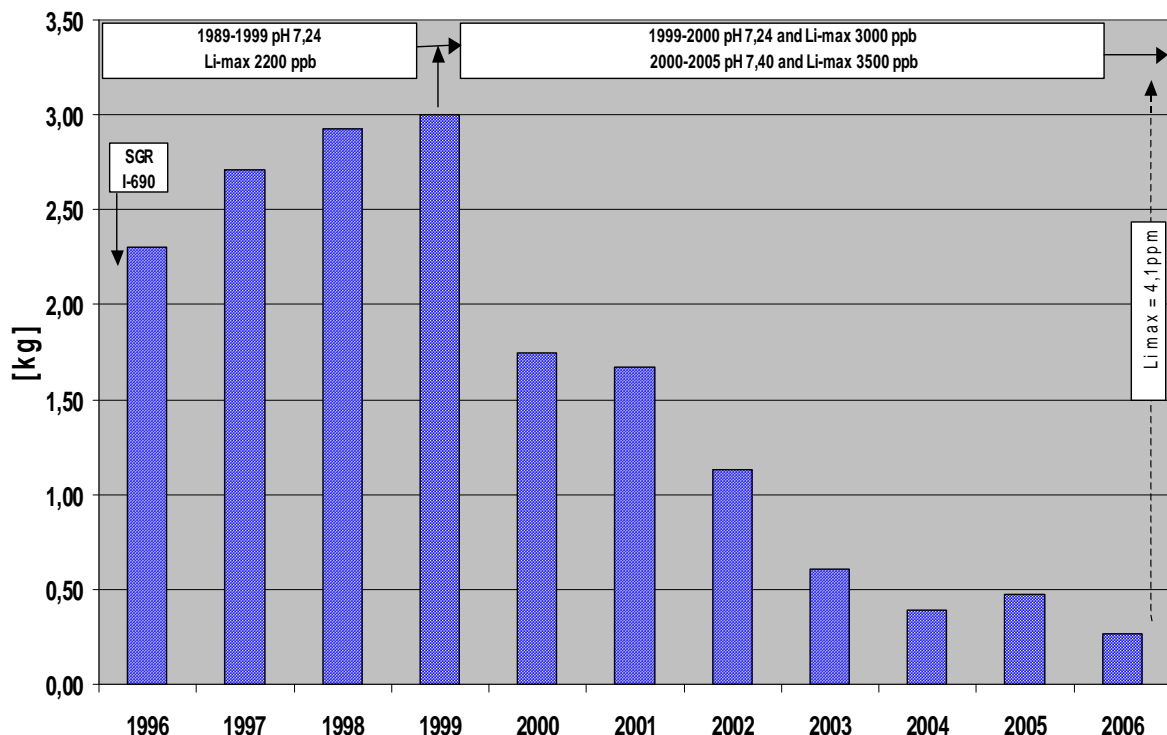


**Figure 39:** R3: Accumulated removal of Ni during different outages

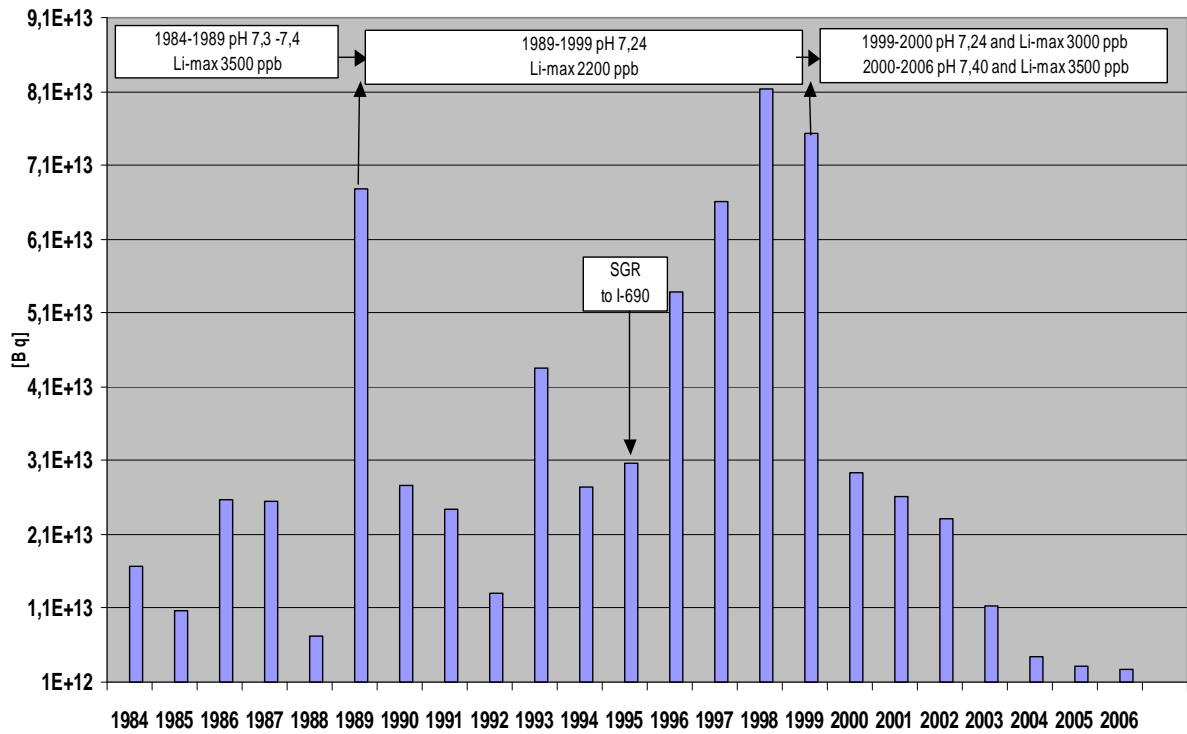


Figure 40: R3: Accumulated removal of Co-58 during different outages

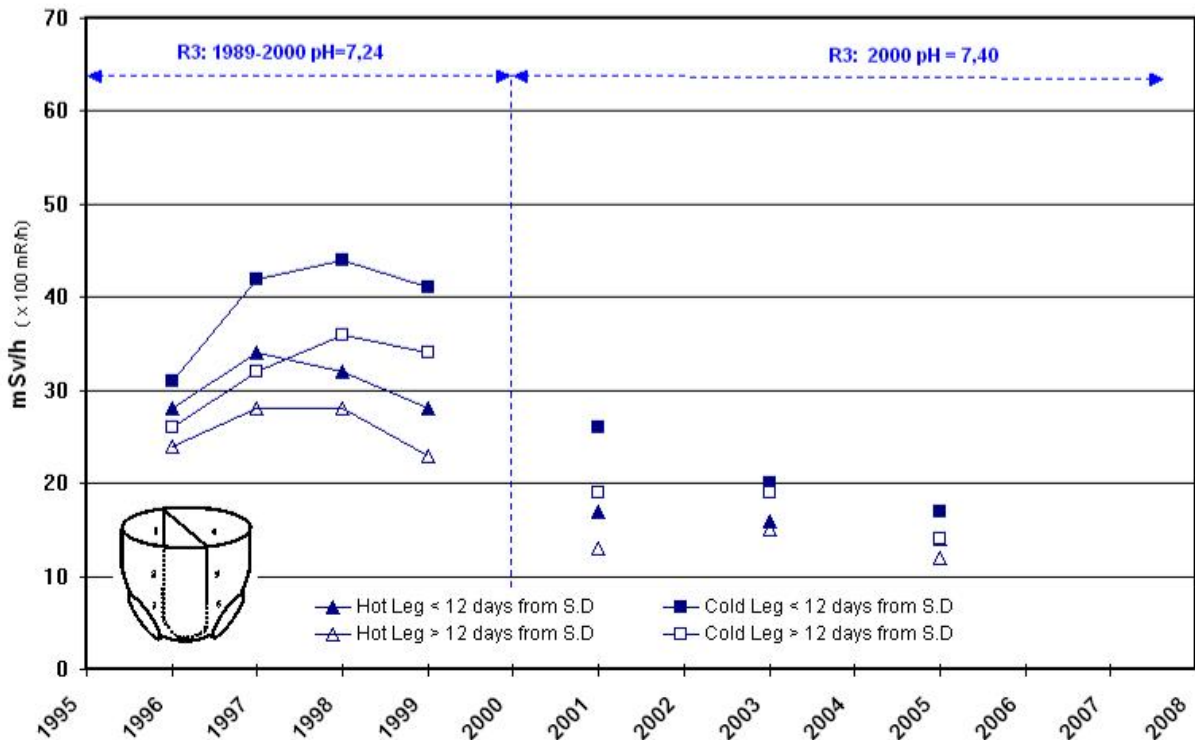


Figure 41: R3: Radiation levels in SG channel heads

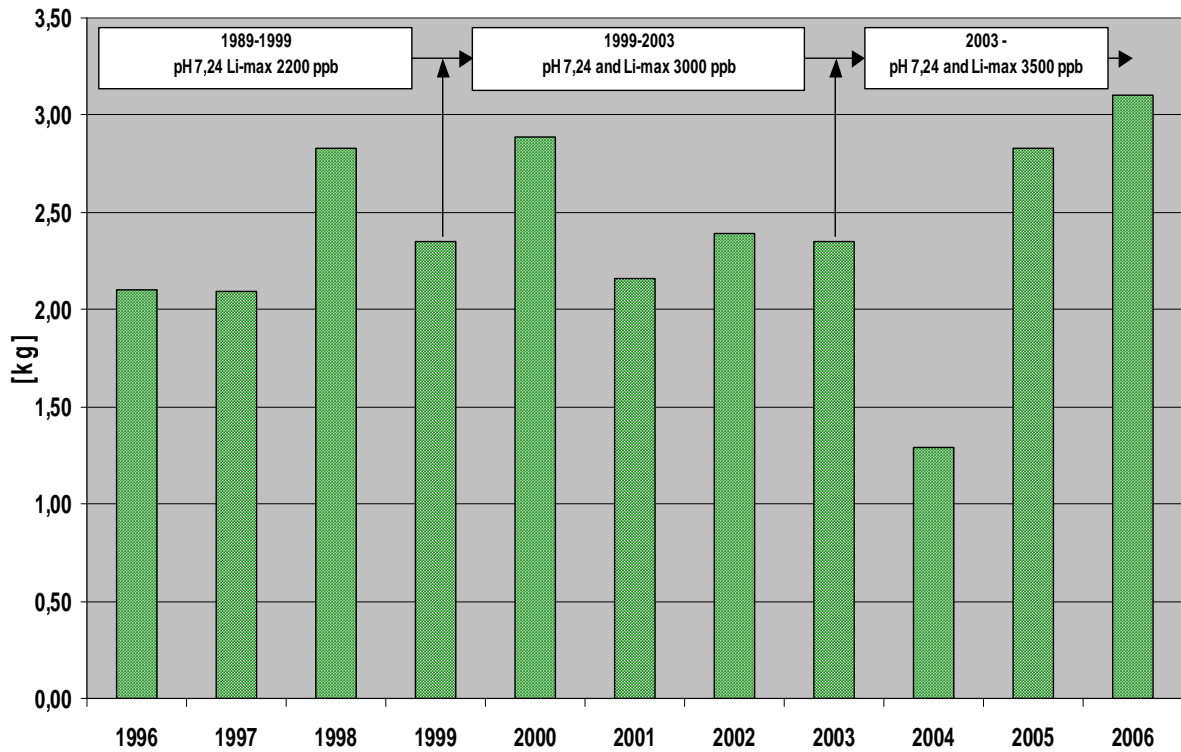


Figure 42: R4: Accumulated removal of Ni during different outages

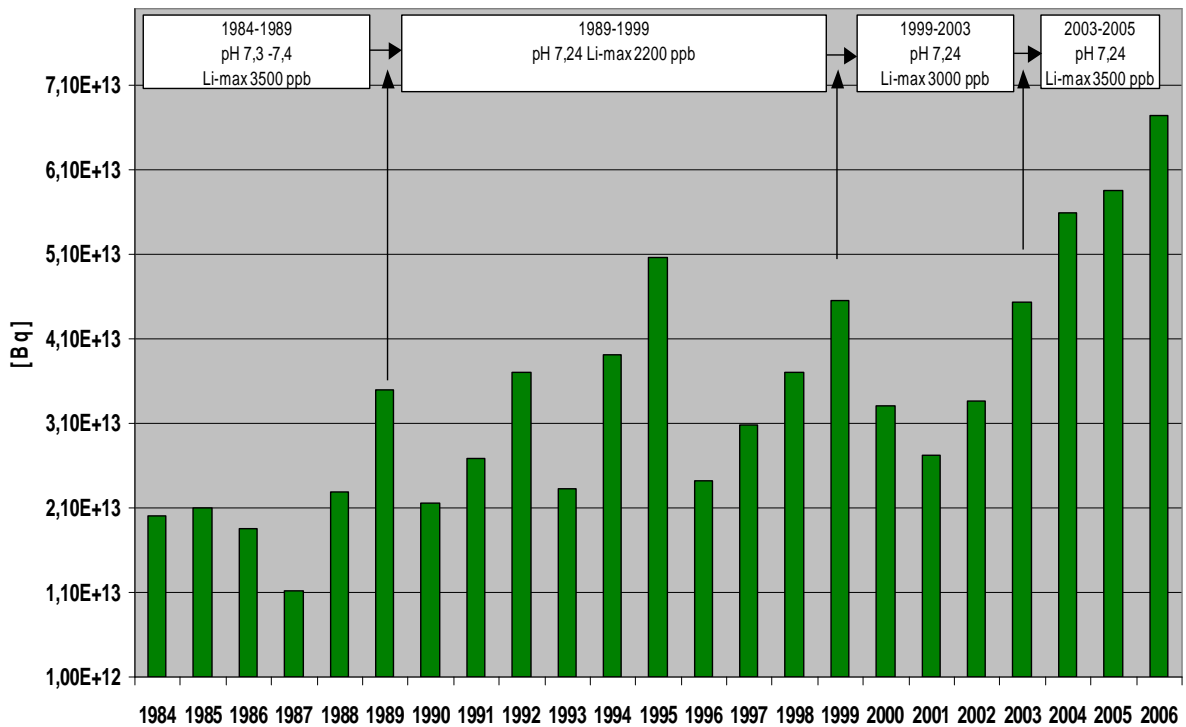


Figure 43: R4: Accumulated removal of Co-58 during different outages

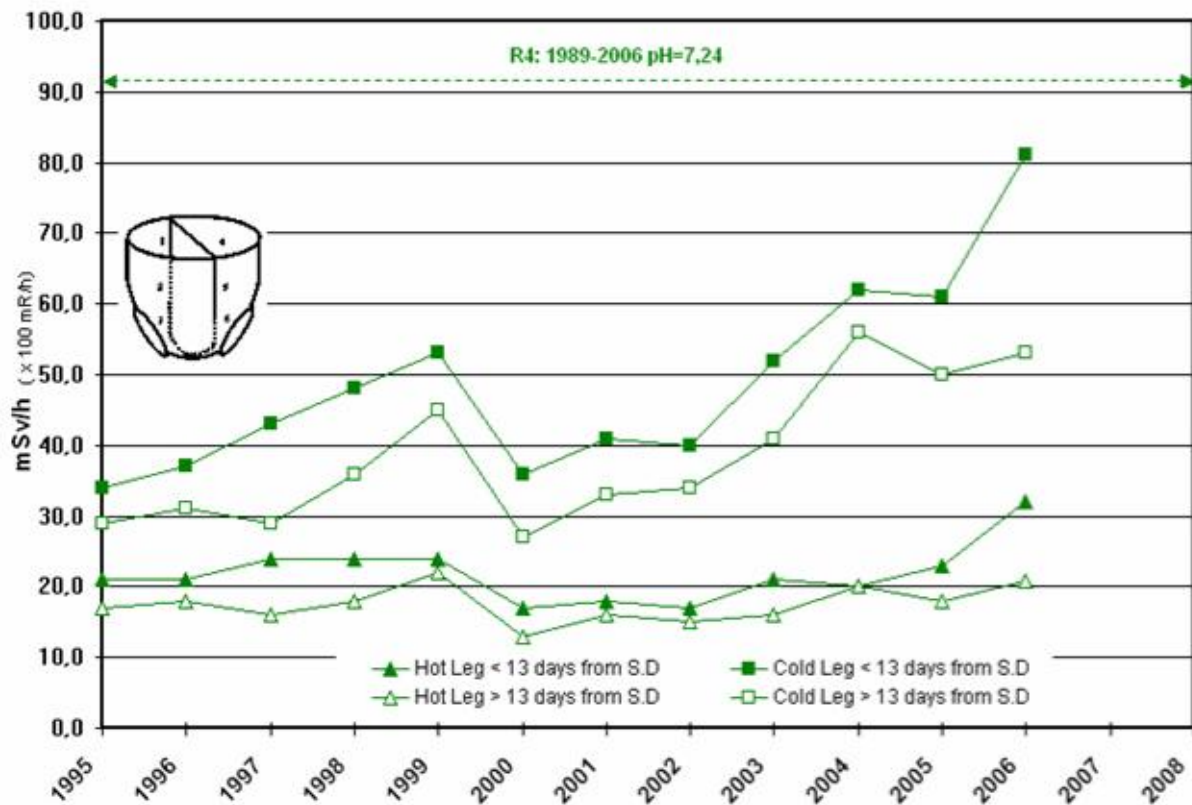
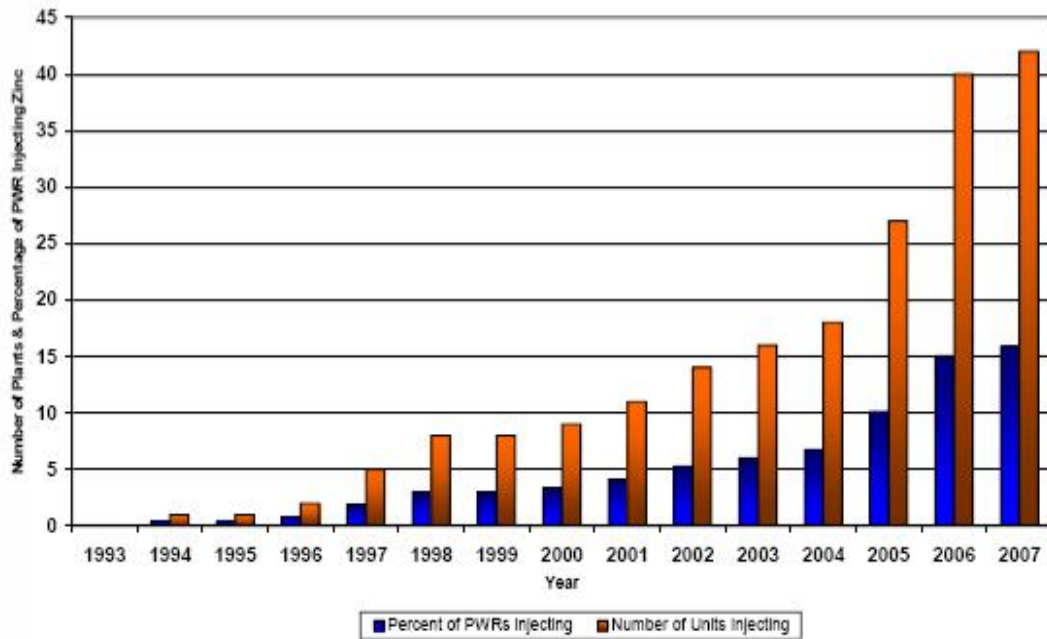


Figure 44: R4: Radiation levels in SG channel heads

The above data on the pH effect on Ni corrosion release from Inconel are proposed to be used in the model validation.

### 3.4 Influence of zinc

PWRs or WWERs injecting zinc have not been included in the present review. Internationally, however, a large number of PWRs are operating with zinc injection, **Figure 45**. Today about 15% of the PWRs worldwide are injecting zinc. The main reasons for injecting zinc are to decrease radiation fields and to mitigate stress corrosion cracking. Some published data are shown below that may be used in the modelling efforts.



*Figure 45: Application of Zinc in world PWRs /EPRI/*

Laboratory data indicate that operation with about 20 ppb of zinc in the water significantly reduces the corrosion release rate from both Inconel and stainless steel, see **Figure 46**. The reduction is a factor 5-6 for Inconel, and about half that value for stainless steel. Operation experience from PWR plants shows a corresponding reduction of radiation fields, see **Figure 47**.

The presented data in form of quantitative trends are proposed to be used in the model validation work.

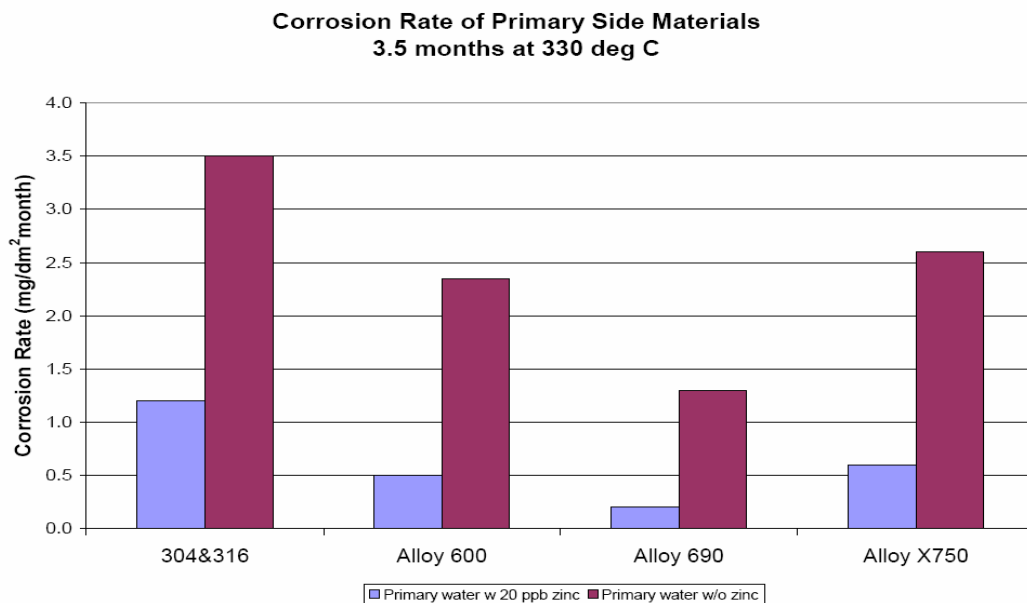


*Figure 46: Experimental corrosion release rates with and without Zn /EPRI/*

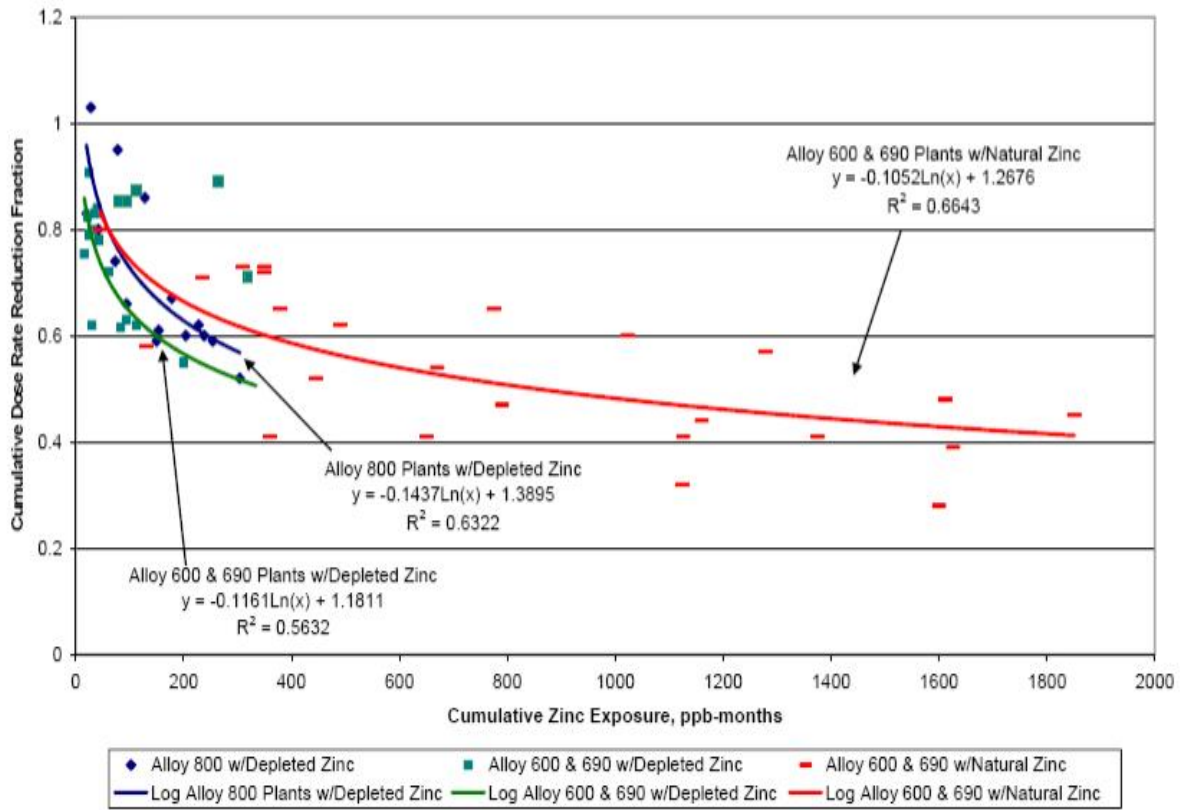


*Figure 47: Cumulative dose rate reduction based on zinc exposure /EPRI/*



## 4 Summary and conclusions

A main finding of the data review is that the surface adsorption rates during PWR operation are quite high for several radionuclides, and that these high rates significantly affect the reactor water sampling efficiency when using long hot stainless steel sampling lines. This effect has been possible to verify by recent Ringhals PWR data where cold sampling lines have been used in parallel to the hot lines. Most reactor water activity data used in the present review are based on measurement in the hot sampling lines, which has to be considered in the evaluation.

The following conclusions are drawn from the presented results that are proposed to be used as input to the validation of the oxide model being developed in the ANTIOXI project:

- The activity build-up of most nuclides is controlled by the normal operation conditions and not the shutdown transient. Examples of such nuclides are: Co-57, Co-58, Co-60, Fe-59, Cr-51, Zn-65 and Mn-54. The activity build-up seems to follow the general form suggested in **Eq. 2**, i.e. a surface adsorption step followed by diffusion into the oxide layer. The evaluation of actual adsorption rates is biased by the observed problems with hot sampling lines, but the rates for the different nuclides are found to be ranged in the following order:

$$\text{Co-57, Co-58, Co-60} \geq \text{Cr-51, Fe-59, Zn-65} > \text{Mn-54}.$$

The difference in rate between the Co and Mn isotopes is close to one order of magnitude. No considerable difference is seen between the WWERs and the PWRs. On the other hand, a considerable difference is seen between the PWRs/WWERs and the BWRs /2/, with one to two orders of magnitude higher adsorption rates in the former.

- The activity build-up of some other nuclides, Sb-122, Sb-124 and possibly Ag-110m, seems to be controlled by the shutdown transient instead of normal operation conditions, i.e. follow **Eq. 3** in this report. Some differences between plants, as well as year-by-year variations, are observed, e.g. the adsorption in the WWER plants is significantly higher than in the PWR plants.
- A considerable difference is observed between activity build-up on stainless steel and Inconel, with about one order of magnitude higher build-up on stainless steel.
- The activity build-up on cold legs is normally slightly higher than on the hot legs. This difference, however, varies between plants. Especially plants that have experienced a significant activity build-up, e.g. LO2 before the decontamination campaign and recent data from R4, show rather large difference.
- The main effect of operation with a slightly increased high temperature pH in some of the Ringhals PWRs, pH<sub>300</sub> 7.4 instead of 7.24, seems to be a considerable reduction of the corrosion release rate of Ni from Inconel. This decrease is close to one order of magnitude. The decrease in corrosion release is counteracted by a slight increase of relative adsorption rates of e.g. the Co isotopes; however, the overall effect of the pH increase is a reduction of radiation fields.
- Plants applying Zn injection has not been included in the data review. Literature data have, however, been reviewed showing that the effect of Zn injection

shows large similarities with the effect of increased pH, i.e. significantly reduced corrosion release rates and an overall reduction of radiation fields.

## References

- /1/ Klas Lundgren, Tormod Kelén, Magnus Gunnarsson, Elisabeth Ahlberg, "A new model for activity build-up in BWRs adopting theories for surface complexes and diffusion in oxide layers", SSI P 1203.00 (September 2001).
- /2/ Klas Lundgren, "ANTIOXI - Development of oxide model for activity build-up in LWRs - BWR plant data analysis", VTT Report VTT-R-04127-07 (June 2007).
- /3/ Klas Lundgren, Hjalmar Wijkström, Gunnar Wikmark, "Recent Developments in the LwrChem Radiolysis Code", International Water Chemistry Conference, San Francisco, October 2004.